APPLICATION OF MAGNETIC SUSCEPTIBILTY MEASUREMENTS TO OILFIELD SCALE MANAGEMENT

The Thesis by

SALIM ALGADAFI ALI IMHMED

Submitted for the Degree of

Doctor of Philosophy in Petroleum Engineering

Institute of Petroleum Engineering
Heriot-Watt University
Edinburgh, Scotland, UK

April 2012

ABSTRACT

The management of a petroleum reservoir requires good understanding of the geology and the properties of the reservoir. This understanding can be obtained from the analysis of results of down-hole tests and laboratory measurements. One of the properties that can be measured is the magnetic behaviour of the reservoir fluids and mineral scales.

The build-up of scale is an important process in oil and gas reservoirs, and can have a damaging effect on the flow of fluid in reservoir rocks and in wells. An understanding of the magnetic properties of fluids such as brines, crude oils, brines with a scaling tendency, brines containing scale inhibitors, and of scale minerals is a key objective of this research.

These magnetic techniques have the advantage of being environmentally neutral, non-destructive, rapid and low cost (Potter 2005). Understanding of the magnetic properties of the petroleum reservoir matrix rock may provide new techniques for improved reservoir characterisation, petroleum exploration and production.

Magnetic susceptibility measurements of brines, crude oils and scale inhibitors have been carried out and are reported in this thesis. All fluids are diamagnetic, with distinct differences between them. The magnetic susceptibility values for brines are related to their solute composition, while for crude oils the magnetic susceptibility values are related to their physical and chemical properties. The effect of solute composition and concentration on the magnetic susceptibility of a brine is also measured.

Measuring the magnetic susceptibility of a produced water sample would allow rapid detection of injection water breakthrough at the production facilities, and therefore

improve the prospect of quickly deploying a preventative or remedial action to mitigate the risk of inorganic scale damage in the production system. The proposed method described herein introduces the potential for either an in line system, or at least an immediate analysis of the sample when captured, thus allowing operators to make important scale management decisions much earlier than is currently possible.

Magnetic hysteresis measurements of reservoir scale minerals could be used as a rapid, non-destructive method to characterise and indentify the types of scale minerals occurring (diamagnetic, paramagnetic, ferromagnetic and antiferromagnetic). Changes in the slope (the magnetic susceptibility) of the hysteresis curves may be used to identify different scale minerals. Straight lines with negative slope are due to diamagnetic minerals, whilst straight lines with positive slope are due to paramagnetic minerals. The relative amounts of diamagnetic and paramagnetic minerals contained in a mixture of the two can potentially be quantified by the slope of the straight line at high fields.

ACKNOWLEDGEMENTS

I am grateful to Professor David Potter, formerly of Heriot-Watt University Institute of Petroleum Engineering staff, who first suggested looking at application of magnetic susceptibility measurements to oilfield scale. Also, I would like to express my sincere gratitude to my supervisors, Professor Eric Mackay and Dr Arfan Ali, Prof. Mackay for his continued support and invaluable guidance throughout many difficult times in both academic and non-academic issues. He is always available to discuss, guide, and support. It would have been difficult for me to have reached this point in my academic journey, without the guidance and support from him, which is highly appreciated. I am also grateful to Dr Ali for his valuable support and guidance in magnetic measurements, analysis of results and also the considerable amount of time he spent in revising my thesis and guiding me on various technical issues.

I am also grateful to Mr. Robin Shields for his guidance, and support. I would like to acknowledge Dr. Oleksandr Ivakhnenko, formerly of Heriot-Watt University Institute of Petroleum Engineering staff, and Keith Bell who passed away during the work in this thesis for their help.

I am also grateful to all the members of the Flow Assurance and Scale Team (FAST) who have always been available for help at any time during my stay at Heriot-Watt University. Needless to say, I express my thanks to all the staff members of Heriot-Watt University, academic, administrators, and finance for making my stay at Heriot-Watt comfortable.

My endless gratitude goes to my parents, my beloved wife, my baby Saden, my brothers, sisters, relatives, friends, and well wishers, for their prayers and patience, assistance and concern throughout the time of my study is highly appreciated.

Special thanks to my older brother Adil, who was like a father to me after my father passed away when I was young, I will never forgot his early morning phone call for the support and encourage during my stay in Edinburgh, UK.

I am also grateful to Dr. Salima Baraka-Lokmane of Total, France and Dr. Khafiz Muradov of Institute of Petroleum Engineering, Heriot-Watt University for agreeing to examine this thesis. Their time invested in reading and evaluation of this thesis is appreciated.

TABLE OF CONTENTS

LIST OF FIGURES

LIST OF TABLES

NOMENCLATURE

B	Magnetic Induction
FW	Formation Water
H	Magnetic Field Strength
HS	High Scaling Tendency
Hc	Coercivity of Magnetisation (Coercive Force)
Hcr	Coercivity of Remanent Magnetisation
ICP	Inductively Coupled Plasma
IRM	Isothermal Remanent Magnetisation
LS	Low Scaling Tendency
M	Magnetisation
MD	Multi-domain
MIC	Minimum Inhibitor Concentration
Mrs	Saturation Remanent Magnetisation
Ms	Saturation Magnetisation
MSB	Magnetic Susceptibility Balance
Msp	Spontaneous Magnetisation
mT	Milli (10^{-3}) Telsa
N_d	Demagnetising Factor
NRM	Natural Remanent Magnetisation

NSSW	North Sea Sea Water
PSD	Pseudo-single Domain
ppm	Parts per million
PW	Produced Water
PWRI	Produced Water Re-Injection
SEM	Scanning Electron Microscope
SD	Single-domain
SIRM	Saturation Isothermal Remanent Magnetisation
SW	Sea Water
T	Telsa (Unit of Magnetic Filed)
T_N	Neel Temperature
T_C	Curie Temperature
VFTB	Variable Field Translation Balance
XRD	X-Ray Diffraction
χ, MS	Magnetic Susceptibility
$\chi_{m,}$ MS	Mass Magnetic Susceptibility
χ_M	Molecular Magnetic Susceptibility
χ_v	Volume Magnetic Susceptibility
χ_o	Initial Magnetic Susceptibility
χ_{Hfld}	High Field Magnetic Susceptibility
χ_{Lfld}	Low Field Magnetic Susceptibility
χ_{gas}	Magnetic Susceptibility of Gas Phase

χ_{fluid}	Magnetic Susceptibility of Fluid Phase
χ_{sol}	Magnetic Susceptibility of Solid Phase
χ_{dia}	Magnetic Susceptibility of Diamagnetic Component
χ_{para}	Magnetic Susceptibility of Paramagnetic Component
χ_{ferro}	Magnetic Susceptibility of Ferromagnetic Component
$\chi_{antiferro}$	Magnetic Susceptibility of Antiferromagnetic Component

CHAPTER 1: INTRODUCTION

1.1 Application of magnetic susceptibility measurements in the petroleum industry

The magnetic susceptibility χ_m is a dimensionless proportionality constant that indicates the degree of magnetization of a material in response to an applied magnetic field (more discussion and explanations will be provided in chapter 2).

The use of magnetic techniques in general in the hydrocarbon industry has been limited to magnetic prospecting (Donovan et al., 1979) and petrophysical investigations for the detection of oil and gas reservoirs (Bagin et al., 1973, Bagin and Malumyan, 1976). Magnetic techniques utilizing the Earth's magnetic field or the natural remanent magnetisation (NRM) in the reservoir rocks have also played an important role in petroleum reservoir exploration and research. High resolution magnetic surveys (Eventov, 1997, 2000) utilize the Earth's present magnetic field. Such survey tools measure three orthogonal components of the local magnetic fields, and from these data the tool's inclination, azimuth, and toolface orientation can be calculated. Also, boreholes are commonly surveyed for drilling using the Earth's magnetic field as a north reference (Wilson and Brooks, 2001).

Palaeomagnetism together with standard magnetostratigraphy are beginning to be used for correlation purposes in the petroleum industry (Gillen et al., 1999: Cioppa et al., 2001; Filippycheva et al., 2001). NRM in palaeomagnetism is a key parameter for the orientation of directional properties to geographic coordinates (Hailwood and Ding, 1995), and helping to date hydrocarbons (Symons et al., 1999). Environmental magnetism is also an important discipline for the detection of hydrocarbon seepage (Yeremin et al., 1986; Liu et al., 1996; Costanzo-Alvarez et al., 2000) and contamination (Cogoini, 1998).

A variety of techniques have been used in the past to measure the magnetic properties of minerals including: fractionation with a magnetic separator (Stradling, 1991), Frantz isodynamic separator (Nesset and Finch, 1980 and McAndrew, 1957), magnetometer (Foner and McNiff, 1968 and Lewis and Foner, 1976), SQUID (Sepulveda et al., 1994), resonant coil (Cooke and De Sa, 1981 and Isokangas, 1996) and the inductance bridge (Drobace and Maronic, 1999, Stephenson and De Sa, 1970, Foner, 1991 and Tarling and Hrouda, 1993). These techniques are generally considered laboratory methods due to the length of time required to process the samples (time for preparing, cleaning, measuring, and getting the results).

The developments in instrumentation and software over time have attracted a number of scientists towards the application of magnetic susceptibility methods in the hydrocarbon industry. They include magnetic susceptibility measurement and their integration with magnetometer and other surface geophysical surveys, and with soil magnetic studies accomplished in the laboratory. However, some still think that there will be insufficient contrast in the magnetic susceptibility of sand and gravel compared to clays and other sedimentary rocks in order to differentiate them (Jeffrey et al., 2007).

The development of industrial grade equipment to measure magnetic susceptibility was identified by the Julius Kruttschnitt Mineral Research Centre (JKMRC). The equipment referred to is able to measure complex magnetic susceptibility (i.e. both phase and amplitude of the magnetic susceptibility vector) from 10 Hz to 100 kHz at infinitely adjustable field strengths (Cavanough and Holtham, 2001 and Cavanough and Holtham, 2004). The CS-2 and KLY-2 Kappabridge was used for the measurement of thermal changes of magnetic susceptibility in weakly magnetic rocks (e.g. calcite) (Hrouda, 1994). Low field variation of magnetic susceptibility was used to see its effect on anisotropy of magnetic susceptibility (AMS) (Hrouda, 2002). Magnetic susceptibility and AMS together with the intensity, inclination and declination of the natural remanent

magnetisation have formed the basis of high resolution rock magnetic analyses (Hall and Evans, 1995; Liu and Liu, 1999; Robin et al., 2000).

At present certain magnetic methods and techniques are becoming more known and applied within the petroleum industry, in particular using magnetic susceptibility measurements to predict petrophysical properties such as clay content and permeability (Potter, 2004a; Potter 2004b; Potter et al., 2004; Potter, 2005; Potter, 2007; Ivakhnenko and Potter, 2008; Potter and Ivakhnenko, 2008). Thermomagnetic analysis of the magnetic susceptibility of the permeability controlling minerals can be used to study tight gas reservoirs (Ali et al., 2010). Also magnetic techniques can be used to quantify the effect of core cleaning and core flooding (for permeability determination and formation damage (Potter et al., 2010)).

1.2 Oilfield scale

Mineral scale in hydrocarbon fields is deposited under diverse conditions in the presence of formation water, oil and gas, drilling fluids and surfactants, and can involve low velocity flow in pores and turbulent high velocity flow within tubing (Oddo and Tomson, 1997; Poyet et aI., 2002). Deposition of scale by alteration of fluid chemical and thermodynamic equilibria is caused by several different phenomena. In permeable sediments within oil-producing formation and tubing the scale forms due to:

• Pressure-induced reactions, such as depressurising of the fluids (e.g. release of CO_2 and formation $CaCO_3$ scale).

• Thermal gradient reactions (Phillips, 1991) with fluid migration through a temperature gradient.

• Mixing of incompatible injected (SO_4- rich fluids) and reservoir (Br^{2+}, Ca^{2+} and Sr^{2+} rich fluids) fluids and/or sediment matrix (Economides et al; 1993).

• Evaporation induced reaction, such as halite (NaCl) deposition at low water cuts.

The main consequence of scaling is gradual constricting of fluid flow leading in the worst scenario to total blockage. This process essentially changes the permeability of the sediments through plugging the pore throats and the deposition of solids in the pores of the reservoir rock (Moghadasi et al., 2002). Scale can also be deposited in production facilities such as tubing, especially perforated intervals, downhole pumps and tanks, etc. For example, data from the North Sea oil province indicates that approximately 5.5% of the wells were severely plugged by different scales and fines (Jordan et al., 2001). Scale accumulation compromises safety causing damage to production equipment, such as electrical submersible pumps (ESP) (Mackay, 2003; Voloshin et al., 2003) and by being a health hazard, because some scales are naturally occurring radioactive materials (NORM) (Oddo et al., 1995; Hartog et al., 1996). Other scale-related problems include macro-aggregate corrosion and fluid contamination, especially at the petrochemical manufacturing phase. The potential consequences of scale and corrosion-induced failures of transport, storage and treatment facilities are economically and ecologically catastrophic (Becker, 1988).

The scaling problem is widespread and common for all worldwide oil provinces on-land and offshore. It can occur at any point in upstream and downstream production systems at which there is supersaturation. As a consequence it can cause considerable losses to oil and gas production, requires expensive work to remove the scale and prevent its reappearance, and also compromises safety. The total value of effective scale treatment during field exploitation is estimated in millions of US dollars per year (Jordan et al; 2001), which can have a considerable economical impact in global terms.

To resolve scale-related problems often requires a complex approach, such as an integrated scale control or management program (e.g. Hinrichsen and Brindle, 1989; Hinrichsen and Edgerton, 1998; Mackay and Jordan, 2003). The integrated scale management program (ISMP) is addressed as part of field and/or reservoir management in the CAPEX and OPEX phases (Jordan et al., 2001). The major stages of the ISMP in

the reservoir sediment formation, in the well, and at surface include: scale detection, identification, prevention (inhibition), removal, monitoring and prediction.

Scale detection is an important stage in order to determine the early occurrence of scale deposition. In the identification stage the determination of the scale's location, concentration, and composition are required. At present the conventional methods of scale detection are physical observation or monitoring the dynamics of abnormal fluid pressure drop and hydrocarbon production decline (Poyet et al., 2002). A few on-line and in-situ methods have been proposed in the literature such as electrochemical (Emmons et al., 1999; Moritz and Neville, 2000), ultrasonic (Gunarathne and Keatch, 1995), nuclear (Wyatt et al., 1994; Bamforth et al., 1996), or nuclear attenuation methods (Allen and Walters, 1999; Poyet et al., 2002). However, many of the above mentioned techniques have very limited use and none of them are in common practice.

Scale inhibition is typically conducted by chemical treatment. Scale removal can be accomplished also by mechanical methods (Cowan and Weintritt, 1976). However, it has been observed that since scale may have multiple components, scale inhibition and removal may be selective and not destroy all of the scale present (Allen and Walters, 1999; Rousseau et al; 2001; Nasr-El-Din and Al-Humaidan, 2001). Magnetic treatment of fluids and scales might provide an alternative option for the prevention and removal of multiple scales (Farshad et al., 2002). Although there are many claims to the effectiveness of magnetic scale control devices, there is very little scientific evidence.

Monitoring and prediction (Jordan et al., 1994) of scale are particularly important where scale causes severe operational problems. To guarantee the success of the integrated scale management, a complex approach based on multi-physical principles may be necessary, which could include magnetics for scale detection, identification and monitoring.

1.3 Scale types in the petroleum industry

Scale deposits constitute several forms. In general petroleum scale can be mineral, chemical, or organic type formed as a result of fluid-fluid (and fluid-substrate) interactions leading generally to their supersaturation. Scale mainly deposited from aqueous supersaturated solutions of formation waters is defined as inorganic (Hinrichsen and Edgerton, 1998; Civan, 2000). Organic scale is formed from crude oil compounds.

Structurally, scale can be single phase or multi-phase. For instance, Voloshin et al; (2003) detected scale deposition on electrical submersible pumps (ESP) consisting of calcium and magnesium carbonate, chlorite, quartz and gypsum. In some deposits siderite and iron oxides were also present. Therefore the widespread presence and variety of scale constituents in the petroleum industry represent a complex foundation for scale classification. The main classification criteria include chemical and mineralogical compositions, origin mechanisms, structural forms, spatial-technological distributions and scale treatment methods.

Most inorganic scales can be classified by the anion type in one of the following seven classes:

• The carbonate scales, formed by cations and bicarbonate (HCO_3) ion precipitation in fluids, and include $CaCO_3$ and $FeCO_3$.

• The sulphate scales, formed as a result of precipitation of cations and sulphate ions (SO_4), which include $BaSO_4$, $SrSO_4$, and $CaSO_4$.

• The sulphide scales, formed by cations and sulphide (S_2) ion precipitation, for example FeS, FeS_2, PbS, and ZnS.

• The chloride scales, formed mainly by brine evaporation and sodium (Na) and chloride (Cl) ion precipitation, yielding NaCl.

• The fluoride scales, caused by reaction of cations and fluoride (F_2) ions, including CaF_2 and FeF_2.

• The aluminium-silicon group of scales, formed by reaction of cation-silicon or aluminium-silicon elements, for example $(Mg,Fe)(Si,Al)_3O_5(OH)_4.4H_2O$.

• Native scales, formed exclusively by native cations or cation covalent bonds, including Pb, SiO_2.

1.3.1 Calcium scale group

The two most common types of Ca scale found in hydrocarbon fields are calcium carbonate ($CaCO_3$) and calcium sulphate ($CaSO_4$) (Lasetr et al., 1968; Vetter and Farone, 1987; Todd and Yuan, 1991., Moghadasi et al., 2003a). The occurrence of calcium carbonate scale (Bezmer and Bauer, 1969; Vetter et al., 1987) is of primary origin due to the partial pressure of CO_2, temperature and pH changes of the production fluid, while the formation of calcium sulphate scale is of secondary origin associated mainly with the mixing of soluble incompatible brines of the injection and formation waters (Vetter et al., 1982; Leon and Scott, 1987; Moghadasi et al., 2003b). The necessary components for calcite ($CaCO_3$) scale formation are often present in hydrocarbon field formation waters and the field's associated production systems.

Dissolved calcium occurs in formation fluids in significant concentrations. Normally in the production treatment calcium carbonate scale is typically softer than calcium sulphate scale and tends to be more acid-soluble.

Calcium sulphate scale can be present in three different phases, gypsum ($CaSO_4.2H_2O$), hemihydrate ($CaSO_4.1/2H_2O$), and anhydrite (CaS04). Other calcium scales include $CaMg(CO_3)_2$ dolomite scale, which forms through calcium replaced by magnesium in a solid-solution series. Hydrofluoric acid in a calcium enriched environment tends to form fluorite (CaF_2) scale (Kotlar and Hove, 2003).

1.3.2 Barium scale group

Barium scales are represented by two main mineral constituents: barium sulphate scale ($BaSO_4$) and barium carbonate scale ($BaCO_3$). Barium sulphate, barite, is considered to be the most prevalent scale in the Ba group (Gaffney et al., 1988; Jordan et al., 1994; Graham et al., 1997). Barium sulphate scale forms by the mixing of two types of incompatible waters (e.g. formation water and injection water) with respective Ba cations and SO_4 anions leading to $BaSO_4$ precipitation. Barium carbonate scale occurs primarily due to CO_2 gas decompressing in Ba saturated formation waters. Altogether, the Ba scale group is considered to be the most stable against chemical removal agents.

1.3.3 Iron scale group

The Fe scale group consists of six anion classes: carbonates, sulphides, sulphates, oxides, hydroxides and fluorides. It is the most varied of all the scale groups. The Fe scales form compounds with two-valence ferrous and three-valence ferric iron. Fe scales are less ubiquitous in petroleum fields than Ba and Ca group scales. Fe scale deposition is, however, a significant hydrocarbon field problem that has been ignored for the most part because of the considerable difficulty in its conventional identification, and its prevention.

Siderite scale ($FeCO_3$) has a primary origin due to partial pressure drops of CO_2, temperature and pH changes of the iron enriched production fluid (Przybylinski, 2001;

Voloshin et al., 2003). Sulphide scales such as troilite (FeS), pyrrhotite ($Fe_{1-x}S$), pyrite (FeS_2), and greigite (Fe_3S_4) are formed in the presence of a high concentration of hydrogen sulphide (Przybylinski, 2001). It is assumed also that mackinawite, $FeS_{(1-x)}$, can be present in sulphide scales (Przybylinski, 2001; 2003). Orthorhombic marcasite (FeS_2) is observed to be more unstable than cubic pyrite when exposed to air, forming a range of iron sulphate hydrates such as szomolnkite ($FeSO_4.H_2O$) and melanterite ($FeSO_4.5H_2O$) (Deer et al., 1966; Weast and Astle, 1978).

Ferrous sulphide scale may be removed by dissolution in acid when it causes a problem in downhole equipment. Unfortunately, acid removal is not efficient as iron sulphides can oxidize to magnetite and hematite, thus transforming to minerals that are difficult to dissolve. In addition, iron sulphides have the tendency to become oil-wet scale constituents, creating a protective organic coating that resists attack by the water-soluble acids. Thus, the scale from the iron group becomes the hardest to remove and is often insoluble.

Ferric hydroxide ($Fe(OH)_3$) most commonly occurs as a result of mixing of iron ions in the source waters with the reservoir fluids causing formation damage (Krueger, 1986).

Alternatively, ferric hydroxide is generated during acidic stimulation (Crowe, 1985). Acid injected into the formation dissolves iron-containing minerals such as chlorite, siderite, and hematite causing precipitation of low solubility $Fe(OH)_3$.

1.4 Precipitation and Scaling

The precipitation process makes use of the solubility product of a compound containing an ion that is considered deterimental. If an excess of an ion is introduced, the solubility is slightly depressed.

One of the fundemental principles of precipitation is that the size of the precipitate increases if the chemical reaction is encouraged to happen on previously precipitated particles. Thus the precipitation of scale-forming minerals occurs by the nucleation and growth of crystals.

Scale is that portion of the precipitate which attaches itself to a fixed surface, such as the side of tubing or the internal surface of the rock. It is known that nucleation in formation brines is considered to be heterogeneous, so it is possible that scale will form directly on the surface. Scaling is usually associated with precipitation. It is recognized that precipitation does not necessarily lead to scaling, but scaling is often thought to result from precipitation followed by the adhering of precipitates to the surrounding surfaces.

1.5 Scaling Probability

Solubility is defined as the limiting amount of solute which can dissolve in solvent under given physical conditions. The mineral salts dissolved in water are present in their ionic form. The solubility of a particular solid, however, is true only when the numbers of cations are equal to the number of anions or, when the solution is stoichiometrically balanced. If an excess of either ion is introduced, the solubility is depressed markedly.

As the solubility of salt is decreased, the supersaturation becomes a disproportionately higher percentage of total salt in the solution. The supersaturation represents the amount of salt present in excess of the solubility and thus represents the amount available for precipitation from solution until the solution returns to its equilibrium state. The precipitate may remain in suspension or form a coherent scale on a surface.

The main factors that may influence scaling probability in the oilfield are:

1- Pressure drop:

The water produced from formation to the wellbore, and then to surface is subjected to a continuous reduction in pressure. As the pressure is reduced, dissolved gases escape. Loss of one of these gases, carbon dioxide, disturbs the bicarbonate-carbonate equilibrium, increasing the probability of forming a flow-restricting deposit of calcium carbonate. The solubility of calcium sulphate in water increases with pressure. The effect of increased pressure results in reduction in the size of calcium sulphate molecule.

2- Temperature change:

The water produced from formation to the wellbore and then from the wellbore to surface is subjected to a continuous reduction in temperature. This temperature drop favours stability. Conversely, the solubility of calcium carbonate decreases with increased temperature.

Solubility of gypsum, $CaSO_4.2H_2O$ is maximum at 43^oC and falls off as the temperature is increased above or reduced below this value. Barium sulphate solubility increases with temperature but barium sulphate is still quite insoluble even at higher temperatures.

Once produced fluids are above ground, temperature influences take on added importance because many produced brines are heated to break an emulsion, resulting in less stable water with respect to both calcium carbonate and calcium sulphate scale.

3- Mineral Characteristics Change:

A change in mineral characteristics could lead to scale due to the total ionic strength of the solution containing the scaling ions. Water is either trying to dissolve what it contacts or trying to precipitate what has already been dissolved.

Total dissolved salts of water containing calcium carbonate are an important factor. The solubility of calcium carbonate increases with the increase of total dissolved salts.

The presence of NaCl or dissolved salts other than calcium or sulphate ions increases the solubility of gypsum or anhydrite. However, if the pressure becomes high enough; salt water has no greater solubility for calcium sulphate than does distilled water.

The solubility of barium sulphate in water is also increased by foreign dissolved salts. The tendency for water to precipitate calcium sulphate or barium sulphate increases with an increase in sulphate content.

4- Change in mineral characteristics due to mixing of incompatible waters:

A change in mineral characteristics could lead to scale due to mixing of incompatible waters. Waters of widely varying mineral content are mixed in the producing well after injection water breakthrough. In many cases, instability with respect to calcium carbonate, calcium sulphate and barium sulphate is a direct result of this commingling action. In the North Sea fields it is often the case that when two incompatible waters, formation water containing barium ions and sea water containing sulphate ions, are mixed together, barium sulphate scale is formed.

Due to the ongoing nature of a waterflood, water that has not been in contact with rock is continuously being injected and so the system never comes into complete chemical equilibrium. Chemical reactions continuously drive the system towards equilibrium, but never get there. Furthermore, due to changes in pressure, temperature and mineral characteristics, the equilibrium itself is always shifting.

1.6 Scale Prediction

Scale does not form except from a solution which is supersaturated at the point of crystallization. In order to predict the formation of certain type of scales, it is necessary to have accurate information on their solubilities. Successful scale prediction can be made by calculating the solubility product under a wide range of thermodynamic conditions. These thermodynamic conditions constitute mainly pressure, temperature and solution composition variables. Effects of abundant ions of solution composition are only considered to predict the solubility. Solubility calculation procedures indicate the degree of scaling tendency or possibility of scale formation. A calculated scaling tendency in an existing system should be considered an indication of a problem of scale formation. Solubility calculations are an extremely valuable tool, but their absolute value will be greatly influenced by the user's experience and judgement. It is obvious that acquiring meaningful measurements of solubilities is an important factor for the prediction of a scale.

Investigations have been made to enable the prediction of calcium carbonate, calcium sulphate, barium sulphate and strontium sulphate scale which are very much common in the oilfield operations. Basically, the solubility data indicate that calcium carbonate scale deposition increases with temperature and pH increase, with a decrease in solubility and with a decrease of carbon dioxide gas partial pressure.

1.7 Scale Inhibitor Treatment:

Scale inhibitors are chemicals that can be used to prevent scale precipitation in the production system.

A range of techniques can be used in order to introduce scale inhibitors at the most appropriate sites. Basically, this chemical treatment can be performed by one of three techniques:

1- Continuous feed.

2- Batch feed.

3- Squeeze.

In a continuous feed technique, the chemicals are injected continuously through a dedicated chemical injection capillary in the production well, or via the gas lift mandrel.

Scale inhibitors can also be injected continuously topsides to deal with scale developing in the surface facilities.

In a batch treatment, chemical treatment is introduced in a batch at regular intervals. Generally, the chemicals are adsorbed to the system at the time of treatment and then followed by desorption to provide the necessary treating concentration. However, the retention of scale inhibition on tubular, etc. is generally poor, that this technique is not used, and continuous injection is used instead.

When scale starts developing at the bottom of the well as a result of water breakthrough, it may become necessary to introduce chemical treatment down-hole. Relatively low concentrations of water soluble, organic scale inhibitors are known to reduce the rate of scale formation in and around the bottom of a producing well. Consequently, the squeeze technique is started which is considered to be a convenient way to apply an inhibitor downhole in the producing formation, in which a large dose of an aqueous solution of scale inhibitor is displaced into the formation to be adsorbed onto the formation surface. Rock surfaces provide much greater retention than do metal surfaces, especially when there are clay minerals present. When the well is returned to

production, flow of fluid past the adsorbed chemical causes the inhibitor to slowly desorb into the produced fluid to give the necessary treating concentration, which is sufficient to stop scale formation for a period of several months. When the residual concentration of inhibitor drops below a certain threshold level, the squeeze treatment is repeated for another cycle of several months. Long-term success of a squeeze treatment depends on continued slow desorption of inhibitor from the reservoir rock.

Success in downhole chemical treatment to control scale depends upon the availability of the required scale inhibitor at the time when the crystallites first begin to form in the formation. This necessitates the continuous treatment introduced upstream of the point of crystallite formation. It is known to be generally desirable that a scale inhibitor be produced in low concentration within the produced water. It is observed that most of the adsorbed inhibitor on the rock is quickly released.

1.8 Research Objectives

The research project is an experimental investigation into the magnetic properties of reservoir fluids and minerals related to scale. The build-up of scale is an important process in oil and gas reservoirs (similar to the accumulation of scale in a kettle), and can have a damaging effect on the flow of fluid in reservoir rocks. An understanding of the magnetic properties of scale, and establishing new environmentally friendly techniques to detect and monitor scale build-up, are key objectives of this research, and could potentially have very important economic consequences for the oil and gas industry.

1.9 Organization of the Dissertation

Chapter 1 is the introductory chapter for the application of magnetic susceptibility measurements in petroleum industry, oilfield scale and its types in petroleum industry. Chapter 1 is also used summarize scaling precipitation, probability, prediction, and inhibitor treatment.

Chapter 2 describes general aspects of magnetism. The magnetic classes and properties are described in relation to the petroleum industry. The main magnetic methods and experimental procedures are detailed.

Chapter 3 details the application of magnetic susceptibility to oilfield fluids analysis, the main magnetic properties of petroleum reservoir fluids such as brine, crude oil, scale inhibitors, and solute composition. In addition, the magnetic susceptibility of high and low scaling tendency brines over time also has been measured.

Chapter 4 explains the possibility of detection and monitoring of injection water breakthrough. The main advantage of this technique is the reduction in time from weeks to minutes in detecting injection water breakthrough in hydrocarbon production.

Chapter 5 details the magnetic properties of the reservoir scale minerals. In particular, the use of magnetic hysteresis measurements for identifying and quantifying the mineral in reservoir scale samples and drawn of theoretically model templates of various concentration of scale mineral mix. Also a laboratory based thermomangetic analyses on a number of different reservoir scale mineral samples have been measured.

Chapter 6 All innovative aspects of the thesis and recommendations for further work are also summarised in this chapter.

CHAPTER 2: MAGNETIC SUSCEPTIBILITY AND HOW IT IS MEASURED

2.1 Introduction

This chapter contains a survey of published work on mineral magnetic susceptibility with focus on how it relates to the oil industry. The chapter will also explore several laboratory based methods for measuring the magnetic susceptibility of reservoir rocks at various temperatures.

The basic properties, such as magnetic susceptibility, magnetic classifications, and magnetic hysteresis, of the various constituents of petroleum reservoirs are described.

2.2 Categorization of magnetic properties in relation to rock minerals associated with hydrocarbons.

Minerals are categorised as magnetic if they cause magnetic induction in the presence of a magnetic field. This categorisation based on their interaction (strength, and type) with the magnetic field is the basis of the classification. Mineral magnetism (M) is related to the applied field strength (H) by the equation

$$M = \chi H \qquad 2.1$$

where χ is the magnetic susceptibility of the material. It is a dimensionless quantity which expresses the efficiency with which a substance may be magnetized.

Universally, all mineral substances exhibit magnetic susceptibility at temperatures above absolute zero (Tarling and Hrouda, 1993), and this information has been used to detect mineral deposits and other natural resources. The principal types of interaction of a substance with a magnetic field are classified into five major divisions: diamagnetism, paramagnetism, ferromagnetism, ferrimagnetism and antiferromagnetism.

2.2.1 Diamagnetism

Diamagnetism is produced when electrons precess and oppose an applied magnetic field. This phenomenon is observed in the orbital motions of electrons. When a magnetic field is applied to a substance in which the electron shells are paired with an even atomic number, the electron spins and produces a negative magnetisation in the opposite direction to that of the magnetic field.

The magnetic susceptibility in diamagnetic materials (magnetisation divided by the applied field) is always negative.

In zero magnetic field the electron shells of an atom have no net dipole. Consequently, once the external magnetic field is removed electron spins randomise and any diamagnetic effects disappear.

2.2.2 Paramagnetism

The paramagnetic susceptibility usually is larger than the diamagnetic contribution at standard temperature and in moderate magnetic fields. Paramagnetic susceptibility is influenced by reduced temperatures (much less than 100K) or in cases where the magnetic field is very high (Moskowitz, 1991). One of the most explicit atoms with unpaired electrons is iron, and paramagnetic susceptibility is often proportional to the total iron content of the substance.

The atoms or ions in this class of materials have a net magnetic moment due to unpaired electrons in their partially filled orbits. Many salts of transition elements are also paramagnetic. The individual magnetic moments do not interact magnetically in transition metal salts, the cations have partially filled d shells, and the anions cause separation between cations. This weakens the magnetic moments on neighboring cations (Spaldin, 2003). The Langevin model states that each atom has a magnetic moment which is randomly oriented as a result of thermal energies (Langevin, 1905). Therefore in zero applied magnetic field, the magnetic moments point in random directions. When a field is applied, a partial alignment of the atomic magnetic moments in the direction of the field results in a net positive magnetization and positive susceptibility (Tarling, 1983). At low fields, the flux density within a paramagnetic material is directly proportional to the applied field, so the susceptibility $\chi = M/H$ is approximately constant. Unless the temperature is very low or the field is very high, paramagnetic susceptibility is independent of the applied field. Most iron bearing carbonates and silicates are paramagnetic. At normal temperatures and in moderate fields, the paramagnetic susceptibility is small. However the strength of paramagnetic susceptibility depends on the concentration of paramagnetic minerals present in the sample. In most cases, it is larger than the diamagnetic susceptibility contribution. In samples containing ferromagnetic/ferrimagnetic minerals, the paramagnetic susceptibility contribution can only be significant if the concentration of ferromagnetic/ferrimagnetic minerals is very small.

The efficiency of the magnetic field in aligning the magnetic moments is opposed by the randomizing temperature effects. This results in a temperature dependent paramagnetic susceptibility, when the intensity of a paramagnetic response to an external field is decreasing as the reciprocal of temperature.

For a substance to have paramagnetic properties, its component atoms or ions must possess a permanent magnetic moment. These moments are a result of angular

momentum of unpaired electrons in partially filled orbitals. With the application of an external magnetic field a torque acts upon the dipoles, forcing them into a uniform alignment, which is parallel to the direction of the applied magnetic field. (This parallel alignment results in a net positive magnetisation and positive magnetic susceptibility). The alignment of the magnetic moments is only partial due to the randomising effect of the thermal motions (Tarling, 1983). Upon the removal of an external field the paramagnetic magnetisation is rapidly randomised by these thermal effects (Figure 2.1). Therefore, the extent of paramagnetic alignment is a balance between the absolute temperature and the strength of the magnetic field. In contrast to paramagnetism, diamagnetism is effectively temperature independent. Therefore with increasing temperature the diamagnetic properties dominate the overall magnetic properties of a material. In paramagnetic and diamagnetic substances the magnetisation is induced and conditionally temporal, because the observed net magnetic moment disappears upon removal of the applied field.

The resulting magnetisation is termed the spontaneous magnetisation (Msp). The spontaneous magnetisation is the net magnetisation that exists inside a uniformly magnetised microscopic volume in the absence of a magnetic field. The magnitude of Msp is dependent on the spin magnetic moments of electrons at temperature 0 K. A related term to Msp, which can be measured in the laboratory, is the saturation magnetisation (Ms).

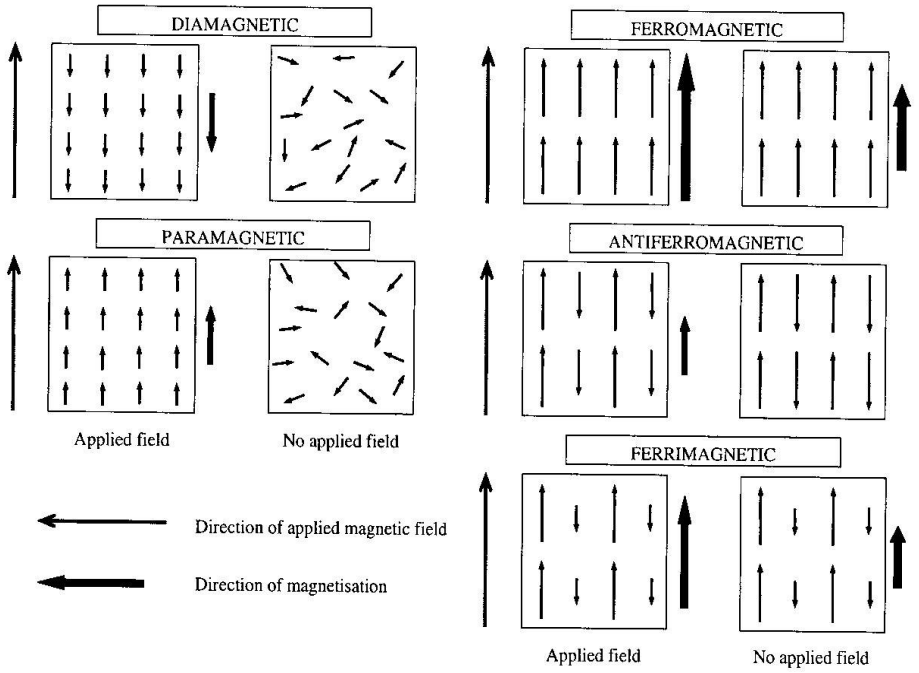

Figure 2.1: Diamagnetic, paramagnetic, ferromagnetic, antiferromagnetic and ferromagnetic classes of substances. Modified after Tarling and Hrouda (1993).

2.2.3 Ferromagnetism

Ferromagnetic materials behave in a similar way to paramagnetic materials forming net magnetic moments that are parallel to the direction of an applied field. The atomic magnetic moments in ferromagnetic materials exhibit very strong interactions resulting in a parallel or antiparallel alignment of their magnetic moments. This produces a strong magnetization even in the absence of an applied magnetic field, then after the field is removed ferromagnetic materials retain a remnant of the acquired magnetism. This effect was postulated to be caused by the presence of a molecular field within the ferromagnetic material, suggesting that magnetic materials consists of small regions called magnetic domains within which all the atomic magnetic moments are aligned in the same direction. On the application of an external applied field, the response of these

magnetic domains to the applied field determines the magnetic susceptibility of the material.

Ferromagnetic materials present in reservoir rocks and the Fe-Ti oxides form the majority of them including goethite (an iron oxyhydroxide), pyrrhotite, greigite (iron sulphides), and hydrated iron sulphate which results from the hydration of pyrite and marcasite (relatively unstable minerals when exposed to air). As ferromagnetic materials are heated, the thermal agitation of the atoms implies that the degree of alignment of the atomic magnetic moments decreases and hence the saturation magnetization also decreases. Eventually the thermal agitation becomes so great that the material becomes paramagnetic. The temperature of this transition is called the Curie temperature (T_c), or Curie point, the temperature above which a ferromagnetic substance loses its ferromagnetism and becomes paramagnetic. Above the Curie temperature, the susceptibility varies according to the Curie-Weiss law. The Curie-Weiss law describes the magnetic susceptibility of a ferromagnetic in the paramagnetic region above the Curie point.

In ferrimagnetic substances the exchange coupling mechanism causes adjacent magnetic moments to align anti parallel, but not exactly of the same magnitude. The ferromagnetic structure is composed of two magnetic sublattices separated by the anions. Thus, the exchange interactions are mediated by the anions, normally oxygen. In such case the exchange interaction is indirect or superexchange. The indirect interaction results in an anti parallel alignment of spins between two sublattices with magnetic moments (Figure 2.1). This imbalance is a product of the two lattices having different ionic populations or different crystallographic structures.

2.2.4 Ferrimagnetism

Ferrimagnetism is only observed in compounds, which have more complex crystal structures than pure elements. The exchange interactions enable the parallel alignment of atomic magnetic moments in some parts of the crystal and anti-parallel alignment in others (Figure 2.1d). These break down the material into magnetic domains. Ferrimagnetic materials are very similar to ferromagnetic materials in terms of spontaneous magnetization and Curie temperatures. After the applied magnetic field is removed ferromagnetic and ferrimagnetic materials acquire and retain remanent magnetisation. Magnetite is an example of a ferrimagnetic material.

The two sublattices formed in ferrimagnetic materials have substantially different orientation and value of magnetic moments leading to a dominant net magnetisation, which is consequently weaker than for a ferromagnetic material. After the applied magnetic field is removed ferromagnetic and ferrimagnetic materials acquire and retain remanent magnetisation. However, in general ferromagnetic and ferrimagnetic materials have different magnetic ordering.

2.2.5 Antiferromagnetism

Antiferromagnetic materials cause the antiparallel alignment of the atomic magnetic moments to happen during the exchange interactions. This is in contrast to ferromagnetic materials where the atomic magnetic moments are aligned in parallel. If the magnitude of atomic magnetic moments are equal and they are completely opposite in direction, this will result in a net zero spontaneous magnetization and the material is a perfectly compensated antiferromagnetic. Such materials have zero remanence, no hysteresis, and a small positive susceptibility that varies in a peculiar way with temperature. Ilmenite is such an example.

When the cancelling of the magnetic moments is not complete a small net moment is observed and the system is described as imperfect antiferromagnetism. This imbalance can have a number of possible origins such as lattice defects, crystal impurities or the spin-canting when the cation-anion-cation exchange bonds are slightly tilted ($< 1^{o}$) or canted. Canted antiferromagnetism exhibits the typical magnetic characteristics of ferromagnetic and ferrimagnetic materials. Hematite is an example of a canted antiferromagnetic mineral.

Unlike ferromagnetic materials which show paramagnetic behaviour above their Curie temperature, the antiferromagnetic materials show paramagnetic behaviour above Néel temperature (T_N). This is the temperature above which an antiferromagnetic material becomes paramagnetic. The paramagnetic behaviour is indicated with a negative intercept indicating negative exchange interactions.

2.3 Magnetic Susceptibility

2.3.1 Theory of Magnetic Susceptibility

Magnetic susceptibility is the ratio of the intensity of magnetisation to the applied magnetic field strength. Mathematically the mass susceptibility is given as:

$$\chi = J/H \qquad 2.2$$

where J is the magnetisation per unit mass, and H is the magnetic field strength. The volume susceptibility is given as:

$$\chi_v = M/H \qquad 2.3$$

where χ_v is the volume susceptibility and M is the magnetisation per unit volume. The third type of susceptibility is the molar susceptibility defined as:

$$\chi_{mol} = M\chi = M\,\chi_v/\rho \qquad 2.4$$

where ρ is density and M is molar mass in Kg/mol.

Magnetic susceptibility is dimensionless while J, M and H are in amperes per meter (A/m). Magnetic quantities are often given in c.g.s. units in literature. However, converting quantities between SI units and c.g.s. units can be confusing as both H and B (the magnetic induction) have the same physical dimensions in SI system but are different in the c.g.s. system. According to Hearst et al (2000) the difference is due to the way force relates to charge and current in the two systems. For the purpose of clarification the equations will be given in SI units while their equivalent equations in c.g.s units will be in brackets.

Following equations 2.2 and 2.3, there is a linear relationship between magnetisation and magnetic field strength and this implies that a linear relationship also exists between magnetic induction (B) and field strength (H) as shown in the following:

$$B = \mu H \quad [B = \mu H] \qquad 2.5$$

where μ is the magnetic permeability and it is dimensionless both in SI and c.g.s units. The magnetic permeability (μ) is mathematically expressed as:

$$\mu/\mu_o = 1+ \chi \qquad [\mu = 1 + 4\pi\chi] \qquad 2.6$$

Where μ_o is free air magnetic permeability. Thus μ/μ_o in SI is the same as μ in c.g.s. Thus, converting susceptibility from c.g.s to SI units is simply done by multiplying the c.g.s. susceptibility value by 4π. Magnetic induction (B) is measured in a unit called Tesla (T) and its dimension in SI units is Newton per ampere-meter (N/Am). Two more expressions can be used to show the relationship between B, J and H as follows:

$$B = \mu_o (J + H) \qquad [B = H\ 4\pi J] \qquad 2.7$$

$$B = \mu_o (1+\chi)\ H \qquad [B = (1+4\pi\chi)\ H] \qquad 2.8$$

Generally materials are paramagnetic, diamagnetic or ferromagnetic (ferro - and ferrimagnetic). Materials with positive susceptibility (χ) such that $(1+\chi) > 1$ are called paramagnetic materials. That implies that the applied magnetic field is strengthened by the presence of the material. Molecular-wise, it is the nature of the electrons in the material that determines the magnetic properties of the material. Since free electrons add to magnetic forces, a material becomes paramagnetic when the number of free unpaired electrons is high. In the situation where susceptibility (χ) is negative such that $(1+\chi) < 1$ the material is said to be diamagnetic. In this case the magnetic field is weakened by the presence of the diamagnetic material- molecular-wise the material lacks free unpaired electrons.

The measurement of magnetic susceptibility is achieved by quantifying the change of force felt upon the application of a magnetic field to a substance. For liquid samples it is measured from the dependence of the natural magnetic resonance (NMR) frequency of the sample on its shape or orientation. Ivakhnenko and Potter (2004) successfully used other methods to measure fluids and ninerals susceptibilities, for example, Sherwood Scientific Magnetic Balance (MSB) Mark I. The susceptibility values of common reservoir rock/ minerals as summarised by Potter et al (2004) and Hunt et al (1995) is given in table 2.1.

Type of mineral	Mineral	Mass Magnetic Susceptibility ($10^{-8}m^3/Kg$)	Volume Magnetic Susceptibility (10^{-6} SI)
Diamagnetic minerals	Quartz	-0.55	-13 to -17
	Calcite	-0.3 to -1.4	-7.5 to -39
	Kaolinite	-2.0	-50
Paramagnetic minerals	Illite	15.0	410
	BVS Chlorite	13.6	
	Pyrite	2.0	35 to 5,000
Ferrimagnetic minerals	Magnetite	20,000 to 110,000	1,000.000 to 5,700,000

Table 2.1: Magnetic Susceptibility of Common Reservoir Minerals and Fluids.(After Potter et al 2004 and Hunt et al 1995)

2.3.2 Factors that affect the magnetic susceptibility

In natural rocks the susceptibility depends on a variety of factors, among them the composition of the actual rock, the shape and distribution of the ferromagnetic minerals, as well as possibly magnetic grain interaction and sample shape.

Important factors other than those mentioned above are:

(1) Magnetic Field Strength

It has been found that the susceptibility of ferromagnetic materials increases with an increase in the applied field up to a point (typically ~150 Oe for magnetite-bearing rocks) and then decreases again.

Worldwide measurements of paleointensities suggest that the amplitude of the Earth's magnetic field has not changed substantially over most of geological history (Tarling, 1971). Thus, any rocks which are used will have come under the influence of this field, and therefore it is advantageous to measure susceptibility in applied fields of the order of magnitude of the present field. In such low fields susceptibility can be considered to be nearly, but not completely, independent of the field.

(2) State of Magnetization

Contradictory evidence has been published on the effect of the remanent magnetization of a sample on its susceptibility. However, it is found that, generally, the susceptibility decreases with increasing remanent magnetization (Strangway, 1967).

(3) Grain Size

For a given material the susceptibility tends to increase with increasing grain size. This is especially important for diameters less than 50 microns and the rate of increase of χ is greatest when this size approaches a value determined by the transition from single-domain to multi-domain structure, since single-domain grains are magnetically hard and so tend to have low susceptibilities. Multi-domain grains are easier to magnetize since it is easier to move domain walls than to rotate magnetization vectors.

(4) Temperature

The changes in susceptibility produced by changes in the temperature depend on the type of material used. For diamagnetic materials there is no temperature dependence, whereas paramagnetic substances obey the Curie law $\chi = C/T$, where χ is the susceptibility per mol, T is the absolute temperature and C is a constant. Ferromagnetic materials are strongly temperature dependent. For single crystals, the susceptibility generally decreases with increasing temperature until the Curie temperature, T_c. Above T_c the materials are paramagnetic, obeying the Curie-Weiss law $\chi = C'/(T-T_c)$ where C' is a constant.

Since rocks are much more complex than a single crystal, the susceptibility variation as a function of temperature fits no simple expression. It has been found, however, that susceptibility generally increases on heating, occasionally by a large factor, before falling off sharply at the Curie temperature. Generally, if this increase is reversible, it will be due to the 'Hopkinson Effect' (Nagata, 1961 p.143).

(5) Previous Magnetic History of the Rock

This depends largely upon the age and mode of formation of the rock, and hence its thermal history and upon the origin and subsequent modifications of its remanent magnetism.

(6) Mineralogical Composition

The presence of ferromagnetic minerals other than magnetite, and hence with different susceptibilities will, of course, affect a susceptibility estimate based upon magnetite content alone.

Another mineralogical factor is crystalline anisotropy, which can give rise to susceptibility anisotropy. This is generally negligible in cubic minerals such as titanomagnetite, but can be important when the susceptibility of rocks containing predominantly pyrrhotite or minerals in the ilmenite-hematite series is to be measured, as these minerals exhibit strong crystalline anisotropy with the minimum susceptibility being directed perpendicular to the basal plane of the crystal. In an assemblage of particles the directions of the axes of the susceptibility ellipsoid (which corresponds to the property of anisotropic susceptibility as a second-rank tensor) are not necessarily randomized, so that crystal anisotropy may have caused the remanent magnetization direction in rocks containing the above minerals to be deflected from that of the original magnetizing field.

(7) Petrological Characteristics

Factors such as homogeneity in rock composition, the presence of fractures, or the degree of metamorphism, may have varying influence on the value of bulk susceptibility. Again an important factor can be susceptibility anisotropy, as this may be

caused not only by crystalline anisotropy, but also by anisotropy of shape; i.e., elongated ferromagnetic grains can have a shape controlled direction of remanence even when crystalline anisotropy is negligible. Hence anisotropy in the bulk rock susceptibility may be caused by non-random packing of the grains. While igneous rocks are usually magnetically isotropic, the susceptibility of some sedimentary rocks as measured parallel to the bedding planes can be appreciably different from that measured perpendicular to it.

2.3.3 Initial magnetic susceptibility at room temperature

The mass magnetic susceptibilities of diamagnetic minerals possess relatively lower magnitudes compared to the paramagnetic and ferrimagnetic classes (Figures 2.2 and 2.3).

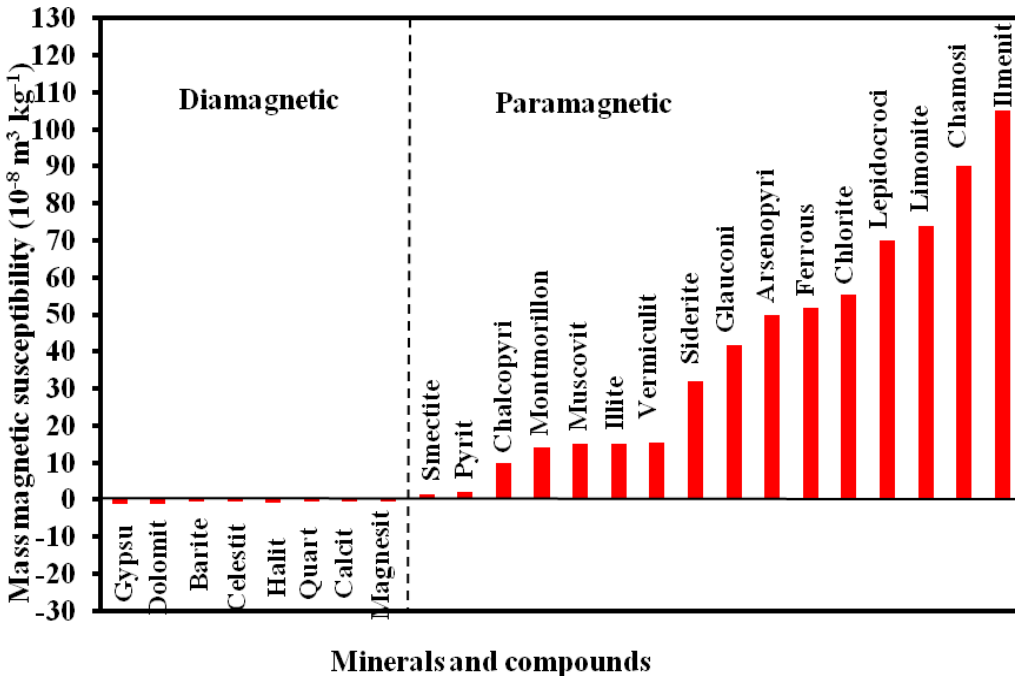

Figure 2.2: Mass magnetic susceptibility of diamagnetic and paramagnetic minerals related to hydrocarbon reservoirs and their sedimentary environment (Ivakhnenko, O.P., 2006 thesis).

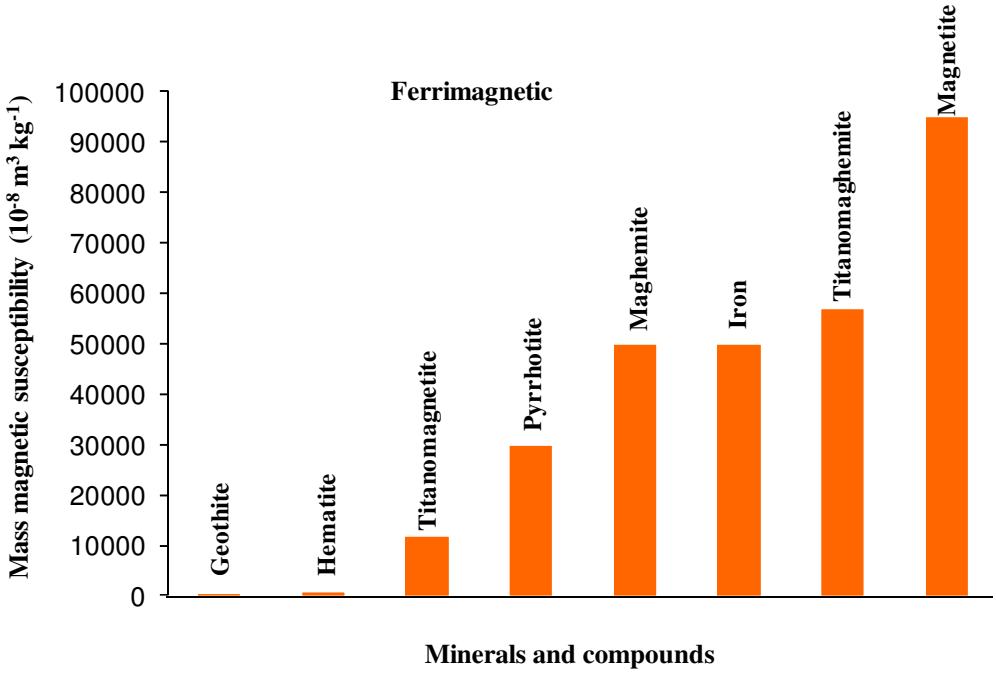

Figure 2.3: Mass magnetic susceptibility of ferrimagnetic minerals (including ferro/ferri/antiferro) related to hydrocarbon reservoirs and their sedimentary environment (Ivakhnenko, O.P., 2006 thesis).

.

Primary magnetic susceptibility *(χ)* or low-field (L_{fld}) magnetic susceptibility (χ_{Lfld}) is measured normally in a low steady field (1 mT). It can also be measured in a low alternating magnetic field. The initial susceptibility as detailed in Section 2.3.1 is defined as the ratio of the magnetisation to the applied magnetic field. It is also the gradient of the magnetisation curve in a magnetic hysteresis loop.

The magnetic susceptibility that is usually measured in the laboratory by the most standard equipment is the extrinsic or apparent initial magnetic susceptibility *(χ_o)* (Moskowitz, 1991), which is different from the intrinsic magnetic susceptibility (χ_i). The difference is due to the effects of substance self-demagnetisation. Hence, the intrinsic susceptibility is the "true" magnetic susceptibility after removal of the effects of internal demagnetising fields in the substance.

Inside a magnetic mineral the applied field (H) is modified by the demagnetising field within the mineral resulting from surface charges. The magnitude of the demagnetising field is N_dM, where N_d is the demagnetising factor, and M is the magnetisation. Consequently, inside the grain the internal magnetic field H_i is:

$$H_i = H - N_dM \qquad 2.9$$

The magnetisation is given by

$$M = \chi_i H_i \qquad 2.10$$

Therefore, extrinsic magnetic susceptibility has the following relationship to the intrinsic susceptibility:

$$\chi_o = \chi_i /(1+N_d \chi_i) \qquad 2.11$$

For strong ferromagnetic and ferrimagnetic materials, such as magnetite, $N_d \chi_i > 1$.

Since the magnitude of the measured susceptibility also depends on the volume concentration of the ferromagnetic minerals (C_{ferro}), it is convenient that for ferromagnetic minerals of strong susceptibility, $\chi_o \approx 1/N_d$, so that in most instances the initial magnetic susceptibility is equal to the following

$$\chi_o = C_{ferro}\,\chi_o \approx C_{ferro}/N_d \qquad 2.12$$

In natural samples containing magnetite with spherical grains the demagnetisation factor is near 1/3. Therefore, the approximate volume fraction of magnetite can be estimated as (Thompson and Oldfield, 1986):

$$C_{ferro} \approx \chi_o/3 \qquad 2.13$$

Initial magnetic susceptibility of ferromagnetic and ferrimagnetic fractions is induced due to reversible displacement of mobile domain walls in Multi-Domain grains or magnetic moment rotation in Single-Domain particles. For the Single-Domain grains the low magnetic fields are not very effective in rotating Single-Domain moments. Therefore, the magnetic susceptibilities in Single-Domain and Pseudo-Single Domain particles are usually lower than Multi-Domain grains.

Initial magnetic susceptibility mainly depends not only on ferromagnetic but also on paramagnetic and diamagnetic minerals. In sediments the concentration of ferromagnetic minerals is often so low that the measured susceptibility values reflect changes in non-ferromagnetic minerals such as silicates, carbonates and clays. Therefore Equation 2.13 has to be used with caution for reservoir sediments.

Initial magnetic susceptibility is temperature dependent. In ferromagnetic minerals susceptibility increases below the Curie temperature (Hopkinson peak) before decreasing to 0.

In the case of sediments connected with hydrocarbons the volume magnetic susceptibility depends on the sum of the magnetic susceptibility of the solid (minerals, χ_{sol}), fluid (oil, formation water, χ_{fluid}), and gas (methane, etc χ_{gas}) phases and their general content. Hence, the volume magnetic susceptibility of such sediments is given by

$$\chi_v = (1\text{-}Cp) \sum\chi_{sol(n)} V_n + \chi_{fluid} Cp + \chi_{gas} Cc \qquad 2.14$$

where $\chi_{sol(n)}$ is the volume magnetic susceptibility of mineral component n of the of solid phase, V_n is the volume content of mineral component n in the solid phase, χ_{fluid} is the volume magnetic susceptibility of the fluids in the pore space, Cp is a coefficient of general porosity, χ_{gas} is the volume magnetic susceptibility of gases in the rock that contribute to the saturation of the pore space, and Cc is the coefficient of gas concentration in the rock.

Considering the fact that χ_{gas} has much smaller values of susceptibility (for methane χ_v is -0.008 in 10^{-6} SI units, Kobranova, 1989) in comparison with χ_{fluid} and also taking into account difficulties of making χ_{gas} measurements, Equation 2.14 can be reduced to:

$$\chi_v = (1\text{-}Cp) \sum\chi_{sol(n)} V_n + \chi_{fluid} Cp \qquad 2.15$$

For the case where the fluid phase is absent we have the following equation describing the susceptibility

$$\chi_v = (1\text{-}Cp) \sum \chi_{sol(n)} V_n \qquad 2.16$$

Equation 2.16 shows that the magnetic susceptibility of the solid phase (χ_{sol}) depends on the magnetic susceptibility of individual mineral components of the reservoir matrix composition and porosity. Therefore, the magnetic susceptibility of reservoir matrix, χ_{sol}, is defined as:

$$X_{sol} = -(\chi_n V_n)_{dia} + (\chi_n V_n)_{para/antiferro} + -(\chi_n V_n)_{ferro} \qquad 2.17$$

In reservoir sediments the ferromagnetic and ferrimagnetic or anti ferromagnetic components can be extremely low (or even absent) so that the magnetic susceptibility is dominated by the diamagnetic and paramagnetic components. Note that mass magnetic susceptibility is not dependent on the porosity of the reservoir rock samples.

2.3.4 Measurement of Magnetic Susceptibility.

Susceptibility is a fundamental property of a magnetic material and hence a knowledge of the susceptibility of rocks and its dependence on the mentioned factors form a part of the subject of rock magnetism. In magnetic prospecting for iron and other ores, however, susceptibility is a fundamental consideration in the interpretation of the magnetic anomalies. Because of its dependence on the magnetic field strength, it is necessary, therefore, that for prospecting purposes the magnetic susceptibility be measured in magnetic fields of the same magnitude as that of the earth. Since the magnitude of the earth's field is about 0.5 oe., the susceptibility measured is the initial susceptibility, χ_o.

The magnetic susceptibility of a material can be measured by a number of methods, as summarized below.

1. Balance Method

The Balance Method, used by the earliest workers such as Gouy (1889), Kelvin (1890) and Curie and Chenevesu (1903), measures the susceptibility of dia-, para- and ferromagnetic materials in high fields (≈10 oe.), and has been adapted for temperatures ranging from that of liquid helium to greater than 1000^{o} C.

A consequence of the respective properties of paramagnetic and diamagnetic materials in a homogeneous magnetic field is their behaviour in the presence of a field gradient.

Since induction in a magnetic field increases the flux density in a paramagnetic body it will tend to move into the strongest part of a non-uniform field. Therefore if a paramagnetic specimen is kept in an inhomogeneous field and allowed to move only at right angles to the direction of lines of force, it will be attracted in the direction of the increasing field. With the same arrangement a diamagnetic body would be repelled in the diminishing field direction. This attractive or repulsive force F, is a function of the susceptibility χ of the material and so can be determined from a measurement of F (in terms of a mechanical force). Such methods can be applied to ferromagnetic bodies as well.

In the Curie method the mechanical force is measured by a torsion balance, while in the Gouy method the test material is suspended from one of the pans of a chemical balance and magnetized by a non-uniform field varying from a large value to essentially zero

over the length of the rod, the magnetic force on the specimen placed in the field gradient is then measured in terms of its apparent gain or loss of mass.

2. Ballistic Method

The method is based on the principle that the magnetic flux threading a search coil will change as a result of the movement of the magnetic moment vector of a specimen relative to the coil.

This in turn, induces an electric charge which can be measured with a ballistic galvanometer and is a function of susceptibility. The magnetizing field is provided by a field coil-generally a solenoid if high fields are used, and the flux through the search coil is changed either by altering its geometrical relationship with the coil and specimen or by reversing the polarity of the current through the field coils. To avoid the effects of the geomagnetic field, the axes of the field and search coils are usually set perpendicular to the geomagnetic meridian.

3. Induction Balance

In the Hughes Induction Balance, first developed by Hughes, (1879) and used by Grenet (1930), the magnetizing field is produced by feeding the output of an oscillator to the primary of a double solenoid system. The induced elctro motive force (e.m.f.) in the secondary circuit is nullified before and after introducing the specimen by a compensating coil system in conjunction with a small trimming inductance M. The net e.m.f. due to the specimen is then a measure of its susceptibility.

4. Mooney's Susceptibility Bridge

Mooney's (1952) instrument consists basically of three coils, two of these (A and B) being energized by a 1000 cps alternating current, and the third (C) being positioned between A and B. Coils A and B are so wound that their magnetic fields cancel at the position of coil C. Mutual induction between C and the system A, B then reduce to a minimum. If a magnetic material is introduced between C and one of the other coils, the additional coupling produces a net magnetic field, which is a measure of the susceptibility. The extent of the imbalance is measured by an alternating current bridge as an imbalanced resistance, the bridge being calibrated in units of magnetic susceptibility.

5. Torque Meter

In the torque meter method (Stacey, 1960; King and Rees, 1962; and Stone, 1962) the specimen is suspended in a uniform magnetic field by means of a fine fibre. If the specimen is anisotropic, the axis of greatest susceptibility will tend to line up itself parallel to the field. The deflection is proportional to the small susceptibility difference itself.

6. A.C. Transformer Bridge Method

Although the Torque Meter method achieves adequate sensitivity, the specimen has to be subjected to high fields. This is not so in the A.C. bridge method where magnetizing fields of the order of 1 oe. are used. In this method the sample functions as an element in a balanced A.C. bridge circuit which is connected to a detector having sensitivity adequate for measuring the variations of the small error signals that appear as the sample is placed within the test coil in various orientations.

7. Inductance Bridge Method

Bruckshaw and Robertson (1948) developed an inductive apparatus for measuring magnetic susceptibility in a low field of about 0.5 oe. A uniform alternating field is produced by a pair of Helmholtz coils HH carrying an alternating current. A pick-up coil consisting of an inner and outer winding, W1 and W2, wound in series opposition is placed at the centre of the Helmholtz Coil. The turns on the windings are adjusted for a minimum (ideally zero) output e.m.f. in a uniform time-varying field. A rock specimen placed at the centre of such a coil causes a differential output because of its closer coupling with the inner coil. By means of a potentiometric arrangement, the differential voltage is measured in terms of that set up in a third coil, W3, of very few turns, which is wound on the outside of the double coil and excited by the Helmholtz coil. A tuned Campbell vibration galvanometer preceded by a 3 stage low-noise, high-gain amplifier is used as a null detector.

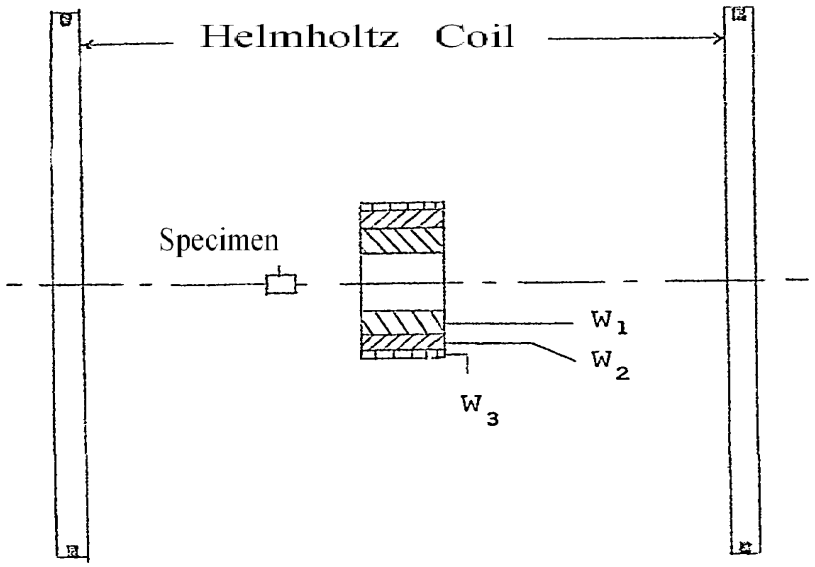

Figure 2.4: Schematic view of the principal parts of the apparatus for measuring the magnetic susceptibi1ity of rocks by means of alternating magnetic field. (After Bruckshaw and Robertson, 1948).

8. D.C. Method

Blackett (1952) used the static magnetometer to determine the susceptibility of rocks. A known field is applied by means of secondary windings on one pair of the 3-component Helmholtz coil system used to obtain a zero field at the magnetometer. The magnetization then measured will be the sum of the permanent and induced magnetizations. The effect of the former can be eliminated through a suitable measuring procedure following which the reversible susceptibility is deduced.

The A.C. method of measuring the susceptibility has the following advantages over the D.C. method:

(1) The output signal due to a specimen varies directly with the frequency of a sinusoidally varying magnetizing field, and hence the sensitivity can be increased by using higher frequencies. Further sufficient amplification permits the measurement of very weak specimens.

(2) The A.C. method can be used in the presence of time varying magnetic fields and mechanical vibration such as exist in the average laboratory. This is an important practical advantage over the D.C. method.

(3) The time required to make a measurement is not more than 30 seconds - much less than that required by the D.C. method.

Disadvantages of the A.C. method are:

1. The balance condition drifts due to changes in the inductance and resistance of the double coil as a result of temperature variation. This problem is reported to have been successfully solved by use of automatic servo loops which maintain the bridge in approximate balance for long periods (Graham 1964).

It should be noted here that the above methods measure only the apparent susceptibility because of the self-demagnetizing effect of the ferromagnetic minerals contained in the rocks.

2.3.5 Laboratory measurement techniques of magnetic susceptibility

For measuring the mass magnetic susceptibility (χ_m) of fluids, in this project we used the first method described above, the balance method, which enabled us to use very sensitive equipment. Most of the fluid measurements were made on a Sherwood Scientific magnetic susceptibility balance (MSB) Mark I (Figure 2.5). The MSB Mark I or Evans magnetic balance is designed as a reverse traditional Gouy magnetic balance. The Evans method uses the same configuration as the Gouy method except that instead of measuring the force which a magnet exerts on the sample, the equal and opposite force which the sample exerts on a moving permanent magnet is measured. The two magnets are at the end of a beam, and when the sample tube is placed in one of the magnets, the beam is not in equilibrium. A current is applied to the other magnet until the beam is back in equilibrium, and by measuring the current it is possible to measure the magnetic susceptibility, which is proportional to the force exerted by the sample.

The general expression for the calculation of the mass magnetic susceptibility from the measurements is as follows:

$$X_m = L/m(C(R-Ro) + \chi_{vair}A) \qquad 2.18$$

where C is a proportionality constant, R is the reading for the tube and sample, Ro is the empty tube reading, L is the sample length, m is the sample mass, A is the cross-section area of the tube, and χ_{vair} is the volume susceptibility of the displaced air.

Figure 2.5: Sherwood Scientific magnetic susceptibility balance (MSB) Mark I.

2.4 Magnetic hysteresis properties

Magnetic minerals have more than one equilibrium magnetisation state. The magnetisation state is reflected by non reversible behaviour when placed in an applied magnetic field. The resulting hysteresis loops display the dependence of magnetisation within a sample on the magnitude of the applied external magnetic field. A hysteresis curve for an assemblage of single-domain or multi-domain grains with randomly oriented easy magnetisation axes is shown in Figure 2.6. It is seen that at low fields the magnetisation is reversible. However, at some critical field value a remanent magnetisation is formed and the magnetisation process is no longer reversible on removal of the applied field. Complete hysteresis is obtained when the magnitude of the applied field is gradually increased until the substance reaches a saturation magnetisation (Ms, Figure 2.6) and the field cycled further between a positive and

negative maximum value. The area bounded by a hysteresis loop is a measure of the ferromagnetic energy stored by the substance. For instance, a Single-Domain mineral grain that has its easy magnetised axis parallel to the magnetic field can switch between equilibrium states only when the reversed applied field is strong enough to subdue the anisotropy energy barrier. This process results in a square hysteresis loop. When the field is perpendicular to the grain's easy axis there is no hysteresis observed as the equilibrium states have equal magnetisation. Thus, for an assembly of randomly oriented Single-Domain grains the type of curve as illustrated in Figure 2.6 is produced. Multi-Domain grains exhibit more complex behaviour as they may have any number of equilibrium positions which are sensitive to the previous petrological and magnetic history of the grains. Multi-Domain grains in general exhibit narrower hysteresis loops than Single-Domain grains.

Various diagnostic magnetic parameters can be obtained from hysteresis loops as illustrated in Figure 2.6. The main magnetic parameters are saturation magnetisation, saturation remanent magnetisation, coercivity, low-field and high-field magnetic susceptibilities.

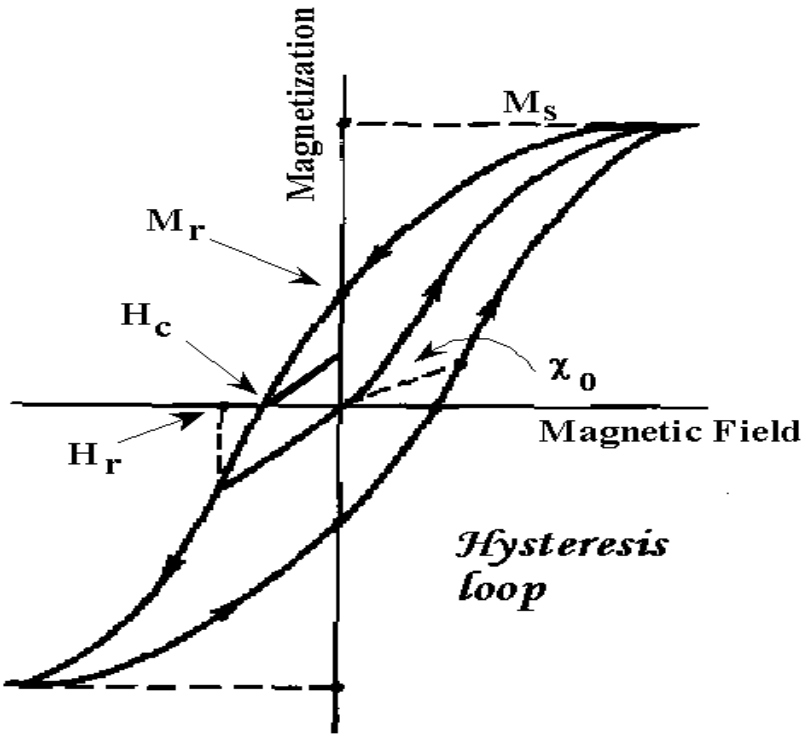

Figure 2.6 Magnetic hysteresis curve of an assemblage ferromagnetic mineral (University of Minnesota).

2.4.1 Magnetic hysteresis procedure

The magnetic hysteresis parameters were measured by the Variable Field Translation Balance (VFTB). The magnetic measurement VFTB (Figure 2.7) is a one-dimensional harmonic oscillator with damping in the forced oscillation mode. It is a horizontal translation balance in which the magnetisation of the sample is measured. The measurements can be made in fields up to 1000 mT. It is also possible to control the temperature using an oven and liquid nitrogen to obtain a temperature range from -170°C to 700°C.

Figure 2.7: The Variable Field Translation Balance (VFTB).

The main advantage of the VFTB is that all the equipment is computer controlled so that once the sample is in the measuring position, many experiments can be applied to the same sample. Thus a whole range of magnetic experiments can be carried out. Normally measurements of IRM acquisition and remanence coercivity are carried out and afterwards a hysteresis loop measurement is followed by the thermomagnetic measurements.

The studied reservoir sample consists of powdered material or sediment chips of known mass (normally about 0.5 g) and was compacted into a non-magnetic container at the end of the sample holder. The sample is very tightly packed into the sample cup

container with quartz wool in order to fix the material and to avoid contamination by air. The sample holder slides into the sleeve at the end of the balance assembly. The obtained data is processed using a software program VFTB Analyser 1.6, written and updated by R. Leonhard (between 1999 and 2005), which allows mass correction for each sample and determination of magnetic properties such as Saturation Magnetisation (M)s, Saturation Remanent Magnetisation (Mrs), Coercivity of Magnetisation (Hc), Coercivity of Remanent Magnetisation (Hcr), Saturation Isothermal Remanent Magnetisation (SIRM), etc.

CHAPTER 3: APPLICATION OF MAGNETIC SUSCEPTIBILITY TO OILFIELD FLUIDS ANALYSIS.

3.1 Introduction

For reservoirs to be effectively managed, we need to have good knowledge of the geology as well as various other properties of the reservoir (permeability, prorosity, reservoir pressure and temperature, etc). These properties are obtained by carrying out analyses of the results that are obtained from the down hole tests conducted in-situ and also from the measurements carried out in the laboratory.

Potter (2005) stated that magnetic techniques have the unique combination of benefits of being environmentally friendly, of low cost and non-destructive. However, relatively little work has been conducted to investigate the potential benefits of applying these techniques to the management of oilfield scale. Thus, the magnetic behaviour of reservoir fluids and mineral scales will be described in this chapter, with a view to developing an understanding of how such measurements could be applied to inorganic scale control.

3.2 Magnetic Susceptibility of Reservoir Fluids

Available literature on the magnetic susceptibility of reservoir fluids is limited. Recent studies (Potter 2005, Ivakhnenko and Potter 2006) have highlighted new potential for the use of magnetic properties of reservoir fluids for improved, non-destructive characterisation of multiple component fluids and reservoir characterisation in petroleum exploration and production. They have provided experimental and theoretical data on the mass magnetic susceptibility (χ_m) and volume magnetic susceptibility (χ_v)

of several crude oils from around the world and refined oils fractions from the North Sea.

Despite the wide use of magnetic methods and techniques in the field of geoscience, very limited research data is available pertaining to the magnetic susceptibility of natural reservoir fluids (crude oils, formation waters and other reservoir related fluids such as injection and drilling fluids). One of the most comprehensive pieces of work on the magnetic susceptibility of reservoir fluids was conducted by Ergin et al (1975) and Yarulin (1979). They established the diamagnetic nature of mass magnetic susceptibility of crude oils that were derived from the former USSR provinces. In this work they showed that the mass magnetic susceptibility of the crude oils ranged from -0.942 to -0.1042 ($10^{-8}m^3kg^{-1}$). However, most of the data fell within the range -0.98 to -1.02 ($10^{-8}m^{-3}kg^{-1}$). Some further work on the volume magnetic susceptibility was carried out by Kobranova (1989), who showed the volume susceptibilities for most of the crude oils to be around -10.4 10^{-6} SI units.

The work of Ergin and Yarulin (1979) also involved the analysis of various crude oil components. From their work, they showed that the most diamagnetic compounds are the alkanes, and the least diamagnetic hydrocarbon compounds are the aromatics (benzol with its homologues, napthenoaromatics and polycyclic aromatic hydrocarbons). The cyclopentane and cyclohexane hydrocarbons have an intermediate position that vary from being the most to being the least diamagnetic hydrocarbon compounds (their mass magnetic susceptibility values range from about -1.00 to -1.13 ($10^{-8}m^3kg^{-1}$)). The magnetic susceptibility of the aromatic hydrocarbons ranged from -0.85 to -0.97 ($10^{-8}m^3kg^{-1}$). The mass susceptibility of sulphur crude oil components have a value that closely matches those obtained for benzol homologues.

Ergin and Yarulin (1979) also established some correlations between the mass susceptibility and notable physical and chemical properties of the oils. They observed that the magnetic susceptibility of the oils increased with depths, with some exceptions. They also established that mass magnetic susceptibility values differ for samples that belonged to different geological formations. Also, there were small differences in the mass magnetic susceptibilities of oil samples obtained from different tectonic areas, and the same for collectors of the same oil deposits. Their work suggested that there is a possibility of distinguishing between the oils from different provinces and different stratigraphic intervals, based on their magnetic susceptibility values.

Other researchers have worked on the ferromagnetic nature of naturally altered hydrocarbons. McCabe et al (1987) establishes the relationship of secondary magnetite with biodegraded liquid crude oil obtained from two remote regions, the Thornton Quarry (IIIinois) and the Cynthia Quarry (Mississippi). Similar work also showed that the final product obtained from the biodegration of solid bitumen is strongly magnetic. Elmore et al (1987) studied the magnetic nature of gilsonite and hydrocarbons containing crystals of calcite in speleothems. The work carried out by Aldana et al (1996), also confirmed the magnetic nature of biodegradable hydrocarbons in Venezuela. Hu (2000) established the ferromagnetic properties of drilling fluids, while Gold (1990, 1991) reported the spatial relationship of hydrocarbons with ferromagnetic magnetite concentration.

3.3 Experimental Measurements of the Magnetic Properties of Reservoir Fluids

Reservoir fluids consist of crude oils and formation waters. In addition, fluids may be injected into the reservoir, such as waters for secondary recovery. Chemicals may be injected for Enhanced Oil Recovery, for Flow Assurance purposes, such as when scale inhibitors are deployed. For the purpose of this research a suite of 10 brines, 6 samples of scale inhibitors (PPCA) with 6 different concentrations and 5 crude oil samples

which we have in the laboratory were measured to indentify their mass magnetic susceptibilities. For this, we have used the Sherwood mass magnetic susceptibility balance (shown in chapter 2, Section 2.3.5, Figure 2.5).

3.3.1 Brines

Table 3.1 shows the compositions of 10 brine samples from the North Sea region (both formation and sea water), which are prepared as synthetic brines so that their mass magnetic susceptibilities could be measured as shown in Table 3.2.

Figure 3.1 shows that the mass magnetic susceptibilities of the brines are in a range from -0.8732 to – 0.9313 (10^{-8} m^3 Kg^{-1}). There is a general trend of increasing mass magnetic susceptibility with increasing density, but there is significant scatter in this trend, so we need to calculate the ionic stenght and plot it agains mass magnetic susceptibility.

Brines B-3 and B-9, B-4 and B-7, have nearly the same density but different mass magnetic susceptibility while brines B-9 and B-10 are different in density but nearly the same mass magnetic susceptibility, so more experiment work should be done in brine samples like preparing a set of brines with the same densities but different in compositions. However, brine B-6 has the lowest mass magnetic susceptibility (more negative) and its density fall between brines B-9 and B-3 densities.

Brine No.	B-1	B-2	B-3	B-4	B-5	B-6	B-7	B-8	B-9	B-10
Na^{+}	41183	31275	10890	9000	6566	14025.1	9278	70740	10890	28800
Ca^{2+}	5373	5038	428	100	143	371.41	43	0	0	0
Mg^{2+}	633	739	1368	50	29	85.17	48	0	0	0
K^{+}	233	654	460	200	70	89.97	81	0	460	1820
Sr^{2+}	330	771	0	80	2	1.28	4.9	0	0	110
Ba^{2+}	368	269	0	20	0	0	0	0	0	1030
Fe2+	0	0	0	0	0	0	0	0	0	10
Fe (total)	0	0	0	0	0	0	0	0	0	0
Fe (disolved)	0	0	0	0	0	0	0	0	0	0
Cl^{-}	0	60848	19766	14451	8370	19499	13060	109088.53	19766	47680
SO_4^{2-}	0	0	2960	0	1300	4100	0	0	2960	7
HCO^{3-}	0	0	0	0	0	0	0	0	0	2070

Table 3.1: Synthetic Brine sample composition.

	Density		Volume Magnetic Susceptibility χ_v		Mass Magnetic Susceptibility χ_m	
	g/cc	Kg/m^3	c.g.s.10^{-6}	SI 10^{-6}	c.g.s. 10^{-8} m^{-3} Kg^{-1}	SI 10^{-8} m^{-3} Kg^{-1}
B-1	1.0820	1082	-0.7706	-9.6787	-0.7122	-0.8945
B-2	1.0637	1063.7	-0.7395	-9.2886	-0.6952	-0.8732
B-3	1.0272	1027.2	-0.7345	-9.2261	-0.7151	-0.8981
B-4	1.0166	1016.6	-0.7402	-9.2972	-0.7281	-0.9145
B-5	1.0036	1003.6	-0.7229	-9.0804	-0.7204	-0.9048
B-6	1.0265	1026.5	-0.7610	-9.5593	-0.7414	-0.9312
B-7	1.0139	1013.9	-0.7333	-9.2113	-0.7233	-0.9084
B-8	1.1186	1118.6	-0.7832	-9.8374	-0.7002	-0.8794
B-9	1.0242	1024.2	-0.7258	-9.1166	-0.7086	-0.8900
B-10	1.0464	1046.4	-0.7415	-9.3139	-0.7086	-0.8901

Table 3.2: Magnetic Susceptibility results for brine samples.

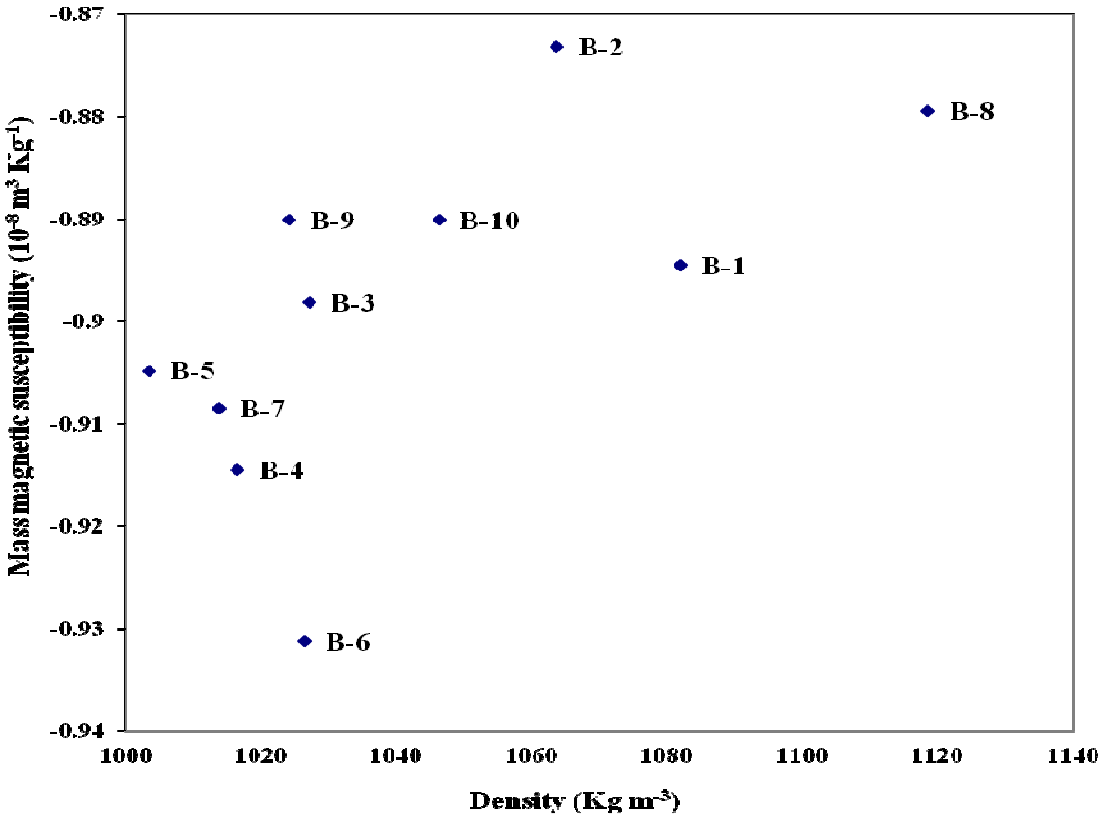

Figure 3.1: Brine density versus mass magnetic susceptibility.

The ionic strength *I* of a solution is a measure of the concentration of ions in that solution. Ionic compounds, when dissolved in water, dissociate into ions. The total electrolyte concentration in solution will affect important properties such as the dissociation or the solubility of different salts. One of the main characteristics of a solution with dissolved ions is the ionic strength.

$$I = \tfrac{1}{2} \sum c_i \, z_i^2 \qquad (3.1)$$

where c_i is the molar concentration of ion, z_i is the charge number of that ion.

The results of ionic strength *I* calculations are sown in table 3.3.

Brine sample	Density Kg/m^3	Mass Magnetic Susceptibility χ_m SI 10^{-8} m^{-3} Kg^{-1}	Ionic strength *I*
B-1	1082	-0.8945	1.231
B-2	1063.7	-0.8732	1.878
B-3	1027.2	-0.8981	0.716
B-4	1016.6	-0.9145	0.412
B-5	1003.6	-0.9048	0.271
B-6	1026.5	-0.9312	0.606
B-7	1013.9	-0.9084	0.392
B-8	1118.6	-0.8794	3.074
B-9	1024.2	-0.8900	0.582
B-10	1046.4	-0.8901	1.355

Table 3.3: Brine Mass Magnetic Susceptibility and Ionic strength

As shown in Figure 3.2, an increase in ionic strength causes an increase in mass magnetic susceptibility (less negative) for most of the measured brine samples, depending on the ion dissolved in the brine and their concentration and charge number for that ions. However, by comparison with Figure 3.1, plotting mass magnetic susceptibility against ionic strength does not show a particulary stronger trend.

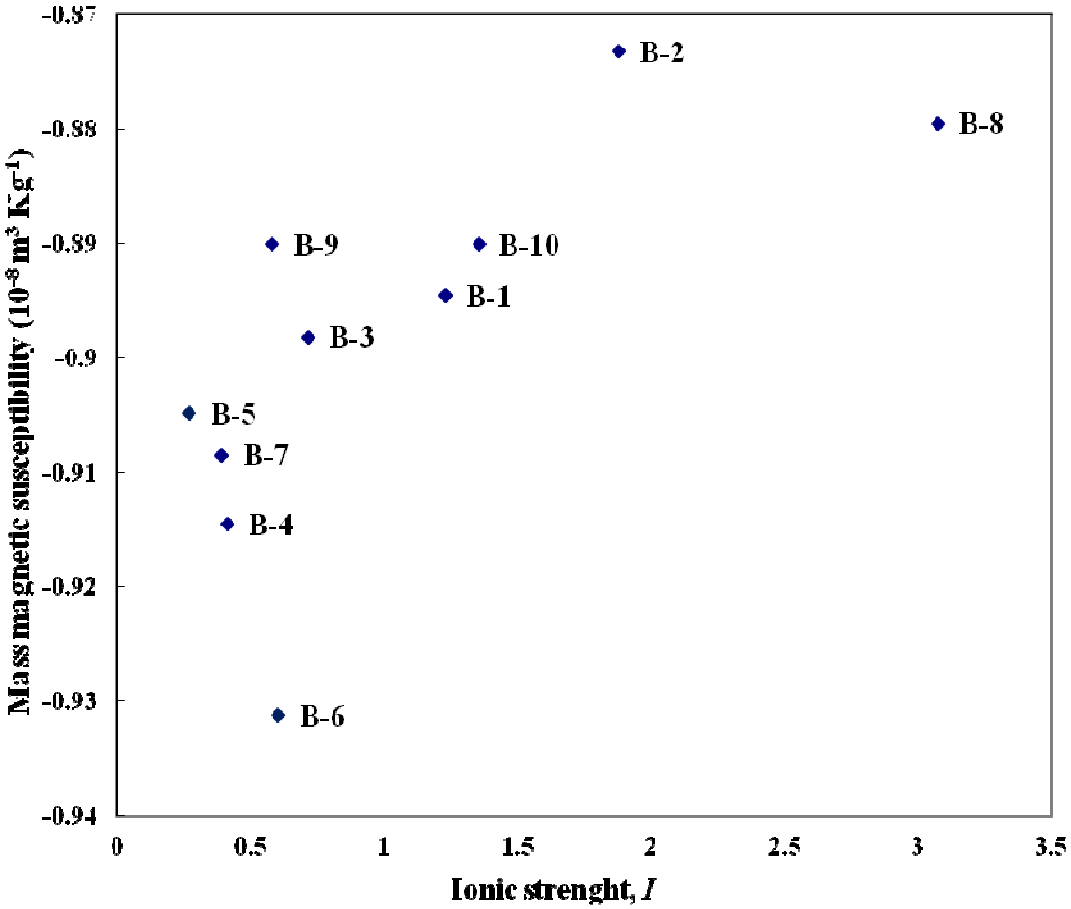

Figure 3.2: Brine ionic strength versus mass magnetic susceptibility.

3.3.2 Crude Oils

Crude oil samples 1 to 3 are taken from North Sea fields, while crude oil samples 4 and 5 are taken from onshore fields in Libya; the results for their mass magnetic susceptibilities are shown in Table 3.3. The mass magnetic susceptibilities of the various crude oil samples versus density are shown in Figure 3.3. The results show that as the crude oil density increases, the mass magnetic susceptibility increase (becomes less negative).

However, two different regions showed different mass magnetic susceptibility, as crude oils (1, 2, and 3) results from the North Sea region show that mass magnetic susceptibility is less negative than for crude oils (4 and 5) results from the Libyan region.

Figure 3.3 shows that the mass magnetic susceptibility of the crude oil ranges between -0.9907 to -1.0291 (10^{-8} m^3 Kg^{-1}).

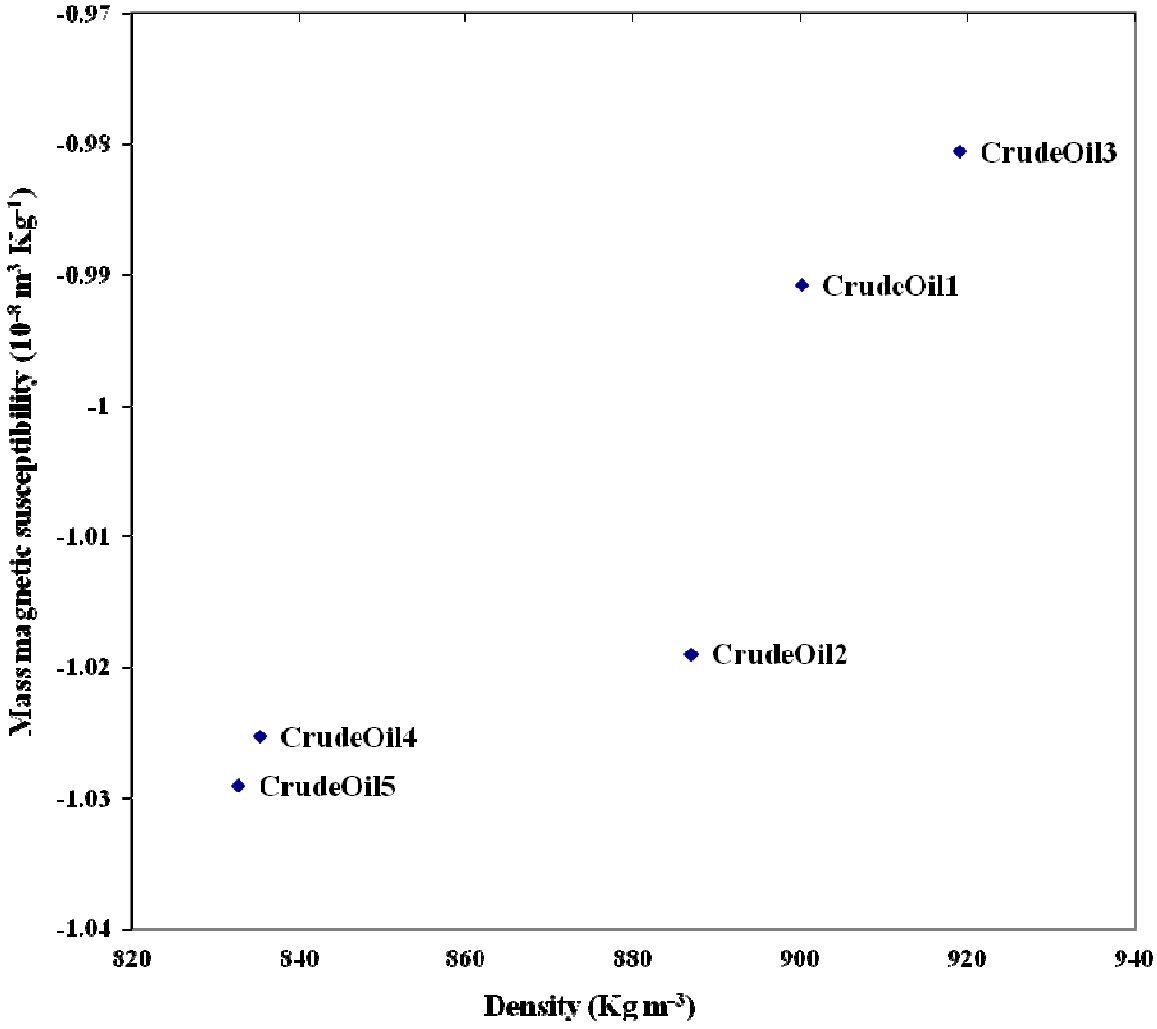

Figure 3.3: Crude oil density Vs mass magnetic susceptibility.

Crude oil						
	Density		Volume Magnetic Susceptibility χ_v		Mass Magnetic Susceptibility χ_m	
	g/cc	Kg/m3	c.g.s. 10^{-6}	SI 10^{-6}	c.g.s. 10^{-8} m^3 Kg^{-1}	SI 10^{-8} m^3 Kg^{-1}
CrudeOil1	0.9002	900.1722943	-0.710080111	-8.918606196	-0.78882689	-0.990766573
CrudeOil2	0.8869	886.9000506	-0.719551611	-9.037568236	-0.811310824	-1.019006395
CrudeOil3	0.9190	919.0212281	-0.717474167	-9.011475533	-0.780693791	-0.980551402
CrudeOil4	0.8353	835.3355036	-0.681915389	-8.564857284	-0.816337132	-1.025319437
CrudeOil5	0.8328	832.7598711	-0.682304056	-8.569738938	-0.819328691	-1.029076837

Table 3.4: Magnetic Susceptibility results for crude oil samples.

3.3.3 Scale Inhibitors

6 samples of scale inhibitor with differenet concenatrations (Table 3.6) are prepared by adding (10, 100, 1000, 5000, 10000, and 20000 ppm) PPCA in North Sea Sea Water (NSSW table 3.5) for mass magnetic susceptibility measurements, results are in Table 3.7.

	NSSW
Ion	ppm
Na^{+}	10890
Ca^{2+}	428
Mg^{2+}	1368
K^{+}	460
Ba^{2+}	0
Sr^{2+}	0
SO_4^{2-}	2960
Cl^{-}	2900
HCO^{3-}	0
TDS	35103.55

Table 3.5: Composition of North Sea Sea Water.

Figure 3.4, shows that an increase in the density of the scale inhibitor solutions results in an increase in their mass magnetic susceptibility (becoming less diamagnetic).

The mass magnetic susceptibility of the scale inhibitors measured ranges from -0.8992 to -0.9241 (10^{-8} m^3 Kg^{-1})

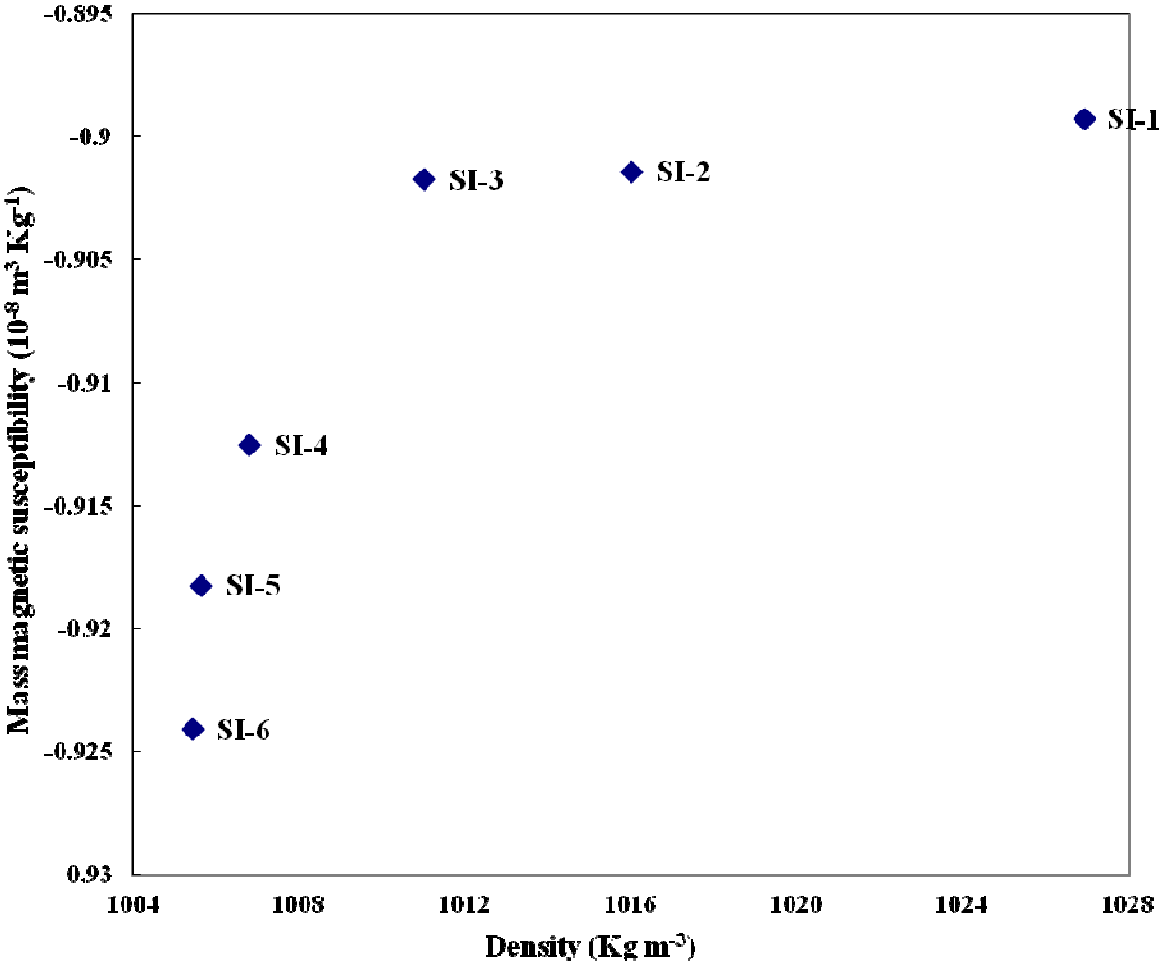

Figure 3.4: Scale Inhibitor Density Vs mass magnetic susceptibility.

Scale Inhibitor No.	Scale Inhibitor Conc. ppm
1	20000
2	10000
3	5000
4	1000
5	100
6	10

Table 3.6: Scale Inhibitor (PPCA) With 6 Different Concentrations.

These measurements on scale inhibitors may be used for the return of a scale inhibitor squeeze; however, in this experiment PPCA inhibitor is only the scale inhibitor which has been used, so other types for scale inhibitors with deferent concentrations should be tested and even the magnetic susceptibility for the scale inhibitor itself should be tested as well.

In Figure 3.5, as scale inhibitor concentration increases results in an increase of mass magnetic susceptibility (become less negative) which is contrast with the results in Figure 3.8, where solute concentration in brine increases results in decrease of mass magnetic susceptibility (become more negative).

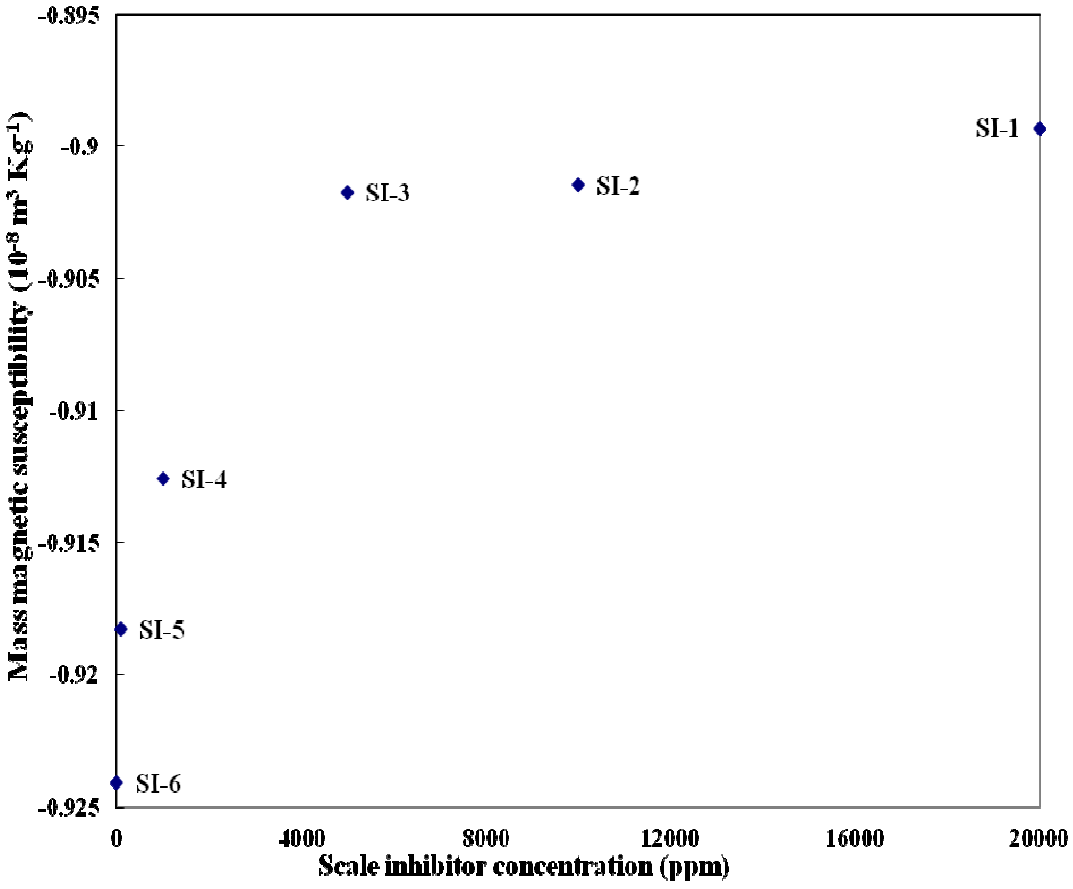

Figure 3.5: Scale inhibitor concentration vs. mass magnetic susceptibility.

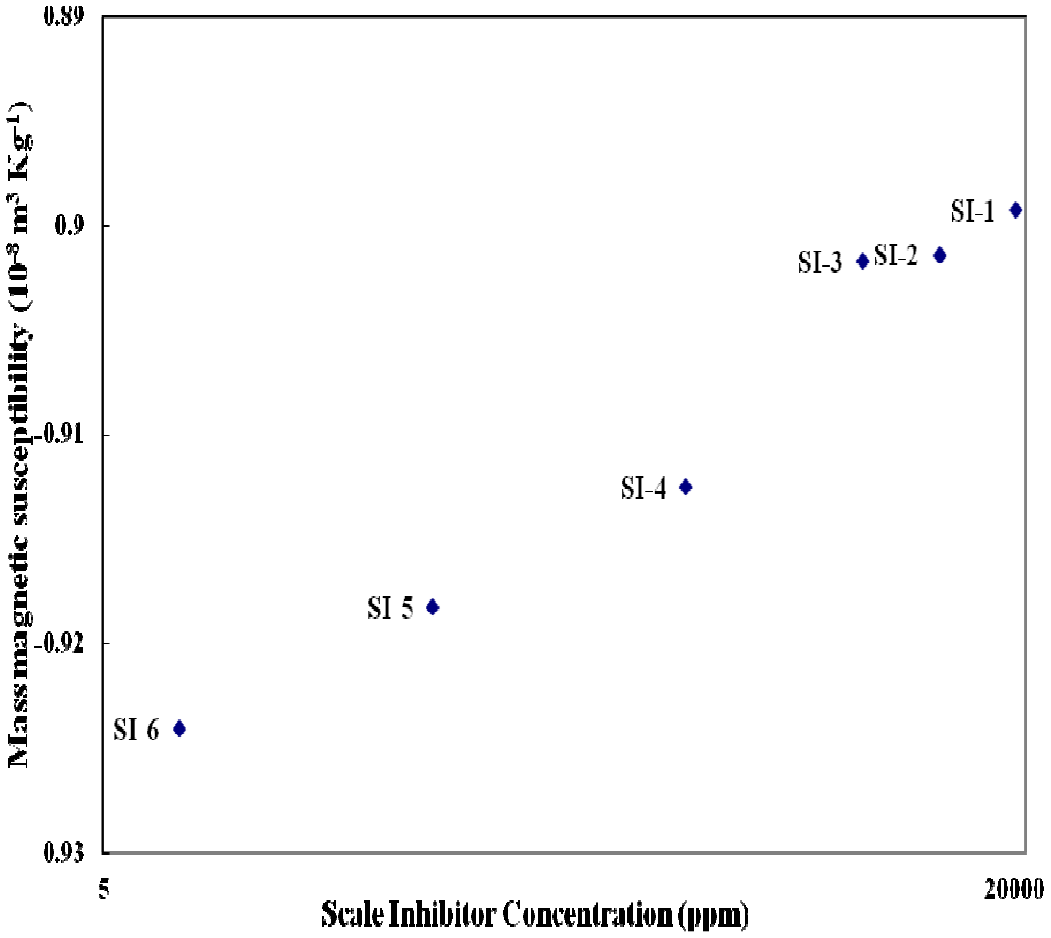

Figure 3.6: Scale inhibitor concentration vs. mass magnetic susceptibility (Log scale for x-axis).

Scale inhibitor						
	Density		Volume Magnetic Susceptibility χ_v		Mass Magnetic Susceptibility χ_m	
	g/cc	Kg/m3	c.g.s. 10^{-6}	SI 10^{-6}	c.g.s. 10^{-8} m^3 Kg^{-1}	SI 10^{-8} m^3 Kg^{-1}
SI-1	1.0269	1026.923092	-0.737009444	-9.256838622	-0.717687089	-0.901414983
SI-2	1.0160	1016.022427	-0.742801852	-9.329591259	-0.731088047	-0.918246587
SI-3	1.0110	1011.016895	-0.723866667	-9.091765333	-0.715978803	-0.899269377
SI-4	1.0068	1006.813624	-0.72282963	-9.078740148	-0.717937871	-0.901729966
SI-5	1.0057	1005.654788	-0.730661111	-9.177103556	-0.72655261	-0.912550078
SI-6	1.0054	1005.437539	-0.739738889	-9.291120444	-0.735738283	-0.924087284

Table 3.7: Magnetic Susceptibility results for Scale Inhibitor.

All the samples we have studied in this chapter are diamagnetic in their magnetic behaviour even the distilled water and deionized water. However, some of them are quite distinguishable from others in terms of their magnetic susceptibilities. For instance, in Figure 3.7, brine and crude oil samples plot in distinct areas on the cross plot of density vs. mass magnetic susceptibility.

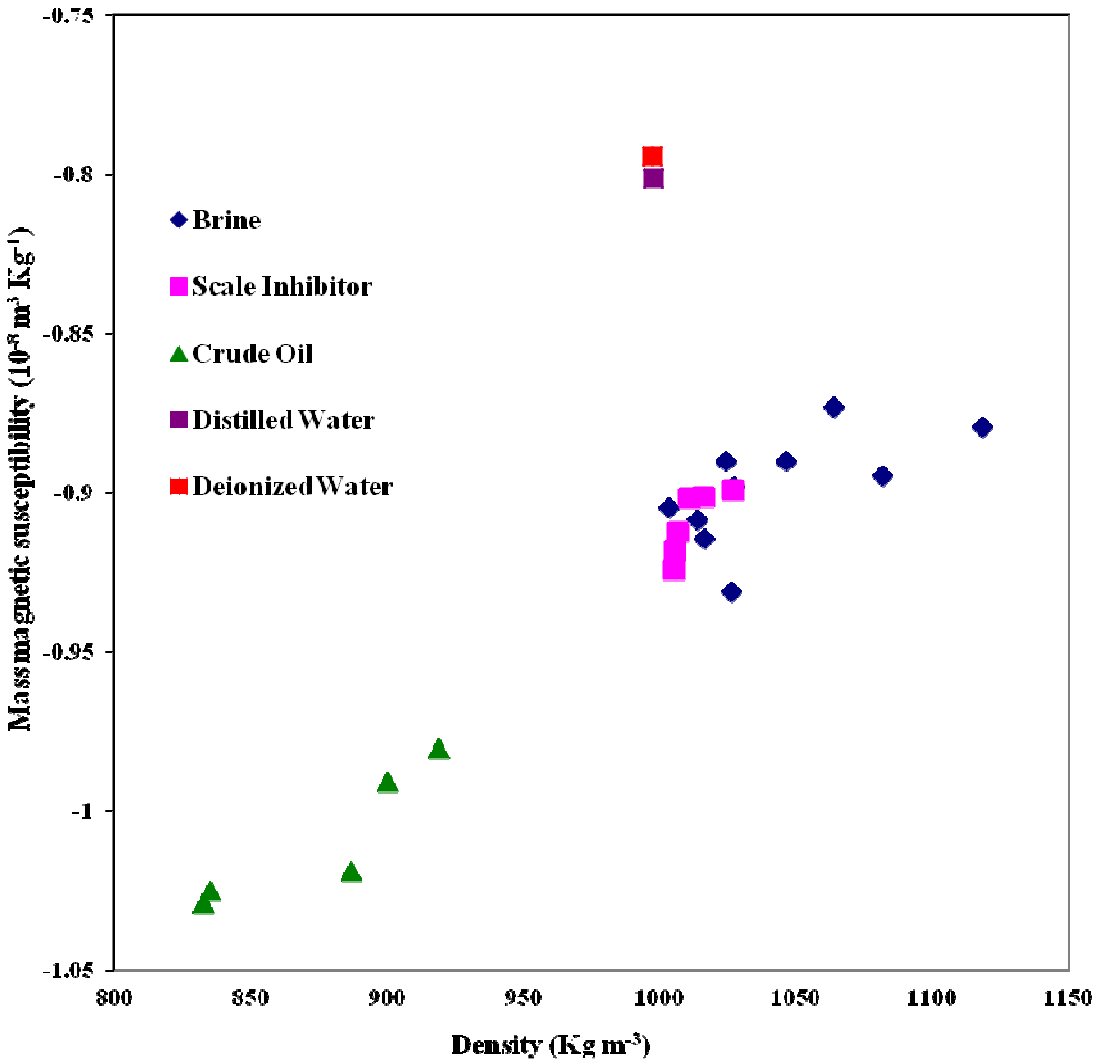

Figure 3.7: Densities of all measured fluids vs mass magnetic susceptibility.

3.3.4 Effect of Solute Composition and Concentration on Mass Magnetic Susceptibility

Figure 3.8 shows the impact that changes in the concentration of brine solutes have on the mass magnetic susceptibility. Five brine solutes were used in this study, ($CaCl_2$, $BaCl_2$, $NaSO_4$, NaCl and $MgCl_2$). Figure 3.8 shows that there is a decrease in the mass magnetic susceptibility as the concentration of the brine solutes increases.

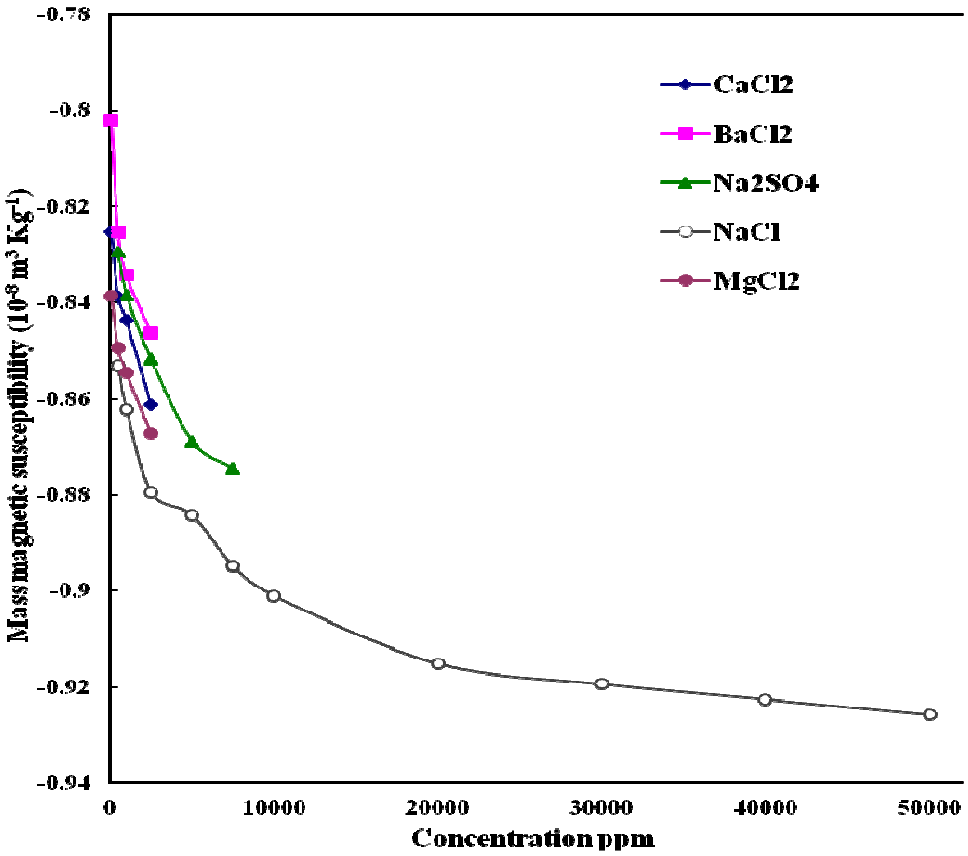

Figure 3.8: Solute concentration vs. mass magnetic susceptibility.

This behaviour contrasts with the behaviour shown in Figure 3.1, since with increasing concentration of salts in the brine, the density will increase, and yet here we see an increase in the mass magnetic susceptibility, not a decrease as seen in Figure 3.1.

3.3.5 Mass Magnetic Susceptibility to Monitor High Scaling (HS) and Low Scaling (LS) Brine Tendencies over Time.

In this section, we show the changes in the mass magnetic susceptibility signal that occurs as scaling brines precipitate scale. This could potentially be useful to detect the extent of scale precipitation in the formation and in production lines.

For a high scaling brine mixture, Miller Formation Water (Miller FW) was mixed with seawater from the North Sea (NSSW). For the low scaling brine, Formation Brine System 2 FW was mixed with Brine System 2 Sea water (SW) as shown in Tables 3.8 and 3.9. A 50:50 ratio was used for both high scaling (HS) and low scaling (LS) samples and mass magnetic susceptibility was recorded at time zero before scale formation commenced, and thereafter. The magnetic susceptibility increases as seen in figure 3.9, from a value of -0.928 10^{-8} m^3 Kg^{-1} until it reaches a value of -0.823 10^{-8} m^3 Kg^{-1} for the HS solution. At this value, the magnetic susceptibility remains almost steady and it may be concluded that all the scale has been deposited or in other words less ions present in the solution. For the LS solution the same trend is observed, until the value reaches to -0.8318 10^{-8} m^3 Kg^{-1}. Again it is assumed that all the scale has been deposited by this time.

Scaling Tendencies	Miller FW	NSSW	50:50 Mix
Na+	28800	10890	19845
Ca2+	1060	428	744
Mg2+	115	1368	741.5
K+	1820	460	1140
Sr2+	110	0	55
Ba2+	1030	0	515
Cl-	47680	19766	33723
SO42-	0	2960	1480
HCO3-	0	0	0

Table 3.8: High scaling tendency brine composition.

Scaling Tendencies	Brine System 2 FW	Brine System 2 SW	50:50 Mix
Na+	32689.1	10800	21744.55
Ca2+	1077.3	430	753.65
Mg2+	309.5	1400	854.75
K+	244	400	322
Sr2+	210.2	8	109.1
Ba2+	96.1	0	48.05
Cl-	53640	19753	36696.5
SO42-	0	2750	1375
HCO3-	0	0	0

Table 3.9: Low scaling tendency brine composition.

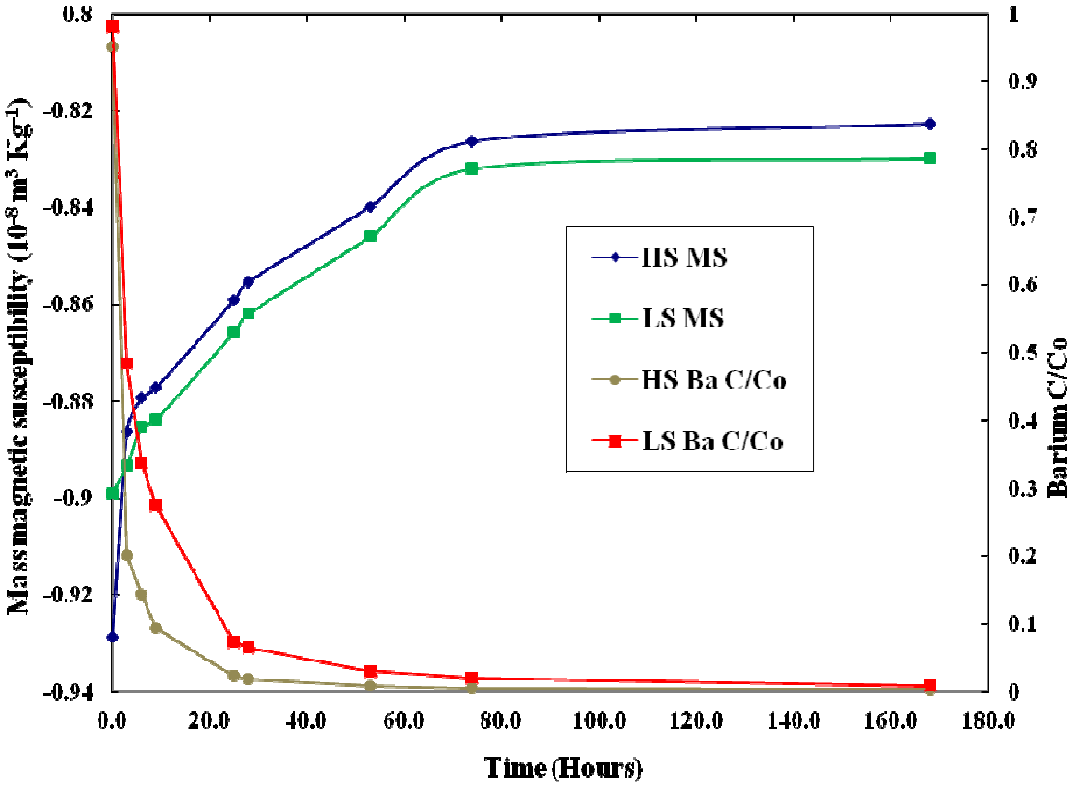

Figure 3.9: Mass magnetic susceptibility and barium concentration vs. time.

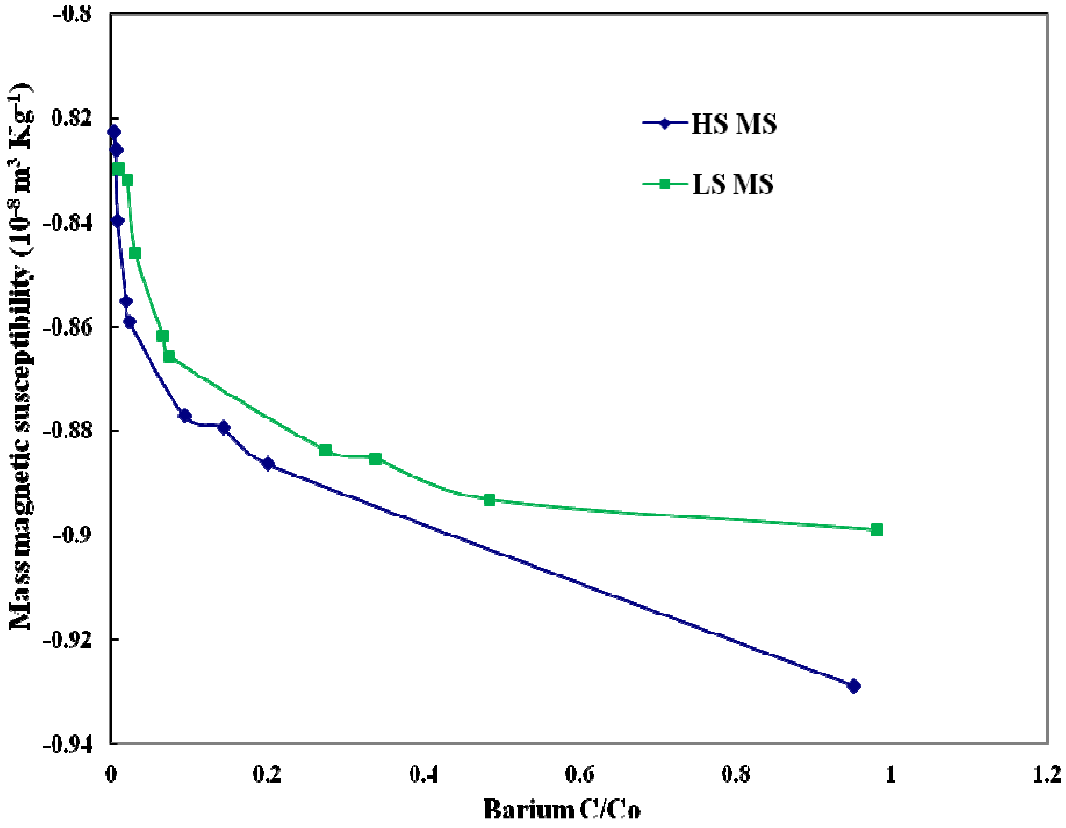

Figure 3.10: Mass magnetic susceptibility vs. barium concentration.

When the mass magnetic susceptibilities in the HS and LS samples (no scale in sample) were measured, samples were also taken for ion chromatography (ICP) analyses. This was done to show the trend of barium concentration dropping out in the samples (HS and LS) with time as the scale precipitates as shown in Tables 3.10 and 3.11 respectively.

Time (hrs)	HS Ba C/Co	Mass Magnetic Susceptibility χ_m 10^{-8} m^3 Kg^{-1}
0	0.9521	-0.9287
3	0.2009	-0.8863
6	0.1439	-0.8792
9	0.0947	-0.8771
25	0.0238	-0.8589
28	0.0194	-0.8552
53	0.0085	-0.8397
74	0.0058	-0.8261
168	0.0039	-0.8226

Table 3.10: Magnetic susceptibilities and barium concentration results for high scaling tendency brine.

Time (hrs)	LS Ba C/Co	Mass Magnetic Susceptibility χ_m 10^{-8} m^3 Kg^{-1}
0	0.9816	-0.8989
3	0.4842	-0.8931
6	0.3380	-0.8853
9	0.2743	-0.8837
25	0.0744	-0.8657
28	0.0661	-0.8618
53	0.0304	-0.8459
74	0.0200	-0.8318
168	0.0085	-0.8298

Table 3.11: Magnetic susceptibilities and barium concentration results for low scaling tendency brine.

The interesting thing to note here is that as the barium concentration decreases with time (due to more and more scale precipitation), the magnetic susceptibility of the samples increases (they become less diamagnetic). This shows a great potential for the magnetic technique to be used in measuring barium concentration in fluids where there is a risk of scale build up. Thus, magnetic measurements can potentially provide a rapid and high resolution means of scanning fluid samples in production lines.

The Figure 3.11 shows the first day results for mass magnetic susceptibility and variation in barium concentration over time for the first day, when most of the precipitation takes place. In the high scaling case the precipitation happens faster than in the low scaling case, especially over the first three hours.

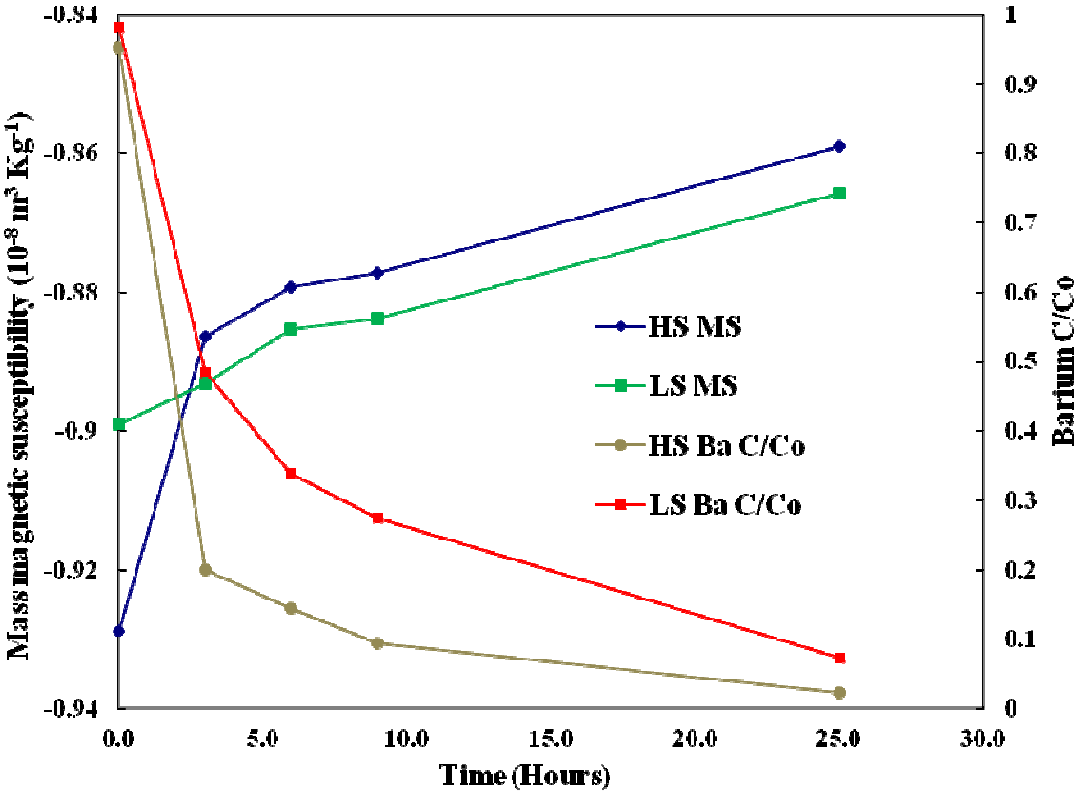

Figure 3.11: Mass magnetic susceptibility and barium concentration over time for the first day.

3.4 Characterisation of Magnetic Properties of Reservoir Fluids at Reservoir Pressure and Temperature (P, T).

The diamagnetic susceptibility is independent of temperature; however, the diamagnetic susceptibility of the fluid phase is substantially affected by certain variations due to changes in the fluid physical properties, especially fluid density, when subjected to compression at reservoir pressure and temperature conditions. The work by Ivakhnenko and Potter (2006) involves the estimation of the effect on magnetic susceptibility at

reservoir conditions; they modelled the susceptibility at reservoir conditions for Dunbar and Forties crude oils and their respective formation waters, and also for an injected sea water sample. They used the equation of state software written and updated by Donghai Xu (between 1988 & 1994). The equation of state (EOS) describes the analytical relation between the fluid temperature, pressure and volume; this relationship is used to simulate the volumetric and phase behaviour of the petroleum reservoir fluids. The generic form of the EOS that was modified to give better prediction of liquid density (Peng and Robinson, 1976; Yu et al., 1986) is defined as:

$$P= (RT/ V-b) - (a_c/ (V^2+ ubV + wb^2)) \qquad (3.2)$$

where the parameters P, T, V and R represent pressure, temperature, molar volume, and the universal gas constant, respectively. The parameters a_c and b are a measure of the degree of the repulsive and attractive forces. The symbols u and w are constants.

The density variation for formation water and sea water were calculated by Ivakhnenko, (2006) using model temperatures chosen between 96^{o}C and 112 ^{o}C, and with the respective pressures of 17.2 and 27.3 MPa, and the conditions for fluid compression were defined by the model above the bubble point. The results showed that the density of formation water and crude oils decreases when compared to ambient conditions. According to Ivakhnenko (2006) the density for Dunbar crude oil drops from 811.2 kg m^{-3} at surface conditions to 786.9kgm^{-3} at 96 ^{o}C and 785.7 kg m^{-3} at 112 ^{o}C. For formation waters the density decrease at reservoir temperatures are more profound compared to that of crude oils. i.e the density of Dunbar formation water decreases from 1021 kgm^{-3} at surface conditions to 982.8 kgm^{-3} at 96 ^{o}C and 970.7 kgm^{-3} at 112 ^{o}C. From research conducted by Ivakhnenko (2006) and other researchers, it has been observed that mass magnetic susceptibility decreases (becomes more negative for a diamagnetic fluid) with decreasing density. Conversely, it decreases with an increase in

temperature for the crude oils and formation waters. However, the volume magnetic susceptibility increases slightly at reservoir temperatures, though the change is far smaller compared to the *mass* magnetic susceptibility. The volume magnetic susceptibility of crude oils increases by about 0.08% at 92 ^{o}C and 0.09% at 112 ^{o}C compared to its ambient value. On the other hand, for formation water, the mass magnetic susceptibility increases from 0.065% to 0.125%. The results of Ivakhnenko (2006) and earlier work by Ergin and Yarulin (1979) show similar trends, with a decrease in mass magnetic susceptibility with depth. Hence, there is a possibility that volume magnetic susceptibility at ambient conditions may be a reasonable measure of the volume magnetic susceptibility of fluids at reservoir conditions.

3.5 Summary: potential applications of measuring magnetic susceptibility of reservoir fluids

Magnetic susceptibility measurements can be applied for use as passive sensors in oil or gas reservoirs to differentiate between formation waters and crude oils, a notable example being the use of magnetic susceptibility to determine the onset of water breakthrough in the production line. These sensors will add value as they remove hazards associated with radioactive tracers. The viscosity meters can also be used in distinguishing between formation waters and crude oils. Magnetic sensors, however, offer additional benefits in that they allow the opportunity to detect small concentrations of ferromagnetic minerals (two components) and other migrating fines (such as paramagnetic clays) that may be present in the fluids.

Earlier work by Ivakhnenko and Potter (2006) showed that the magnetic susceptibilities of natural reservoir fluids are more negative than most of diamagnetic matrix reservoir minerals such as quartz and calcite. Due to these variations in magnetic susceptibility researchers believe that magnetic properties may play a unique role in rock-fluid interactions. Ivakhnenko and Potter (2006) also inferred that the relative magnetic

forces that exist between quartz and formation water and also between quartz and crude oil, in the earth field, can be utilised in determining the wettability (water wet or oil wet) of the reservoir rock. Their research also showed that if the reservoir rock contains substantial amounts of paramagnetic clays, such as illite, magnetic roles of the formation water and crude oil can be reversed, and this will influence the wettability that is observed between the clean sandstone (quartz rich with little clay) and muddy sandstone (that contain paramagnetic clays). Work by Guan et al, 2002 has shown the link between nuclear magnetic resonance (NMR) and wettability. Their research also establishes the possibility of a relationship between magnetic susceptibility and wettability.

Magnetic susceptibility of reservoir fluids can be used as a useful parameter for characterising the following;

- Types of reservoir fluids (formation water and crude oil)
- Major physical properties
- To distinguish between the various kinds of crude oils. More research in this area is needed to prove that it is a better method compared to other methods (such as refractive index or fluorescence)
- Fractional and compositional constitution of crude oils, also metal content of chemical elements
- For detecting the presence of fines and contaminants (e.g. pieces of iron).
- Detecting in-situ changes in the physical and/or chemical properties of fluids.

However, work carried out and presented in this chapter identifies that mass magnetic susceptibility measurements may be used to identify changes in water composition, such as when injected seawater breaks through to production wells, and also when scale deposition may have taken place. This topic will be explored in greater depth in the next chapter.

CHAPTER 4: INJECTION WATER BREAKTHROUGH

4.1 The Problem

Water injection into oil reservoirs is used to maintain reservoir pressure, improve the sweep efficiency and increase secondary recovery from reservoirs that have low natural energy or are established mature fields. The deposition of scale minerals in the injection wells, production wells and production facilities, and the risk posed by it has been well studied by various researchers.

Scale build-up is now a source of concern in both the upstream and the downstream aspects of the oil and gas industry. Scales are deposited in the reservoir, in the tubing, in the transportation pipelines and other facilities that are used for processing from the upstream to the downstream. Scale formation now constitutes a major operational problem in both surface and subsurface oil and gas installations. (Todd and Yuan, 1991; Moghadasi et al., 2003a). Scale contributes greatly to equipment wear, corrosion and flow restriction, with the attendant consequences of decreased oil and gas production. Researchers have also attributed scale formation to be a major cause of formation damage (Civan, 2000).

Various researchers have published works on flow restrictions in tubing, and impaired well production as a result of scale deposition within the oil producing formation matrix and the downhole equipment, often involving primary, secondary and tertiary oil recovery operations. (Todd & Yuan, 1991). Scales are formed for various reasons, and the amount and the location of deposits is dependent on a combination of several factors. A supersaturated condition has been attributed as one of the primary causes of scale formation and this occurs when minerals are dissolved in a solution, which are at a higher concentration than their equilibrium concentration. Most researchers also believe that the degree of supersaturation, also known as the scaling index, is the major driving

force behind precipitation, and they equate high supersaturation with greater precipitation.

Since higher salt supersaturated conditions can exist at any point within the production system, scale can be formed at any point within the well. Supersaturation is influenced by changes in brine composition, temperature, pressure, pH, and CO_2/H_2S partial pressure. (Mackay et al, 2003; Moghadasi et al, 2003a).

4.2 The potential of the magnetic susceptibility method

With this technique, it is practicable to monitor and identify brine type from a produced brine system in real time. i.e. the change in ionic compositions and densities result in a change in magnetic susceptibilities of brines. This magnetic susceptibility signal can thus be used to distinguish between brines of varying compositions.

This technique makes it easy and faster to analyse samples and obtain results, since it relies on an inline system. Existing systems for monitoring produced water involve capturing water samples, preserving them, and then sending them to a labrotary for analysis.

With this technique, the facility for carrying out the analysis can be located either onshore or offshore, which will substantially reduce the time required between collecting samples and carrying out the analysis. With this quick time of response, the operator will have more time to make informed decisions about the management of oilfield scale, which will avert production losses due to mineral scale deposition obstructing the flow of hydrocarbon and damage to the sensitive downhole pressure and

temperature monitoring devices, as well as to the very important subsurface safety valves (SSSV).

This proposed system makes it possible for quick detection of injection water breakthrough at the production facilities, through magnetic susceptibility measurements of produced brine samples. With the water breakthrough detected, the operator will be able to quickly deploy appropriate technology that will combat or mitigate the risk posed by inorganic scale damage to the production facility (upstream or downstream facilities). This will result in cost savings for the company.

This technique is easy, fast, environmentally friendly and cost effective compared to the existing methods.

4.3 The Technique

As noted in Chapter 1 of this thesis, one of the main reasons that oilfield scale is formed is the mixing of incompatible water. Two water types are said to be incompatible if, on mixing, salt precipitation results. One example of incompatible water mixing is when seawater, which has a high concentration of SO_4^{-2} is mixed with formation water with a high concentration of Ca^{+2}, Ba^{+2} and/or Sr^{+2}. The mixing of these two types of water at varying pressures and temperatures can result in precipitation of $CaSO_4$, $BaSO_4$ and or $SrSO_4$. Also, disposal water produced from the field may to some extent be incompatible with seawater. Some researchers have suggested the possibility of scale precipitation when produced water is mixed with sea water for re-injection in a produced water re-injection (PWRI) project. (Bayona, 1993; Anderson et al., 2000; Paulo et al., 2001; Stalker et al., 2003).

The reason for water injection into mature fields is to provide pressure support through voidage replacement and improve oil recovery from the producing field. In addition,

water injection with proper well positioning can improve sweep efficiency. As the water is injected, its composition may be quite different from that of native formation brine. However, breakthrough of the injection water from the injection wells to the producing wells results in a mixture of injection water with formation brine at different compositions at varying temperatures and pressures, being co-produced resulting in mineral scale deposition in the hydrocarbon formation matrix and also in the tubular and surface facilities. If the amount of scale deposition is high, within a few days a large amount of production can be lost as a result of flow restriction problems. The method use currently by researchers to identify injection water breakthrough is the ion chromatographic technique. By this method samples of brine are collected routinely on the production facilities and taken to an onshore production chemistry laboratory for analysis using ion chromatography techniques. One of the disadvantages of this method is the delay in getting the results, which often may take two weeks or more, depending on frequency of transportation etc., and if the radioactive tracers are introduced into the injection water stream for detection, cost elements makes it an unattractive option.

This current method makes it possible for close to real time identification of the brine type in a produced brine stream during the process of extracting hydrocarbons. Another advantage of this new technique is that it introduces the potential for the use of an online system or quick analysis of a sample that has been collected, which gives the operator ample opportunity to make informed scale management decisions earlier than will be practicable using the existing system.

Using this method the magnetic susceptibility values that are measured for the brine samples are used to identify injection water breakthrough in the production system. From the research undertaken, it is evident that the majority of reservoir fluids are diamagnetic i.e. they show negative magnetic susceptibility values. This can be attributed to the nature of the compounds that are present in these fluids (i.e. in the sea water and the formation water). Also, work by previous researchers established the fact

that changes in the ionic compositions and densities results in a change in the magnetic susceptibilities of brines (Ivakhnenko and Potter, 2004). Hence, this means that mass magnetic susceptibility signals can be utilised in distinguishing between brines of varying compositions.

Using the present technique, the method was employed to identify the breakthrough in production wells of injections water (i.e. sea water), based on the fact that sea water and the formation water have different chemical compositions. A sea water sample taken from the North Sea Sea water (NSSW) was mixed with field formation brine (initially without barium). Table 4.1, shows the type and the concentration of various compounds present in the two samples.

	FW NoBa	SW NoSO4
Ion	ppm	ppm
Na^{+}	31275	10890
Ca^{2+}	2000	428
Mg^{2+}	739	1368
K^{+}	654	460
Ba^{2+}	0	0
Sr^{2+}	771	0
SO_4^{2-}	0	0
Cl^{-}	5900	2900
HCO^{3-}	0	0
TDS	90578.76	35103.55

Table 4.1: Composition of formation water and sea water.

Sea water samples contain lower ionic concentrations compared to the formation brine. The magnetic susceptibility values as shows in Table 4.2 of water is much higher (less negative) for sea water (-0.8083, 10^{-8} m^3 Kg^{-1}) compared with the value for formation brine (-0.9085, 10^{-8} m^3 Kg^{-1}).

FW NoBa	SW $NoSO_4$	Density		Volume Magnetic Susceptibility χ_v		Mass Magnetic Susceptibility χ_m	
%	%	g/cc	Kg/m^3	c.g.s.10^{-6}	SI 10^{-6}	c.g.s. 10^{-8} m^3 Kg^{-1}	SI 10^{-8} m^3 Kg^{-1}
100	0	1.062	1062	-0.7681	-9.6482	-0.7233	-0.9084
90	10	1.0579	1057.9	-0.7573	-9.5127	-0.7159	-0.8992
80	20	1.0542	1054.2	-0.7421	-9.3218	-0.7040	-0.8842
70	30	1.0495	1049.5	-0.7294	-9.1622	-0.6950	-0.8730
60	40	1.0453	1045.3	-0.7226	-9.0768	-0.6913	-0.8683
50	50	1.0395	1039.5	-0.7122	-8.9457	-0.6851	-0.8605
40	60	1.0372	1037.2	-0.7058	-8.8649	-0.6804	-0.8546
30	70	1.0338	1033.8	-0.6833	-8.5822	-0.6609	-0.8301
20	80	1.0291	1029.1	-0.6779	-8.5156	-0.6588	-0.8274
10	90	1.0241	1024.1	-0.6611	-8.3043	-0.6456	-0.8108
0	100	1.0208	1020.8	-0.6569	-8.2516	-0.6435	-0.8083

Table 4.2: Magnetic susceptibility of sea water fraction in formation water.

The contrast in the susceptibility value is the key factor that is utilised in this current technique. Figure 4.1, shows a graph of the mass magnetic susceptibility of 100%

formation brine and 100% sea water. The susceptibility of mixing different fractions lies in between the two end points. The upward trend towards less negative values indicates an increase in sea water concentrations. This is consistent with higher values (less negative) for sea water mass magnetic susceptibility for the case of this particular research. Hence, by collecting fluids samples from the production stream, and by measuring their magnetic susceptibilities, we can possibly identify the seawater breakthrough at the production wells and from that ascertain the seawater fraction that is present in the mixed sample. Sea water breakthrough, if not quickly addressed, may lead to scale deposition, and consequently flow restriction, which will results in loss of the production wells.

This technique provides a more proactive approach to addressing the challenges of scale deposition in production lines and combat any damage or loss before it occurs, since breakthrough is discovered early and scale management systems can be put in place by the operator. In the conventional technique this quick response time is not practicable and more days are required for results and even response to the situation at hand. Since this method can be performed onsite and early waning signs given to the operator of such a facility, it allows the operator ample time adopt scale prohibition measures, which will result in cost savings and higher net present value of the facility for the operators.

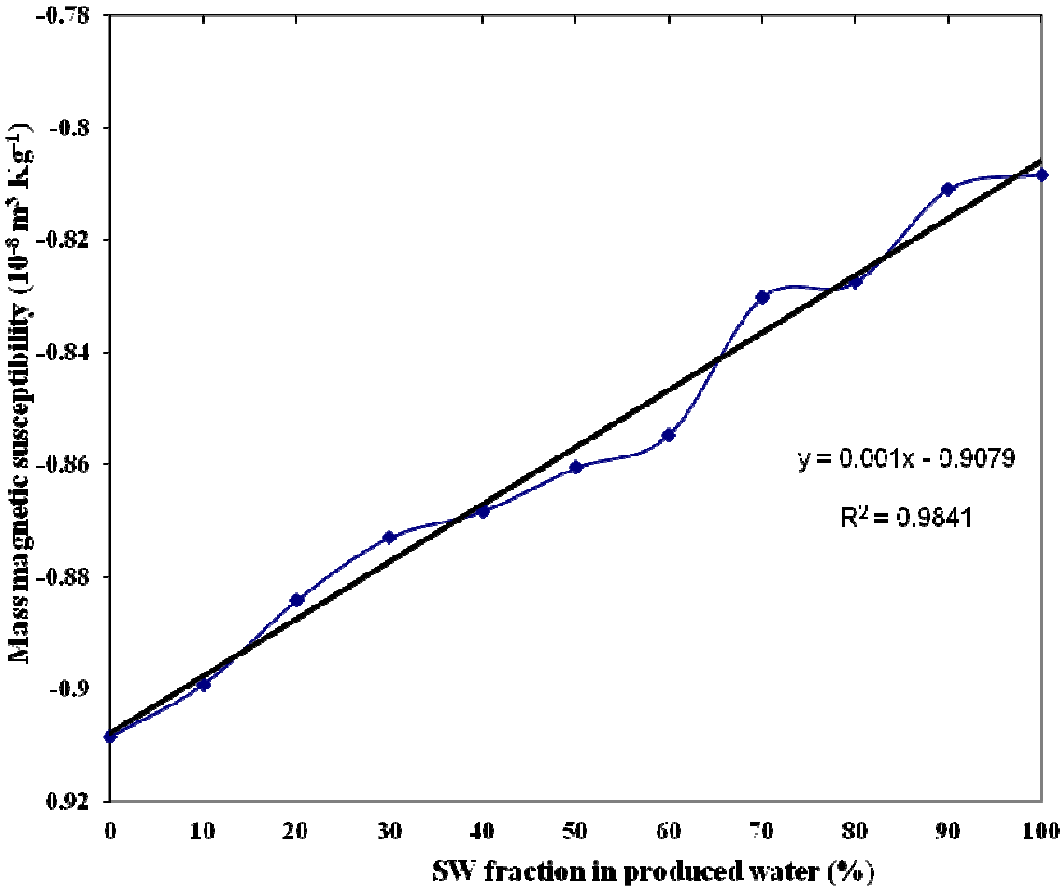

Figure 4.1: Mass magnetic susceptibility of various mixes of sea water and formation water.

4.4 Repeatability

The same technique is repeated by measurement several times for the same representative sea water sample (without sulphate) and formation brine (without barium) the results are shown in Table 4.3.

FW NoBa	SW $NoSO_4$	Mass Magnetic Susceptibility χ_m SI 10^{-8} m^3 Kg^{-1}				
%	%	1	2	3	4	5
100	0	-0.9084	-0.9069	-0.9094	-0.9074	-0.9073
90	10	-0.8992	-0.8977	-0.9002	-0.8982	-0.8981
80	20	-0.8842	-0.8827	-0.8852	-0.8832	-0.8831
70	30	-0.8730	-0.8715	-0.8740	-0.8720	-0.8719
60	40	-0.8683	-0.8668	-0.8693	-0.8673	-0.8672
50	50	-0.8605	-0.8590	-0.8615	-0.8595	-0.8594
40	60	-0.8546	-0.8457	-0.8494	-0.8483	-0.8517
30	70	-0.8301	-0.8316	-0.8321	-0.8291	-0.8290
20	80	-0.8274	-0.8259	-0.8284	-0.8264	-0.8263
10	90	-0.8108	-0.8093	-0.8118	-0.8098	-0.8097
0	100	-0.8083	-0.8068	-0.8093	-0.8073	-0.8072

Table 4.3: The repeated mass magnetic susceptibility of sea water fraction in formation water.

This is necessary due to the sensitivity of the measurements and also to confirm a similar trend of results that are consistent with earlier results. Figure 4.2, shows that the repeated results, which are consistent with the trend earlier obtained, i.e. much lower mass magnetic susceptibility (higher negative) with 100% formation brine and no sea water in the mix. The mass magnetic susceptibility gradually increases (becomes less negative) as the percentage of sea water increases until the highest mass susceptibility (lowest negative) is obtained when the percentage of sea water reaches 100% and there is no formation brine in the mix.

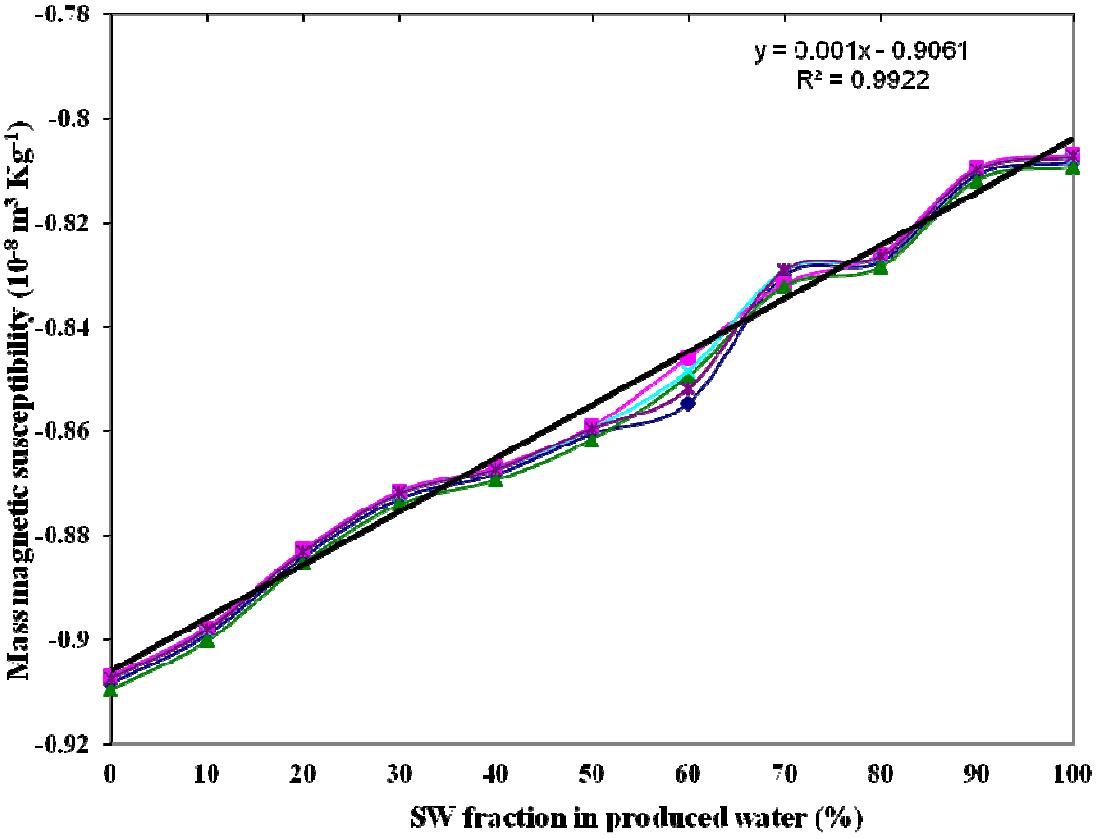

Figure 4.2: Mass magnetic susceptibility of various mixes of sea water and formation water repeatability texts.

Figure 4.3 shows the results for the same representative sea water sample (with sulphate 2960 ppm) and formation brine (without barium), with results for sea water sample (without sulphate) and formation brine (with barium 279 ppm), and only NaCl added to the SW-FW. The trend obtained is consistent with earlier results. This shows the accuracy of the results obtained. Figure 4.3, also demonstrated that sodium chloride is the main constituent that affects mass magnetic susceptibility, but that barium, and sulphate in particular, also add to the effect.

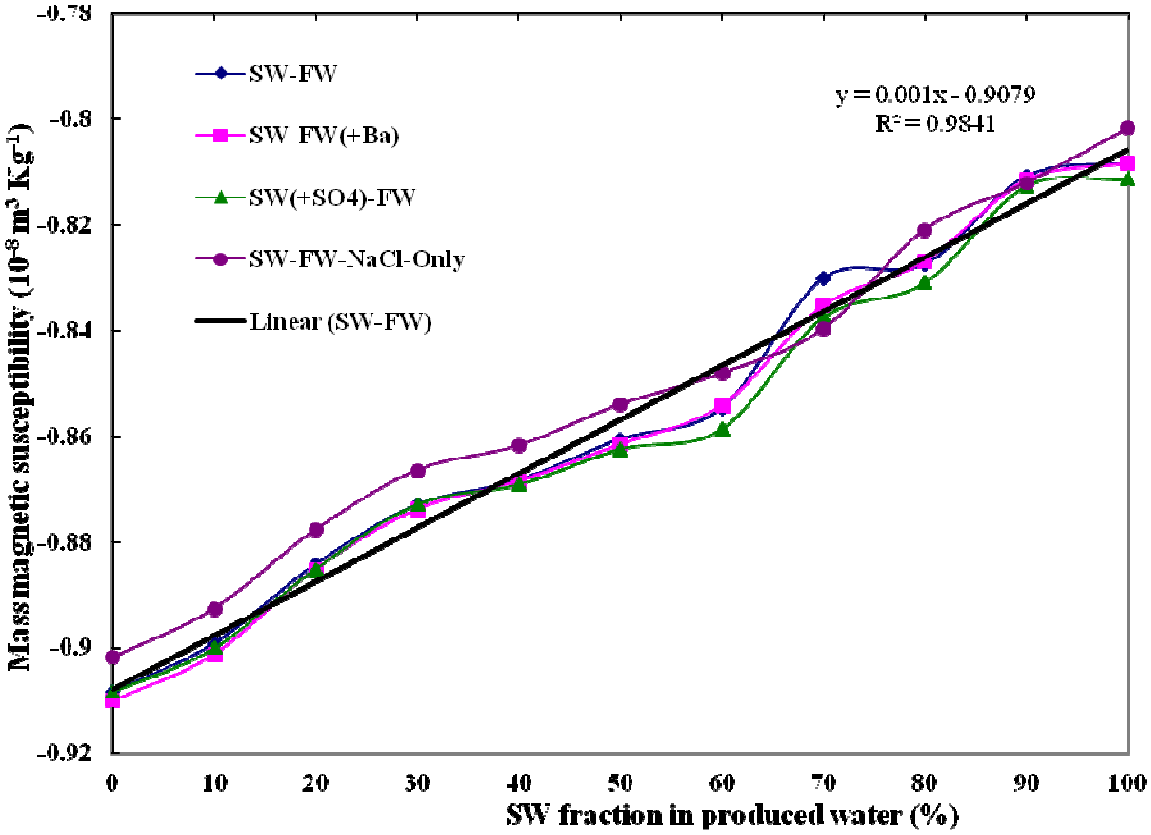

Figure 4.3: Mass magnetic susceptibility of various mixes of sea water and formation water, when the base case seawater has no sulphate and the formation water has no barium, and where e these ions are subsequently included.

4.5 TDS Measurement for sea water in formation water mix

Figure 4.4 shows the sea water fraction in the produced water vs. total dissolved solid and also the sea water fraction in the produced water vs. density. From the graph in Figure 4.5, as the sea water percentage gradually increases to 100% the magnetic susceptibility decreases (becomes less negative) due to a decrease in TDS. Similarly, as the sea water fraction in the mix increases, the density decreases, and as the sea water percentage in the fraction decreases the density increases (Figure 4.6).

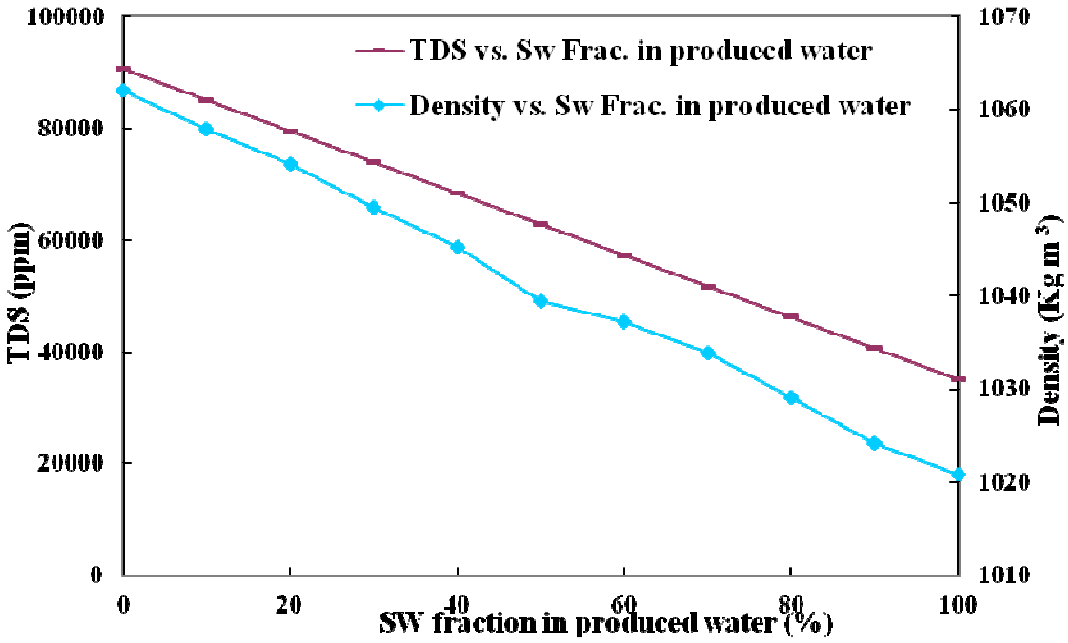

Figure 4.4: Total dissolved solid vs. sea water fractions in produced water and also the density vs. sea water fraction in produced water.

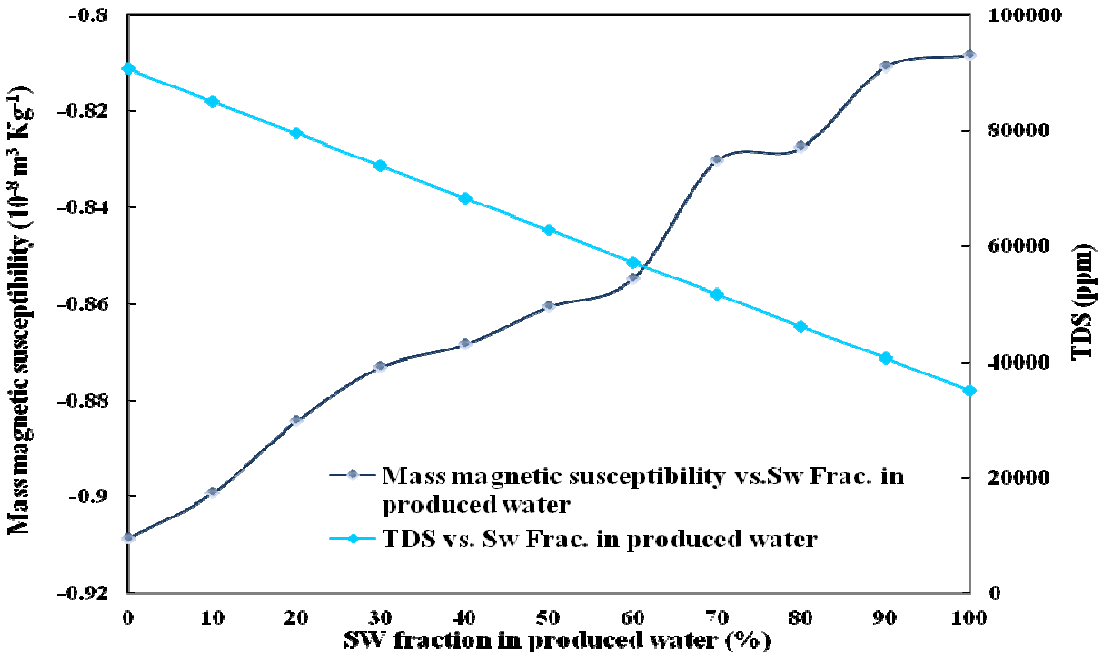

Figure 4.5: Total dissolved solid vs. sea water fractions in produced water and also mass magnetic susceptibility vs. sea water fraction in produced water.

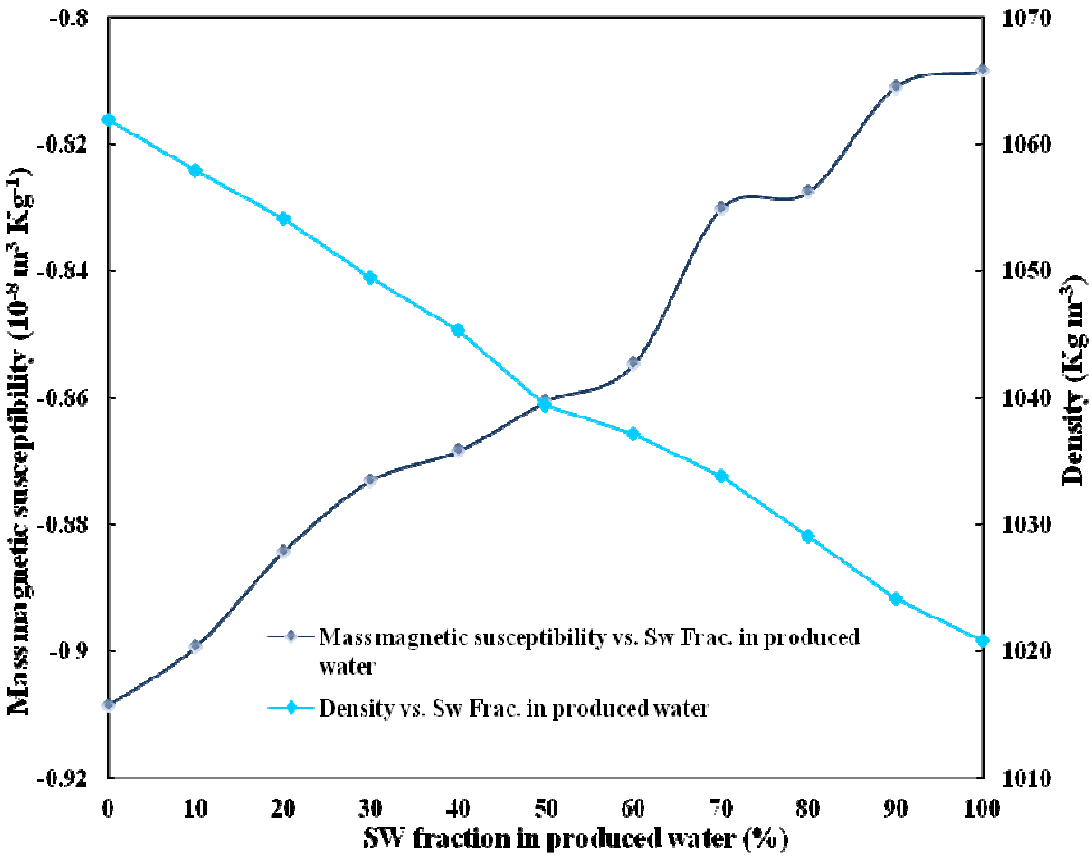

Figure 4.6: Density vs. sea water fractions in produced water and also mass magnetic susceptibility vs. sea water fraction in produced water.

4.6 Summary:

For the technique to be effective there must be a salinity contrast between the formation brine and seawater (or the presence of key ions that affect the magnetic susceptibility at different concentrations in the two brines).

Large metallic objects should not be present in the near vicinity of the magnetic equipment (say within two meters).

At present, we need to extract a brine sample from the production line for onsite magnetic susceptibility measurements. And after that, we have plans to deploy the magnetic sensor in conjunction with a flow cell to measure the brine stream in real time.

The presence of elemental iron would give much higher magnetic susceptibility values. However, this could be another application of the magnetic technology to detect corrosion in injection/production pipelines for instance.

The single main advantage of the technique is the reduction in time from weeks to minutes in identifying injection water breakthrough in hydrocarbon production. This will enable the operator to make decisions about oilfield scale management which may prevent loss of oil production wells due to scale deposition in the production system restricting hydrocarbon flow or damaging sensitive equipment, such as subsurface safety valves, for example.

Blind testing of the method using synthetic brine samples has already proved the method to be very effective. Further testing of the method using scale inducing brines is required. The next example would be to use field samples obtained from an oilfield production system, and compare the results with conventional ion chromatography techniques. The technique would also need to be tested in an environment where there is metallic equipment in a confined space to simulate offshore production facilities, before eventually being field trialled offshore.

CHAPTER 5: IDENTIFICATION AND QUANTIFICATION OF MINERALS IN RESERVOIR SCALE SAMPLES USING MAGNETIC HYSTERESIS MEASUREMENTS

5.1 Introduction

In this chapter, we will make use of magnetic hysteresis measurements to identify and quantify the key scale minerals present in reservoir scale samples. We initially prepared synthetic scale samples in the laboratory using a mixture of reservoir scale minerals. We then performed magnetic hysteresis measurements on these samples using Variable Field Translation Balance (VFTB) equipment described in Chapter 2. The hysteresis curves are a plot of magnetisation (y-axis) versus applied magnetic field (x-axis). Our results show that magnetic hysteresis measurements can identify as well as quantify various scale minerals present in reservoir scale samples. The ease of identification is due to the distinct magnetic behaviour (diamagnetic, paramagnetic, ferrimagnetic) of different reservoir scale minerals (see Chapter 2, Section 2.2 for details).

On the magnetic hysteresis curve, diamagnetic minerals exhibit straight lines of negative high field slope. This is shown in figure 5.1. In contrast, paramagnetic minerals exhibit straight lines with positive high field slope. A mixture of a diamagnetic and paramagnetic mineral will have a slope that is dependent upon the amount of the two minerals present in the sample. Therefore the slope of the hysteresis curves at high applied fields can potentially allow very sensitive and subtle changes in the magnetic mineralogy to be readily identified. Also by quantifying the change in high field slope, we can accurately quantify the content of paramagnetic and diamagnetic minerals (when two componetnts are present). This can be important, since the majority of the scale minerals are either diamagnetic (for instance, barite, anhydrite, celestite, and gypsum) or paramagnetic (for instance, siderite, illite). These subtle mineralogical changes, which can be easily recognised and quantified from the hysteresis curves, are sometimes difficult to detect by other conventional methods such as X-ray diffraction (XRD).

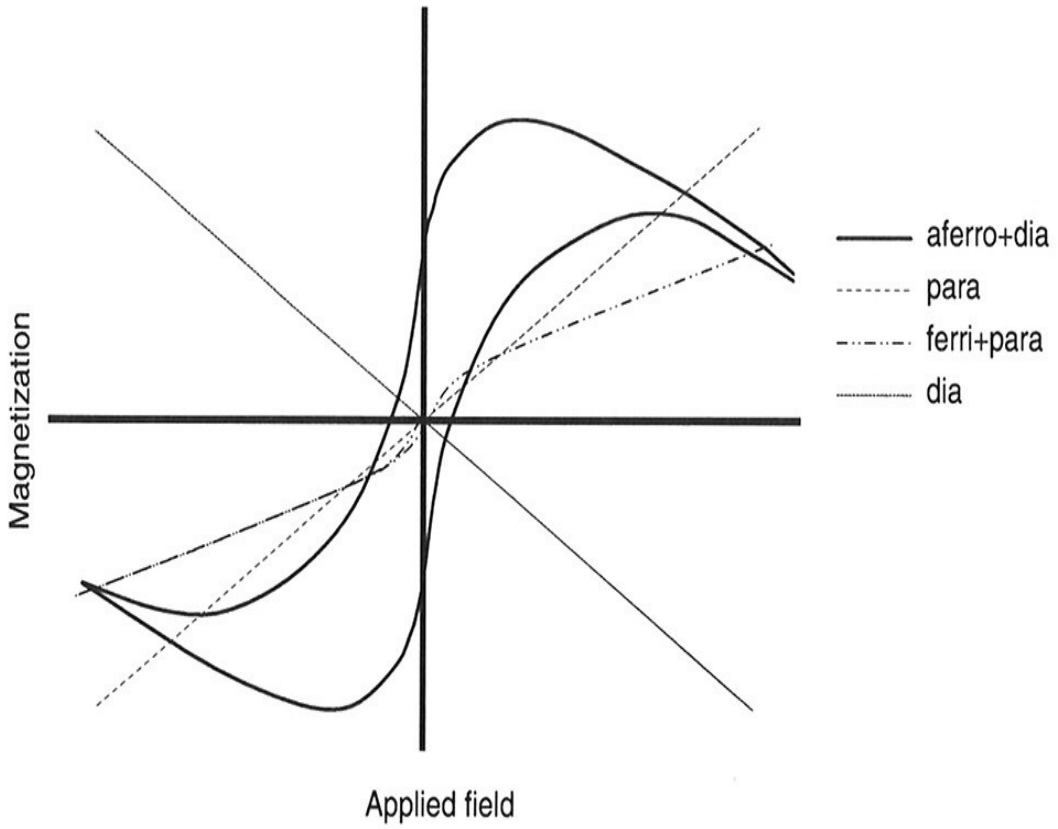

Figure 5.1 Magnetic hysteresis curves of typical diamagnetic, paramagnetic and ferrimagnetic minerals. Modified after Ali and Potter (2010).

Apart from paramagnetic and diamagnetic minerals, magnetic hysteresis measurements can also identify the presence of ferrimagnetic minerals (such as iron oxide magnetite) and canted antiferromagnetic minerals (such as iron oxide hematite) in reservoir scale samples. The presence of these minerals causes "kinks" in the low field region of the hysteresis curves as shown in Figure 5.1. Generally, the higher the kink, the higher is the concentration of these ferrimagnetic minerals.

Another potential advantage of magnetic hysteresis measurements is that they can provide information about the size of the ferrimagnetic particles present in reservoir

scale samples. This is achieved by measuring magnetic hysteresis parameters (Hc, Hcr, Ms, Mrs; their explanation is given in chapter 2) and plotting them on a typical Day type plot. For instance, if the Day plot analyses indicates that the particles are multidomain (rather than being single-domain or superparamagnetic), this would mean that the particles are likely to be around the micron size range rather than the nanometer size range. Apart from grain size information,magnetic hysteresis measurements can also differentiate the presence of magnetite from hematite. The presence of magnetite is indicated by a narrow kink which saturates at relatively low applied fields. If there is hematite present in the sample, the kink becomes relatively wider and also saturates at much higher applied fields (we will show the magnetic hysteresis results for magnetite and hematite in the chapter).

Magnetic susceptibility on the magnetic hysteresis curves is given by the slope of the line which is a ratio of magnetisation over applied magnetic field. The initial low-field magnetic susceptibility *(χ_o)* measures the overall induced magnetisation of all minerals present in reservoir scale sample (this may include one or more of the ferrimagnetic, diamagnetic, paramagnetic, and antiferromagnetic minerals).

$$\chi_o = \chi_{ferro} + \chi_{dia} + \chi_{para} + \chi_{antiferro} \qquad 5.1$$

Since ferrimagnetic minerals saturate at relatively low applied fields, the magnetisation at high applied fields will only be due to the contribution of paramagnetic, diamagnetic, and antiferromagnetic minerals in the sample. Therefore the magnetisation at high applied fields above Ms (saturation magnetisation of ferrimagnetic minerals) can be used to calculate the high-field magnetic susceptibility (χ_{Hfld}).

$$\chi_{Hfld} = \tan(\alpha) = \chi_{dia} + \chi_{para} + \chi_{antiferro} \qquad 5.2$$

where α is the slope of the high field hysteresis line. This is usually determined using magnetic field range >750 mT, where the ferrimagnetic component saturates and therefore do not contribute to the slope of the hysteresis curve.

The difference between the high-field and the low-field magnetic susceptibility of a reservoir scale sample gives the magnetic susceptibility due to the ferrimagnetic component in the sample:

$$\chi_{ferri} = \chi_o - \chi_{Hfld} \qquad 5.3$$

In the remaining description of this chapter, we will call ferro/ferri/antiferromagnetic minerals as ferrimagnetic minerals

5.2 Identification and quantification of diamagnetic reservoir scale minerals.

We initially measured low field mass magnetic susceptibility of four scale minerals in the laboratory using Bartington's MS2B magnetic susceptibility bridge (details of the equipment are given in chapter 2). Table 5.1 shows the results of low field volume magnetic susceptibility measurements and those converted into mass magnetic susceptibility (dividing volume magnetic susceptibility by the density of the sample).

	Density		Volume magnetic Susceptibility χ_v		Mass magnetic Susceptibility χ_m
Sample	g/cc	Kg/m^3	cgs. 10^{-6}	SI 10^{-6}	$10^{-8}\ m^3\ kg^{-1}$
Anhydrite	2543	1.683	-0.5078	-6.3785	-0.379
Barite	1683	2.543	-0.7815	-9.8159	-0.386
Celestite	2189	2.189	-0.6807	-8.5502	-0.3906
Gypsum	857	0.857	-0.3726	-4.6801	-0.5461

Table 5.1: Magnetic susceptibility measurements for pure scale minerals.

Figure 5.2 shows mass magnetic susceptibility values obtained in Table 5.1 for the four reservoir scale minerals. Gypsum shows the highest diamagnetism which is evident by its highest negative mass magnetic susceptibility compared to the other three minerals. Celestite, barite and anhydrite show very similar mass magnetic susceptibility values.

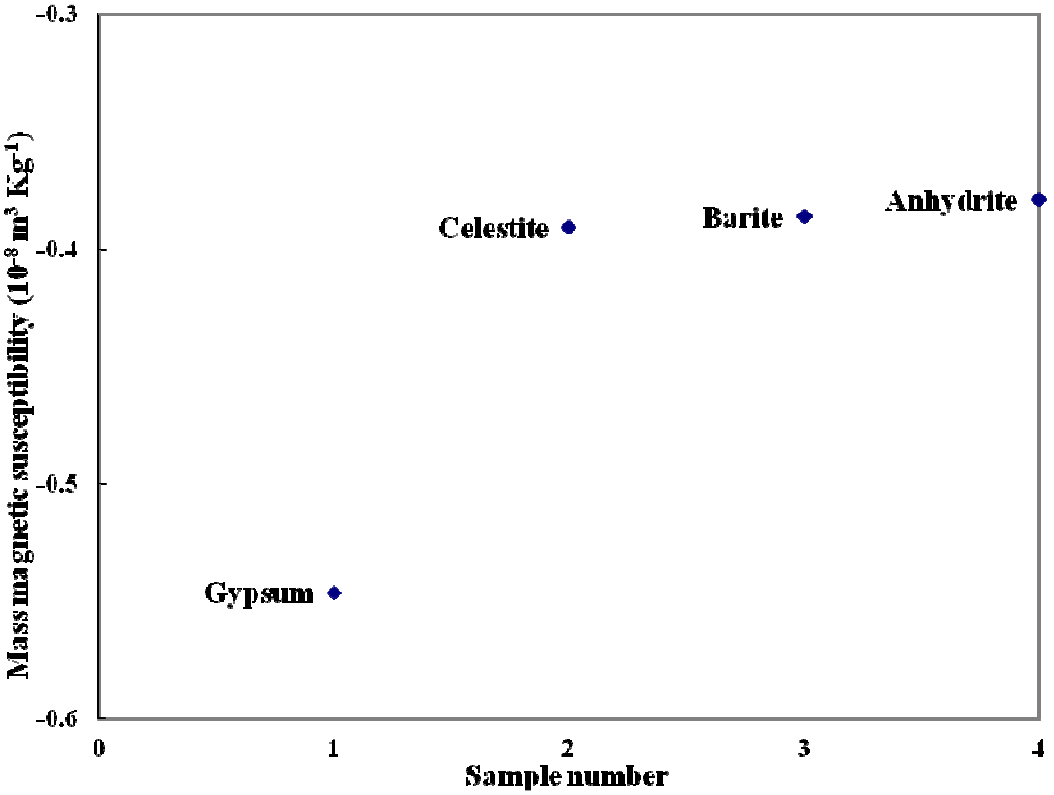

Figure 5.2: Mass magnetic susceptibility of pure scale minerals.

In Figure 5.3 we have plotted magnetic hysteresis curves of the four samples in Figure 5.2 (that is barite, anhydrite, celestite and gypsum). Since we are working with pure synthetic samples, their magnetic hysteresis curves exhibit no kinks at low applied fields indicating there are no ferrimagnetic impurities present in the samples. A negative high field slope for all of the four samples indicates that all of them are diamagnetic. It is interesting to note that minerals such as barite, anhydrite and celestite posses a very similar high field slope which indicates that the three minerals possess a very similar diamagnetism. This is consistent with the low field magnetic susceptibility measurements shown in Table 5.1 where the three minerals show very similar mass magnetic susceptibility values. Figure 5.3 shows that gypsum is relatively more diamagnetic as shown by a more negative high field slope on the hysteresis curve. This suggests that we can potentially distinguish between gypsum and other diamagnetic

scale minerals in reservoir scale samples. We can also quantify different reservoir scale minerals if they have distinct magnetic susceptibilities. For example, a reservoir scale sample containing a mixture of gypsum and barite will have a slope somewhere between 100% gypsum line and 100% barite line depending on the content of the two minerals. The higher the barite content, the more the high field slope would be pushed towards 100% barite line. It is important to mention that the magnetic technique (either low field or high field) mentioned in this chapter works on the basis that the minerals present in a sample have distinct magnetic susceptibilities. If a sample contains a mixture of minerals which have no magnetic susceptibility contrast (for instance a mixture of celestite, barite and anhydrite), it would then be impossible for the magnetic techniques to identify and quantify individual minerals in the sample. We have used mass magnetization in the hysteresis plots as the equipment (VFTB) provides mass magnetization data which is indepent of porosity of the samples.

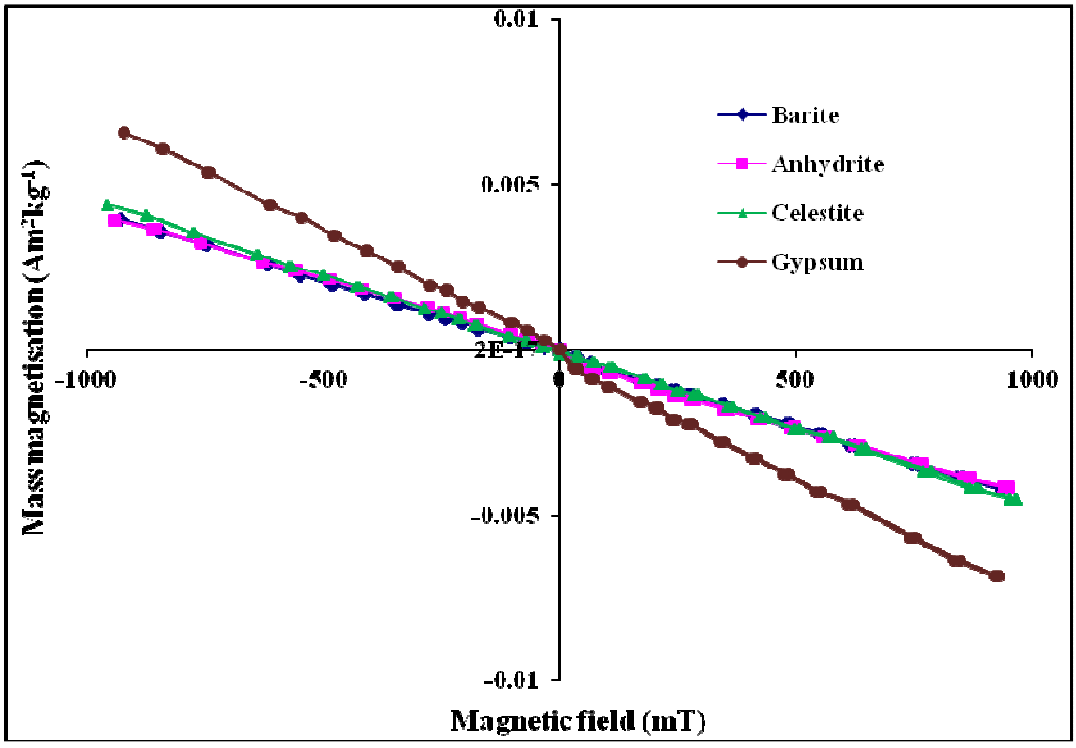

Figure 5.3: Experimental magnetic hysteresis curves of pure barite, anhydrite, celestite, and gypsum.

For mineral quantification, we have created theoretical model templates for various reservoir scale mineral mixtures. Figure 5.4 shows model templates for gypsum and Anhydrite. One can see how sensitive these magnetic hysteresis measurements are in picking small variations in mineralogy.

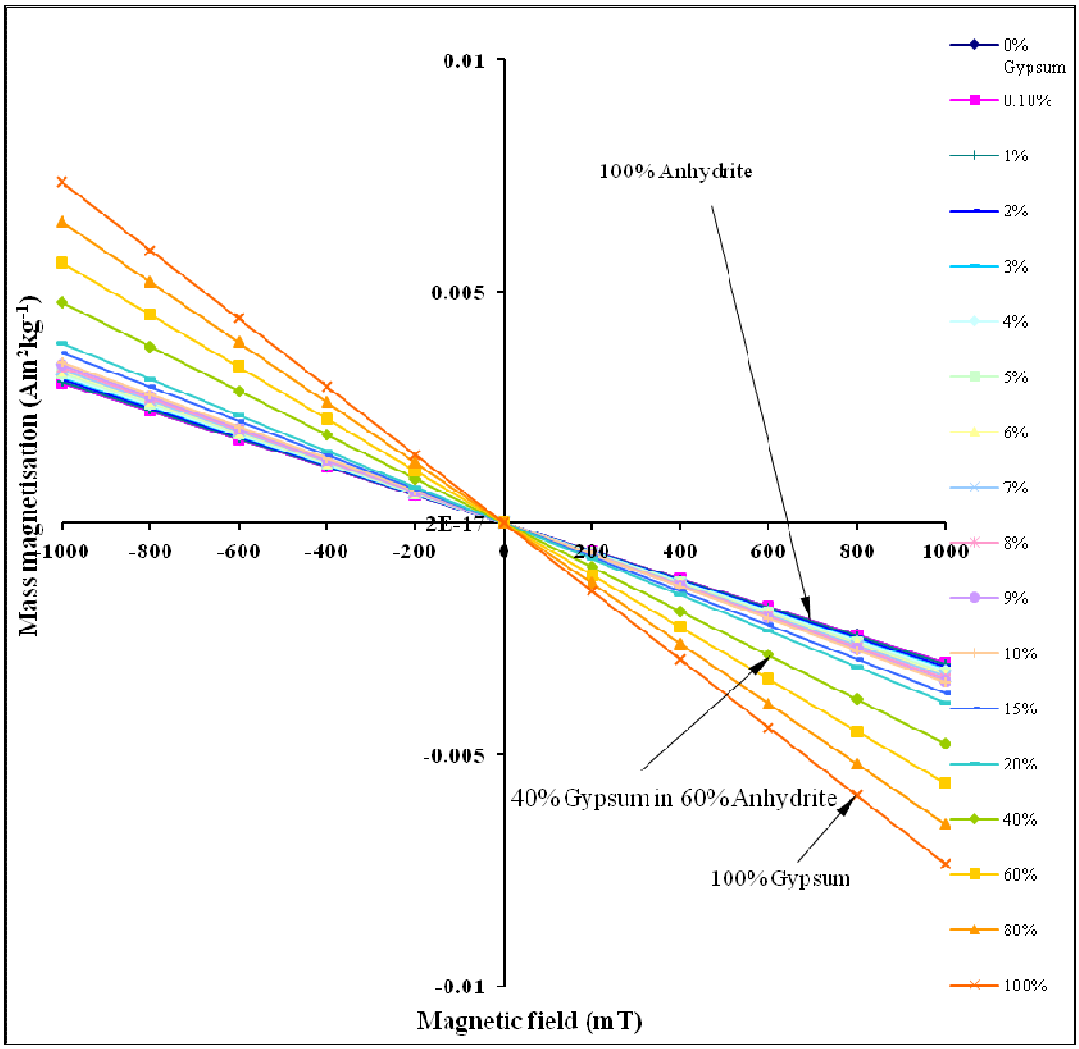

Figure 5.4: Theoretical model templates of various concentrations of gypsum in anhydrite matrix.

5.3 Identification and quantification of paramagnetic reservoir scale minerals.

In figure 5.5 we have shown experimentally measured magnetic hysteresis curve of pure barite (a diamagnetic mineral) and three other hysteresis curves for 2%, 4% and 10% siderite (by weight) in a barite matrix. Since siderite is paramagnetic, its presence would shift the high field slope of the hysteresis curve upwards. The higher the concentration of siderite in a barite matrix, the higher would be the high field positive slope.

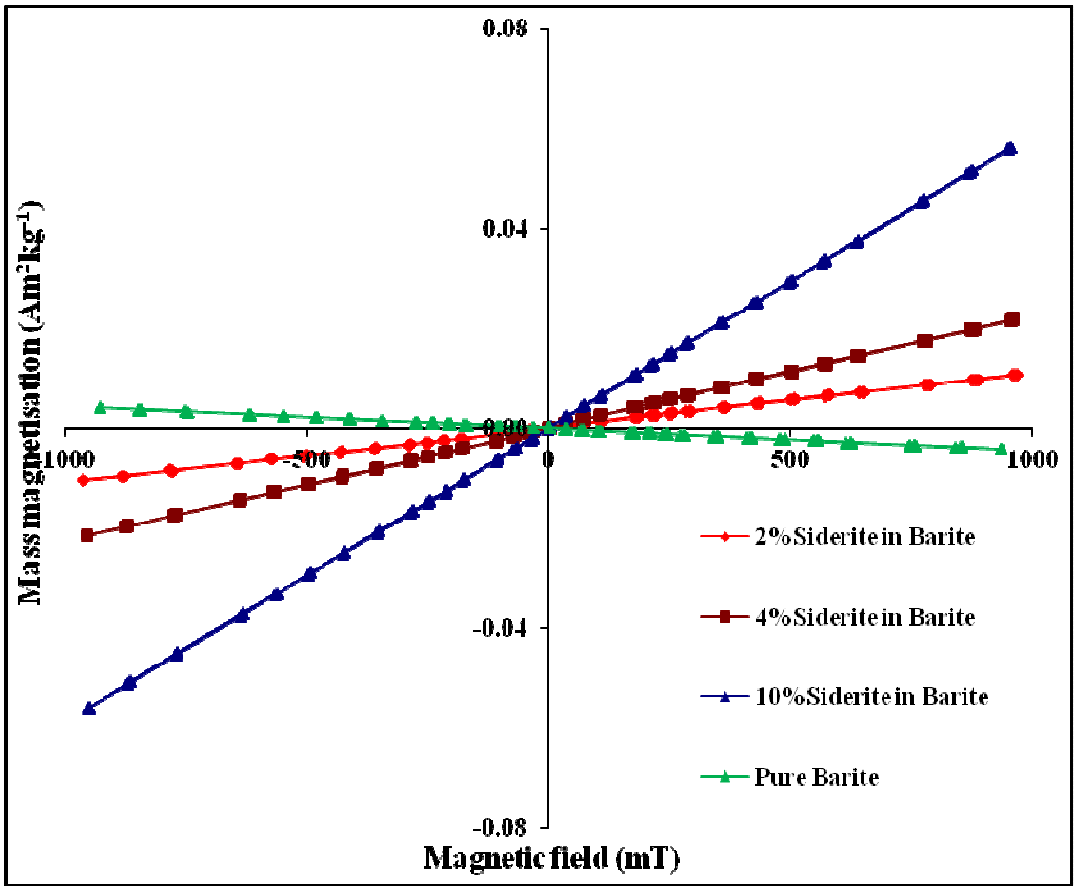

Figure 5.5: Experimental magnetic hysteresis curves of pure barite mineral and a mixture of barite and siderite.

In Figure 5.6 we have drawn theoretical model templates of magnetic hysteresis curves for various concentrations of siderite in a barite matrix. Therefore, by experimentally measuring the magnetic hysteresis curve of a reservoir scale sample and plotting it on the model template of the corresponding mineral (known by X-ray or similar techniques), one can accurately quantify the minerals present in the sample.

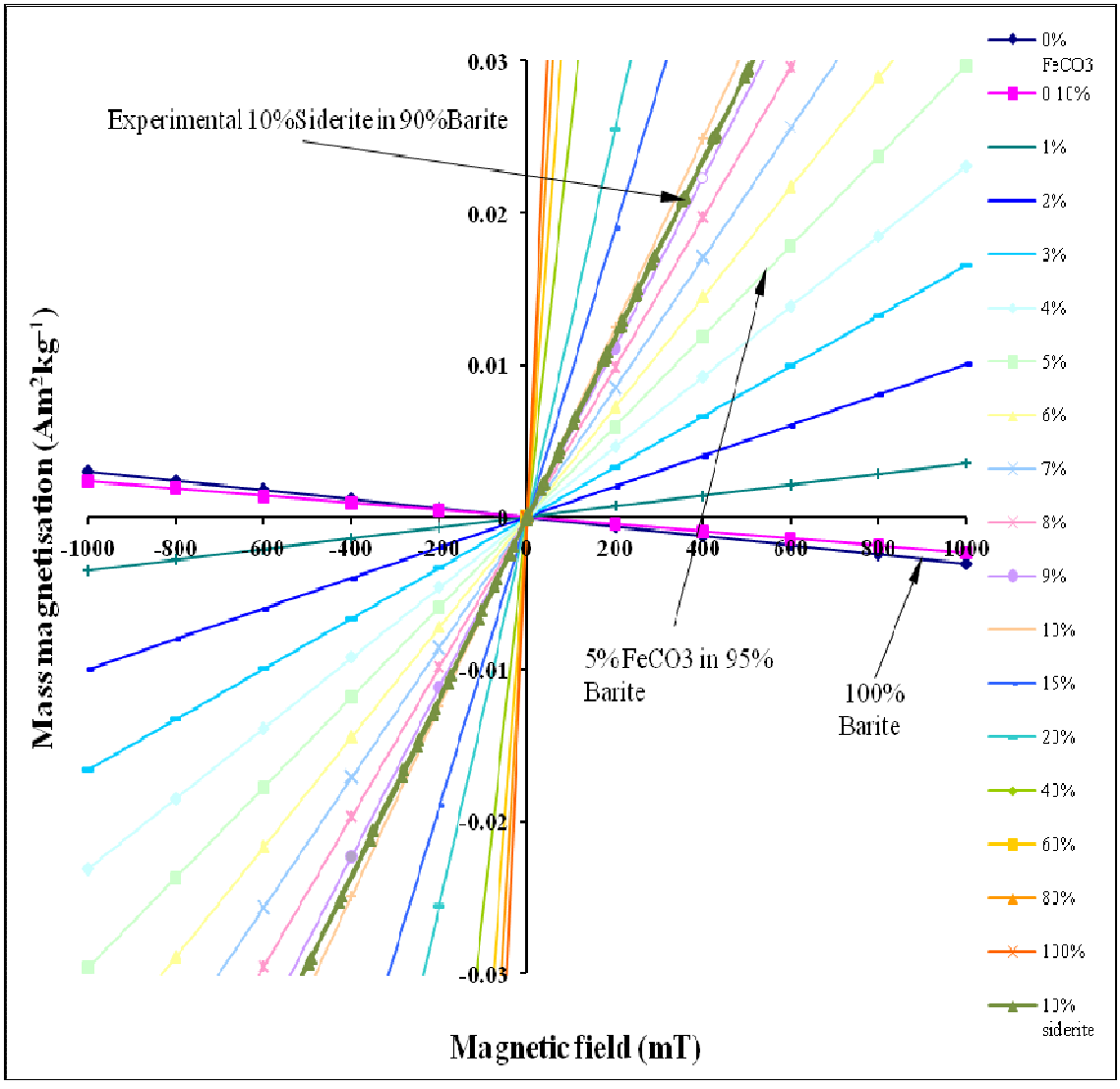

Figure 5.6: Theoretical magnetic hysteresis curves of various concentrations of siderite (FeCO3) in barite matrix. Percentage values in the legend indicate the concentration of siderite in barite matrix. The experimentally measured magnetic hysteresis curve of 10% siderite in 90% barite matrix is shown too.

To verify our model templates, we made up a synthetic sample in the lab consisting of 10% siderite by weight in a barite matrix. Figure 5.6 shows the experimental magnetic hysteresis curve of the synthetic sample which falls almost on the 10% line of the theoretical model template. A slightly lower high field slope of the experimental curve is due to the fact that we could not source a 100% pure siderite mineral. In most cases it is 99% pure and which explains why the hysteresis curve of the experimental samples falls slightly short compared to the theoretical line. This also shows how accurate our magnetic hysteresis measurements are in picking up subtle changes in mineralogy and if there are any impurities present in pure minerals. In this particular case, the impurity is likely to be of diamagnetic nature, the reason experimental hysteresis curve shows slightly lower high field slope. If the impurity would have been of paramagnetic nature, the experimental curve would have still been either lower (supposing paramagnetic susceptibility of the impurity is lower than of siderite mineral) or higher (supposing paramagnetic susceptibility of the impurity is higher than of siderite mineral) compared to the theoretical curve.

In figure 5.7 another theoretical model template of magnetic hysteresis curves has been drawn for various concentrations of illite in a barite matrix and a plot of experimental hysteresis curve of a mixture of 10% illite by weight in barite matrix, and again the experimental curve falls almost on the theoretical template.

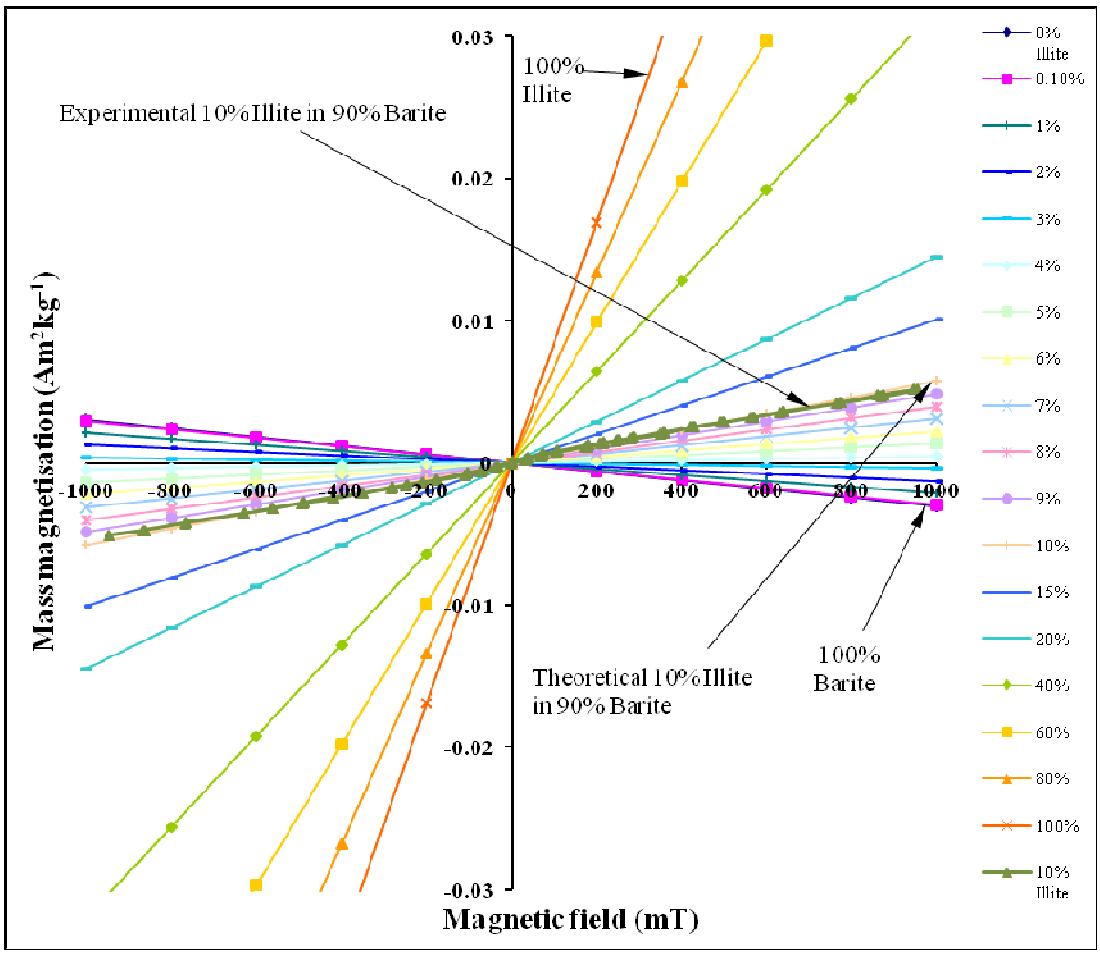

Figure 5.7: Theoretical magnetic hysteresis curves of various concentrations of illite in barite matrix. Percentage values in the legend indicate the concentration of illite in barite matrix. The experimentally measured magnetic hysteresis curve of 10% illite in 90% barite matrix is shown too.

In figure 5.8 we could see from experimentally measured magnetic hysteresis curves of pure barite (a diamagnetic mineral) 10% siderite and 10% illite (by weight) in a barite matrix. Since siderite and illite are paramagnetic, their presence would shift the high field slopes of the hysteresis curves upwards. Even we could see the difference in slopes between the 10% (by weight) of both the paramagnetic minerals in a barite matrix.

Majority of minerals have distinct magnetic susceptibilities and which makes it easy for one to recognize their presence (Figure 2.2 Chapter 2). However some minerals show a range of magnetic susceptibilities. If one has information on the mineralogy from drill cuttings, whole cores or from XRD type analysis, we can then quantify minerals very easily.

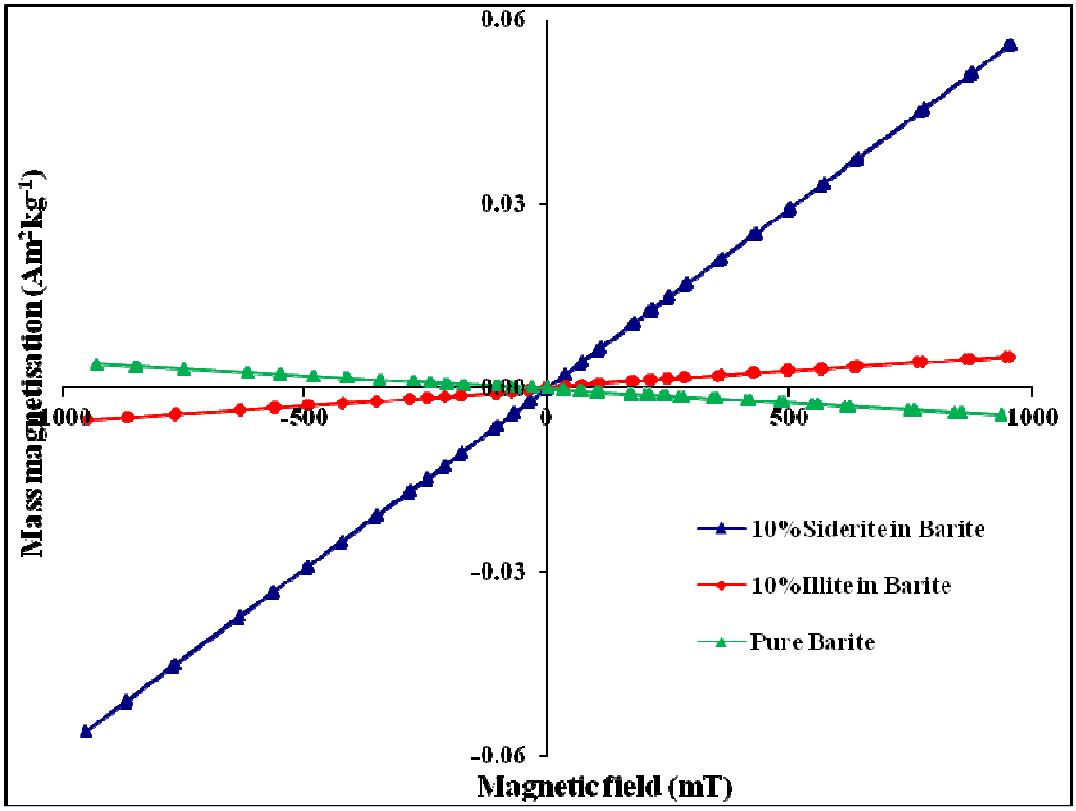

Figure 5.8: Experimental magnetic hysteresis curves of pure barite (a diamagnetic mineral), and 10% siderite and illite (by weight) in a barite matrix.

5.4 Identification of ferrimagnetic minerals found in reservoir scale samples

Magnetic hysteresis measurements enable us to identify the presence of ferrimagnetic minerals in reservoir scale samples. Ferrigamagnetic minerals show a kink at low applied fields which saturates at relatively low applied fields if there is iron oxide magnetite present in the sample, whereas it saturates at much higher applied fields if

there is iron oxide hematite present. Therefore, our measurements cannot only detect the presence of such minerals but also can differentiate between the type of ferromagnetic minerals. Figure 5.9 shows a small fraction of iron oxide magnetite (1% by weight) present in a barite matrix. For comparison, we have also shown two types of iron oxide hematite minerals (designated by A and B) present in a barite matrix (again 1% by weight). Magnetite shows much higher magnetic susceptibilities compared to hematite and this is apparent from the magnitude of magnetisation on the y-axis. One can also note that the sample containing magnetite saturates at relatively low applied fields whereas hematite samples saturate at relatively higher applied fields.

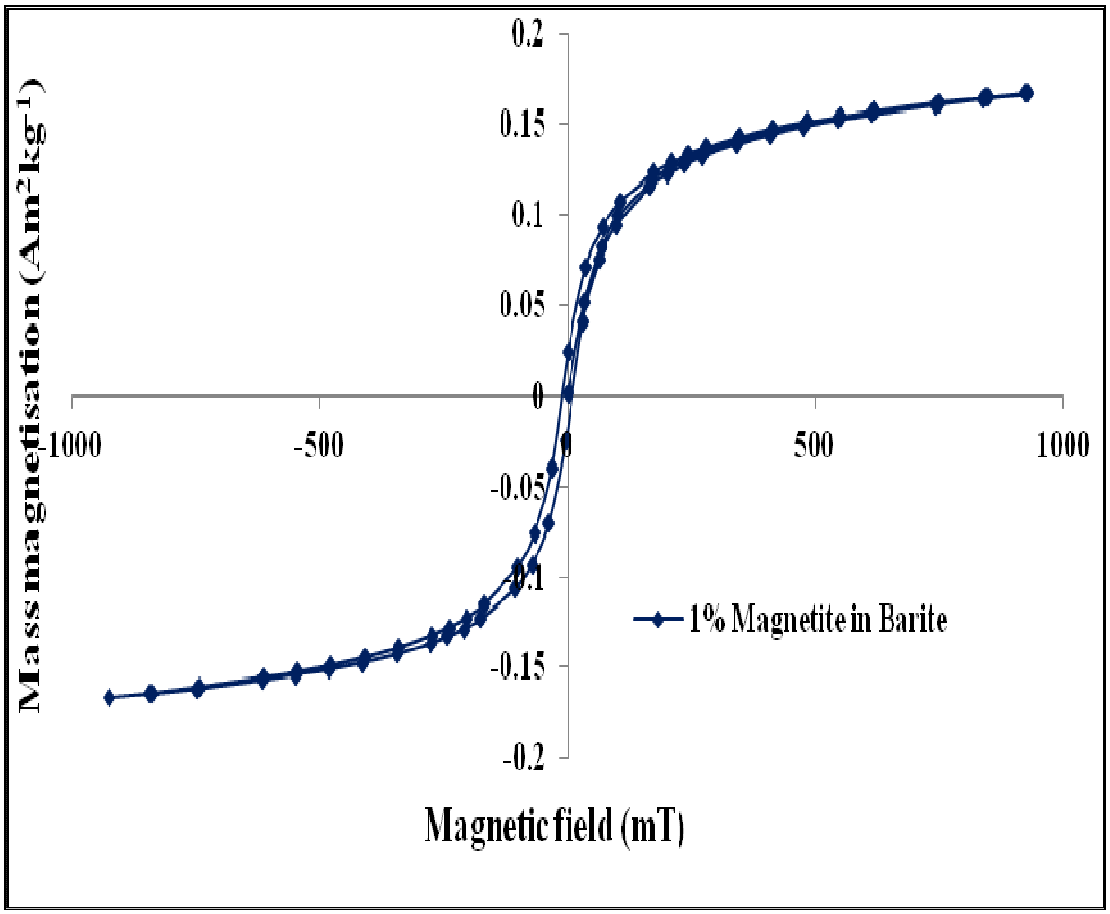

Figure 5.9: Experimental magnetic hysteresis curves of 1% magnetite sample mineral (by weight) in a barite matrix.

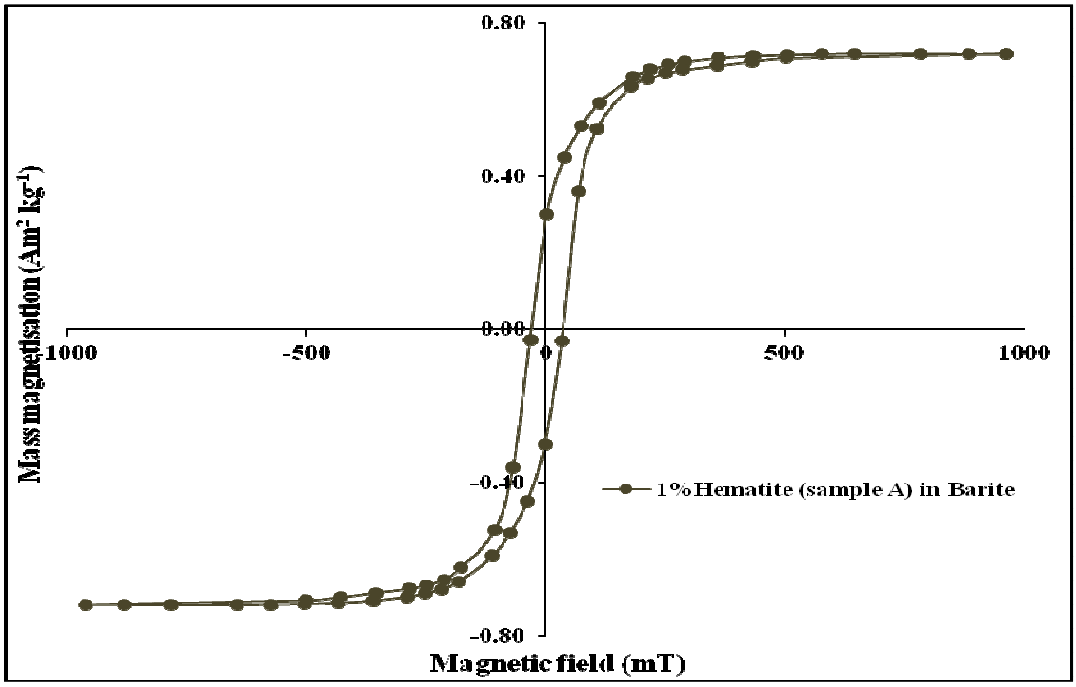

Figure 5.10: Experimental magnetic hysteresis curves of 1% hematite sample A mineral (by weight) in a barite matrix.

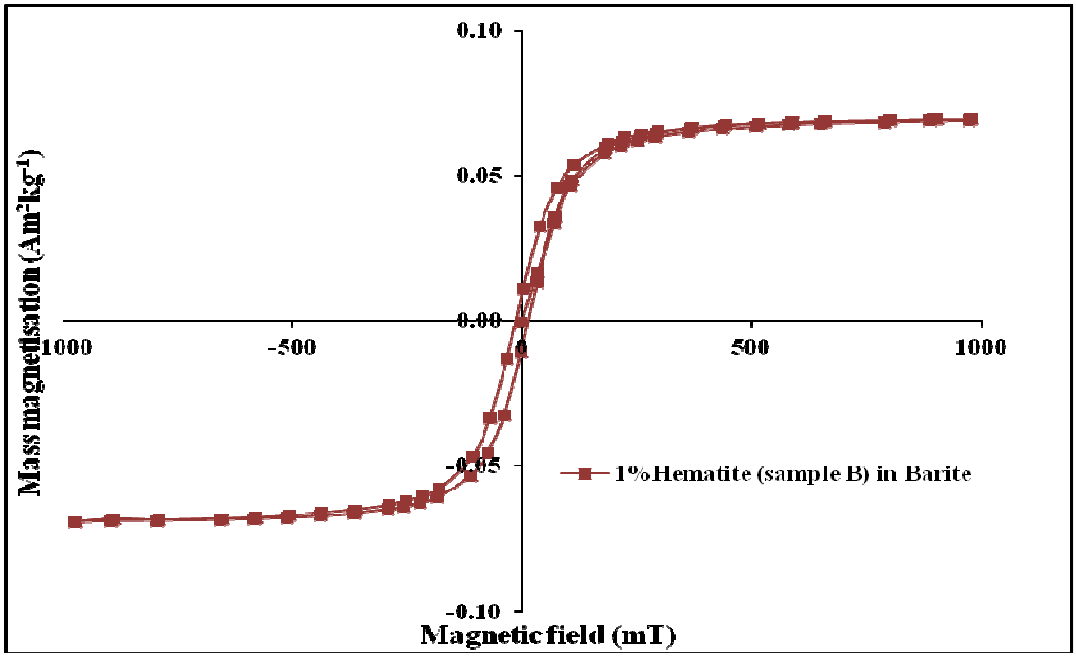

Figure 5.11: Experimental magnetic hysteresis curves of 1% hematite sample B mineral (by weight) in a barite matrix.

5.4.1 Ferrimagnetic minerals – their domain and particle size

A significant property of ferrimagnetic materials is not only that they have a spontaneous magnetisation, but also that their magnetisation can be influenced by the application of low magnetic fields. In order to minimize the magneto static force the magnetisation of a ferromagnetic grain breaks down into smaller units called domains. It is generally considered that domains are uniformly magnetised and the magnetic moments within each domain are parallel (Kittel, 1949). Therefore, a grain will split into zones, which are all magnetised to saturation but in different directions. In a case where the individual domains are arranged randomly the grain will have a total net magnetic moment of zero. Domains are separated by zones, Bloch walls, in which the electron spin moments cant over from the direction of one domain to that of an adjacent domain. Although a wide range of domain sizes is observed, they are still relatively small in the range of 1-100 μm, however much larger than atomic distances.

In an applied strong magnetic field the Bloch walls unroll in such way as to increase the total volume of domains with a magnetisation in the same direction as the applied field. In weak fields the Bloch walls return to their original positions upon removal of the applied field (Thompson and Oldfield, 1986). However, in higher magnetic fields the Bloch walls may move into new minimum energy positions from which they cannot escape after the field is removed. Non-reversible migration of the Bloch walls produces a remanent magnetisation that is stable in the absence of an applied field. Saturation magnetisation of the ferromagnetic material occurs when the extemal field is strong enough to align completely all the domain moments.

The number of the domain subdivisions is a function of particle size and mineralogy. Consequently, the magnetic properties of a particle depend on the domain state of the particle, which mainly is equal to the number of domains. Very large particles have large numbers of domains and they are termed multi-domain (MD). They tend to be

easily magnetised and their magnetic remanence can be easily altered. Small particles that have only one domain are called single-domain (SD). Because the single-domain grains do not contain Bloch walls that can migrate with applied magnetic fields, they tend to be more stable than their multi-domain counterparts. The SD magnetic remanence is harder to change, therefore the SD grains are considered to be the ideal recorders of a palaeomagnetic field.

In our analysis, we tried to identify the domain states and particle size of the two hematite samples we used in Figures 5.10 and 5.11. For this, we measured the magnetic hysteresis parameters for the two hematite samples including coercivity (Hc), coercivity of remanence (Hcr), saturation magnetization (Ms) and saturation remanent magnetization (Mrs) (the details of the hysteresis parameters are shown in chapter 2). The results are shown in Table 5.2.

Sample No	**Hcr mT**	**Hc mT**	**Mrs Am^2kg^{-1}**	**Ms Am^2kg^{-1}**	**Mrs/Ms**	**Hcr/Hc**
Sample A	87.5	35	0.28	0.72	0.388889	2.5
Sample B	56.4	12	0.0085	0.0694	0.122478	4.7

Table 5.2: Hc, Hcr, Mrs, and Ms parameters for hematite samples A and B.

We subsequently plotted these hysteresis parameters as a Day plot (Day et al, 1977) in Figure 5.12. On this plot, SD grains appear on the top left hand corner and MD grains appear on the bottom right hand corner showing a change in particle size (from smaller to bigger particles) as one moves from SD to MD region. When we plotted our hysteresis parameters on this plot, we found out that sample A plots somewhere in the

middle between SD and MD regions whereas sample B plots in the MD region. The analysis potentially shows that hematite sample B contains relatively bigger sized particles compared to sample A. This is also evident by the remanent magnetisations of the two samples with sample A having a higher value (small sized particles retain relatively higher Mrs) compared to sample B.

The measurements we have done on a small powder sample with no independent grain size analysis. However Day type plot provides information on the bulk majority of the grain sizes present in a sample. In real life, yes we can encounter multiple grain sized samples and again the bulk majority of grain sizes would be reflected on the Day plot. For instance, if a sample contains majority of SD grains a fewer MD grains, the point for that sample may plot somewhere between SD-MD region.

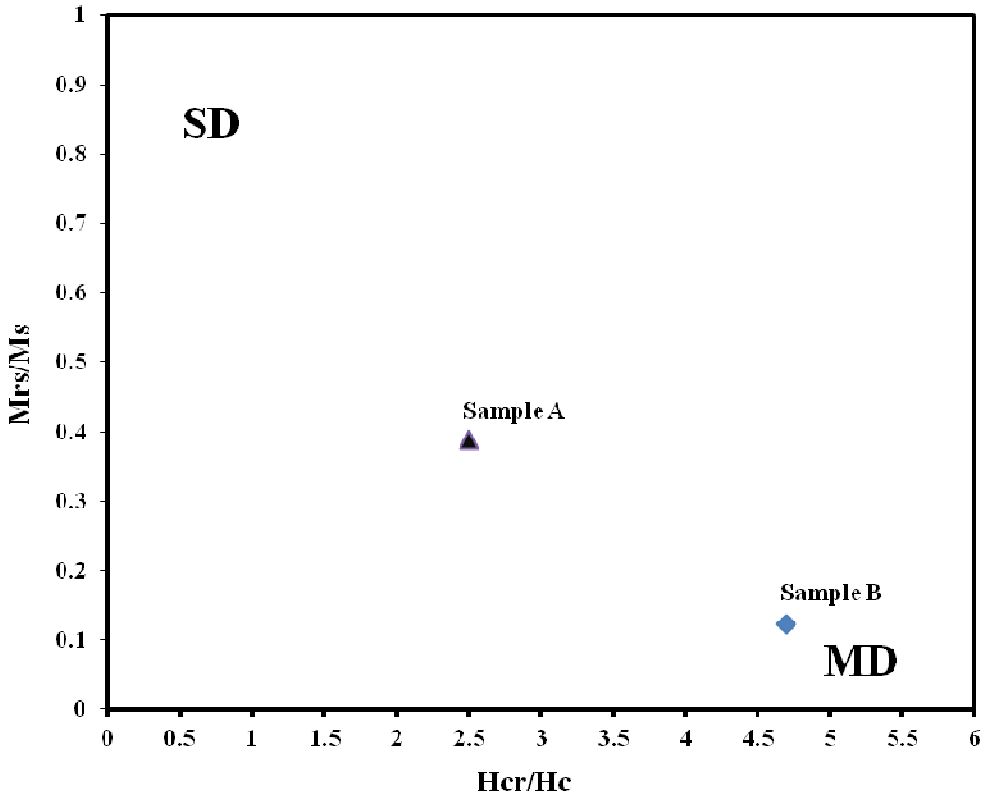

Figure 5.12: Coercivity ratio Hcr/Hc vs. remanence ratio Mrs/Ms for hematite samples A and B.

5.5 Thermomagnetic analysis of reservoir scale minerals

In order to gain an insight into the magnetic properties of reservoir scale minerals at reservoir conditions, the dependence of magnetic susceptibility with temperature has been experimentally determined for the representative reservoir scale minerals. Magnetic susceptibility measurements at low applied field reflect the combined thermal changes in a complex mineral mixture (Henry et al., 2005). For this, we performed magnetic hysteresis measurements on synthetic pure reservoir scale minerals as well as the impurities commonly found in them. Thermomagnetic hysteresis measurements help to model the behaviour of various scale minerals (ferromagnetic, paramagnetic, diamagnetic) at in-situ reservoir conditions. In this study, we performed magnetic hysteresis measurements at three different temperatures (20 ^{o}C, 89 ^{o}C, and 125 ^{o}C respectively). Our measurements showed very interesting results indicating that the change in magnetic behaviour of reservoir scale minerals with temperature depend on the type of magnetic minerals present. For example, diamagnetic scale minerals show a very little or no variation in their high field hysteresis slope with temperature. Whereas for paramagnetic scale minerals, their high field hysteresis slope decreases with an increase in temperature according to the Curie-Weiss law.

Figure 5.13 summarizes thermomagnetic properties of various minerals including paramagnetic (P), superparamagnetic (SP), ferromagnetic minerals including magnetite (MAG) and titanomagnetite (TMAG). It is difficult to interpret thermomagnetic curves when the sample contains a mixture of minerals. In such cases, thermomagnetic curves show a commulative magnetic response from the all the minerals present in the sample, e.g. a mixture of magnetite and paramagnetic minerals will produce an intermediate curve (John Dearing 1999).

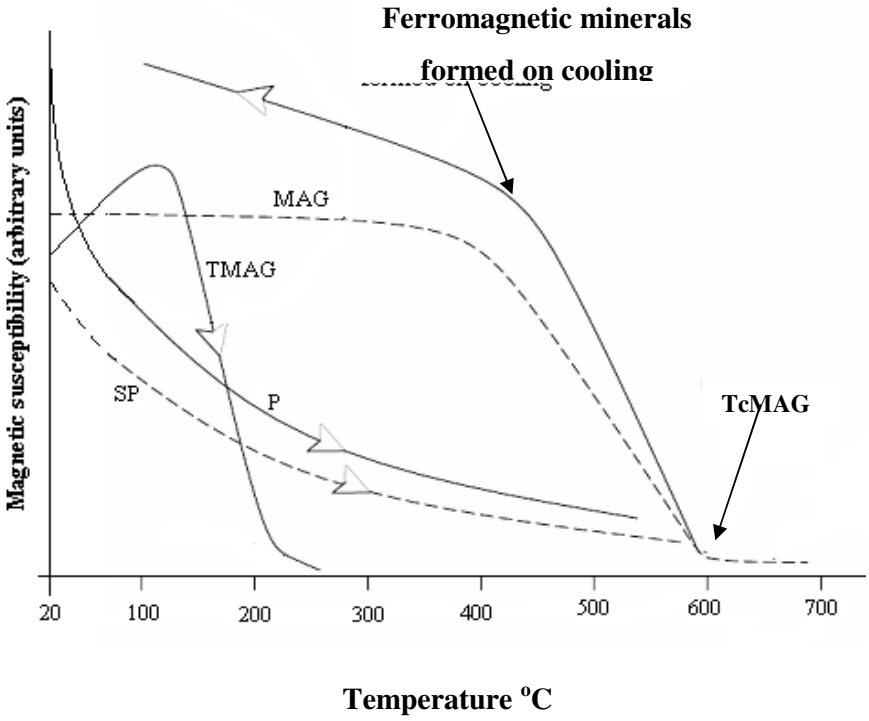

Figure 5.13: Schematic trends and transitions of low field (Lfld) magnetic susceptibility values from room temperature to +700 oC for different minerals and domains; superparamagnetic (SP), paramagnetic (P), magnetite (MAG: Tc 580 oC), titanomagnetite (TMAG: Tc 250 oC). Susceptibility axis not to scale. (based on Thomson and Oldfield 1986).

In Figure 5.14 a barite sample is measured for its magnetic susceptibility changes with temperature from hysteresis loops at a set of specific temperatures (20 ^{o}C, 89 ^{o}C, and 125 ^{o}C). This sample represents almost pure diamagnetic matrix samples with only minor amounts of paramagnetic material. Theoretically the magnetic susceptibility of a diamagnetic substance should be independent of temperature, which is consistent with the experimental results for this barite sample as shown in the figure. Small decreases of H_{fld} susceptibility with temperature may be due to tiny amounts of paramagnetic material, where the magnetic order and paramagnetic susceptibility is destroyed with increasing temperature.

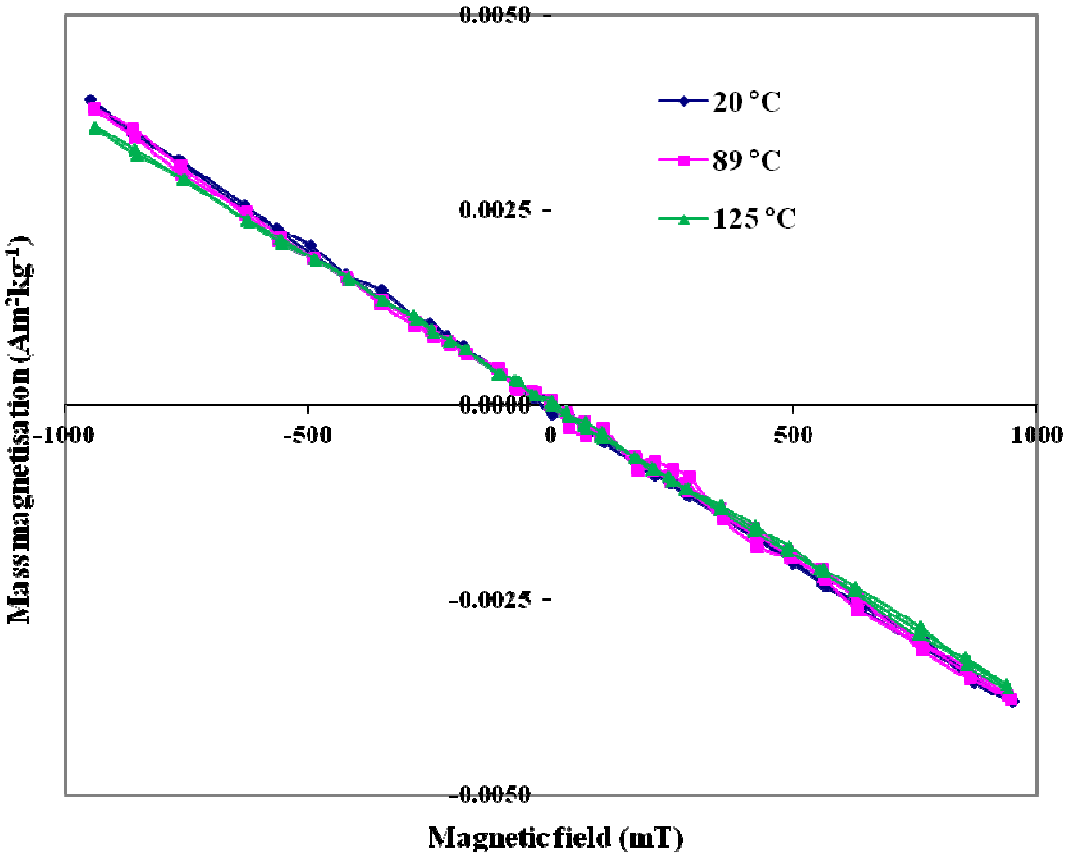

Figure 5.14: Experimental magnetic hysteresis curves for barite sample at respective temperatures (20 ^{o}C, 89 ^{o}C, and 125 ^{o}C).

To see the difference temperature effects on magnetic susceptibility changes between the diamagnetic and paramagnetic, we measure illite sample (paramagnetic) for magnetic hysteresis at different set of temperatures (20 ^{o}C, 60 ^{o}C, 89 ^{o}C and 130 ^{o}C) For the illite sample figure 5.15, the initial positive susceptibility (due to the paramagnetic a susceptibility) decreases with increasing temperature. The decrease in the magnetic susceptibility may be due to more chaotic paramagnetic ordering, leading to a reduction in the paramagnetic susceptibility.

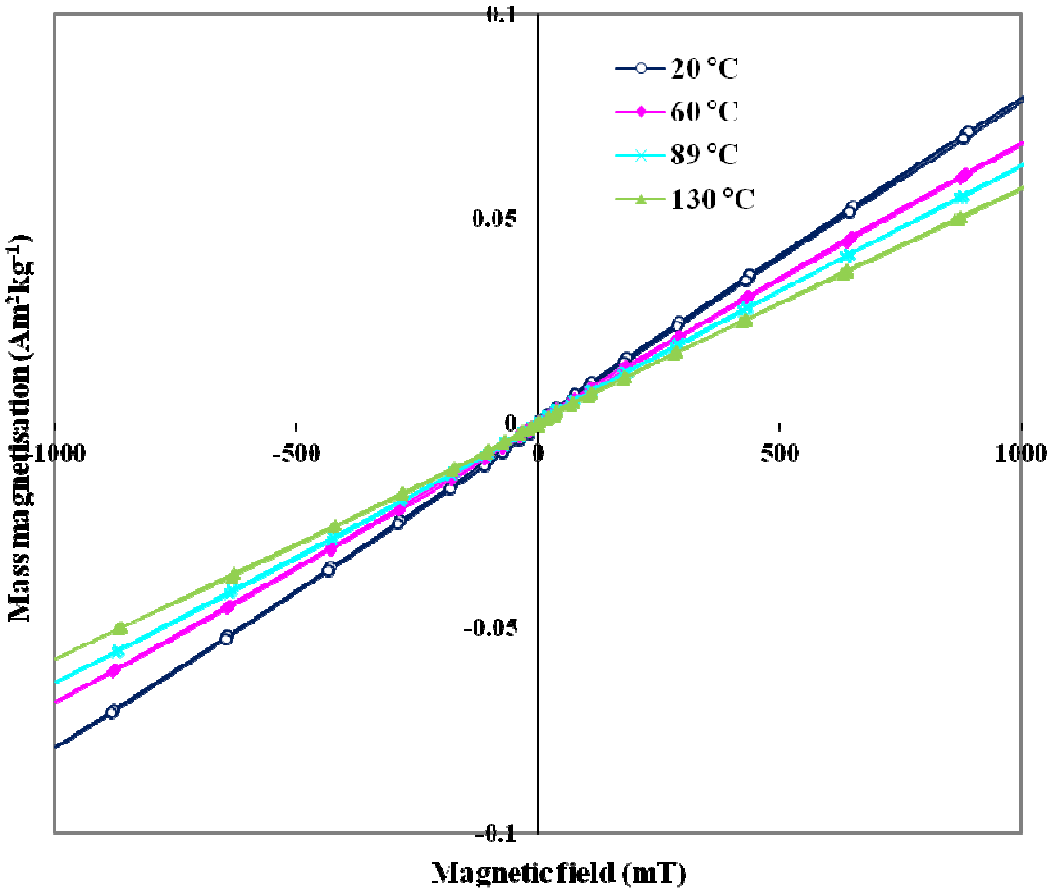

Figure 5.15: Experimental magnetic hysteresis curves for illite sample at respective temperatures (20 ^{o}C, 60 ^{o}C, 89 ^{o}C and 130 ^{o}C).

Using the geothermal gradient the experimental variation of magnetic susceptibility with temperature can be converted into the variation with depth. We have used a gradient of 33 m/^{o}C (Mayer-Gurr, 1976) and used the following equation for conversion of temperature into depth.

$$D = 33T-33(Ts+kt) \qquad 5.4$$

where D is depth in m, T is temperature in ^{o}C, Ts is the average annual sediment surface temperature in ^{o}C, and kt is a geographic constant. We used average annual sediment surface temperature as 9.2 ^{o}C, and kt was taken as 0.8, which is an appropriate value for the UK North Sea region. The conversion of temperature to depth using this equation is shown in Figure 5.26.

Usually there is a thermometer mounted on the tool string which can provide information on the temperature borehole and which we can use to use in our analysis.

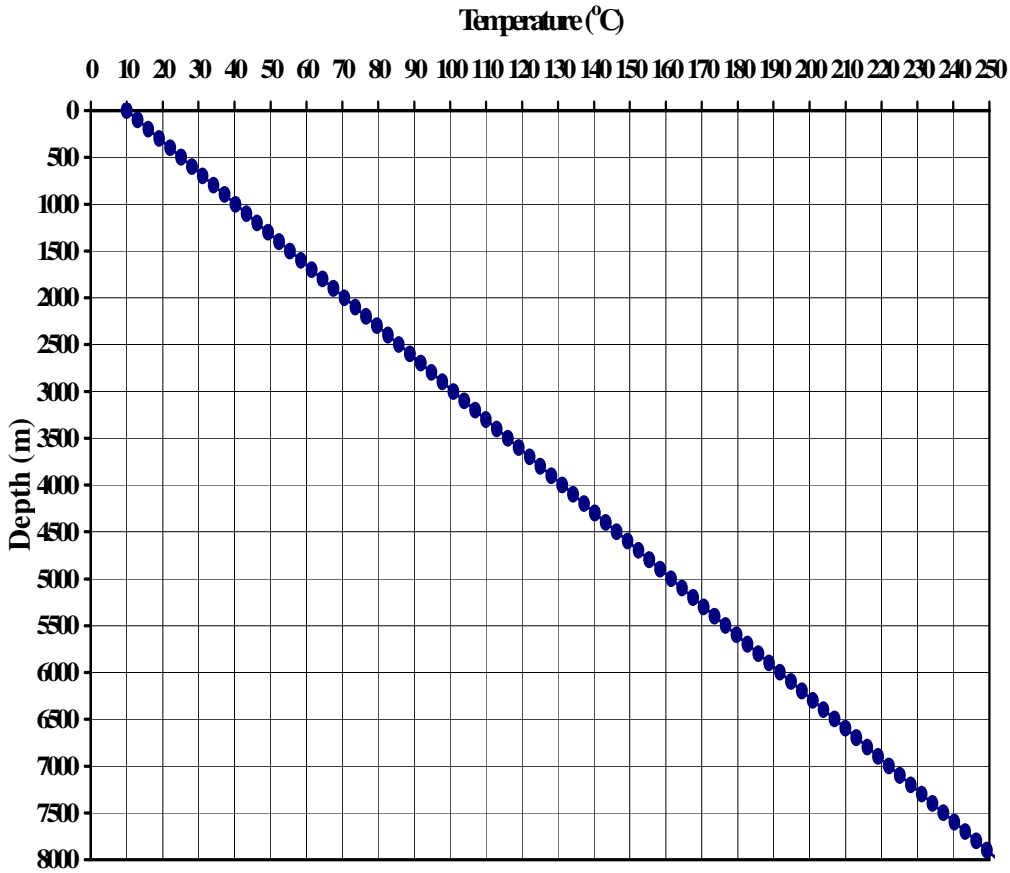

Figure 5.16: In-situ temperature gradient applicable for reservoir rock samples.

Figure 5.17 shows our experimentally obtained mass magnetic susceptibility curves with depth for the illite and barite samples shown in figures 5.14 and 5.15. The magnetic susceptibility values are taken by using the slope of the hysteresis curves. Since we have used synthetic samples in our study, the slope can be taken at any point on the hysteresis curve. If we had ferromagnetic impurities present in our samples, we would then take the slope of the hysteresis curves at high applied fields since ferromagnetic components become saturated at relatively low fields. In our case, the slope is calculated by dividing the magnetization value by the applied field at any particular point on the magnetic hysteresis curves.

Figure 5.17 shows that paramagnetic susceptibility decreases considerably with an increase in depth (or in other words with an increase in temperature). The higher the paramagnetic content in a sample, the higher will be the decrease in paramagnetic susceptibility with an increase in depth. Diamagnetic susceptibility appears to be independent of depth (and temperature). Therefore if we know which reservoir scale minerals we are dealing with, we can accurately model their magnetic response at various depths downhole. Things can be even simpler if one develops model templates for various reservoir scale minerals. Such tempelates could then be used to plot the experimental thermomagnetic data to quickly tell how much of the scale mineral content is present at any particular depth downhole.

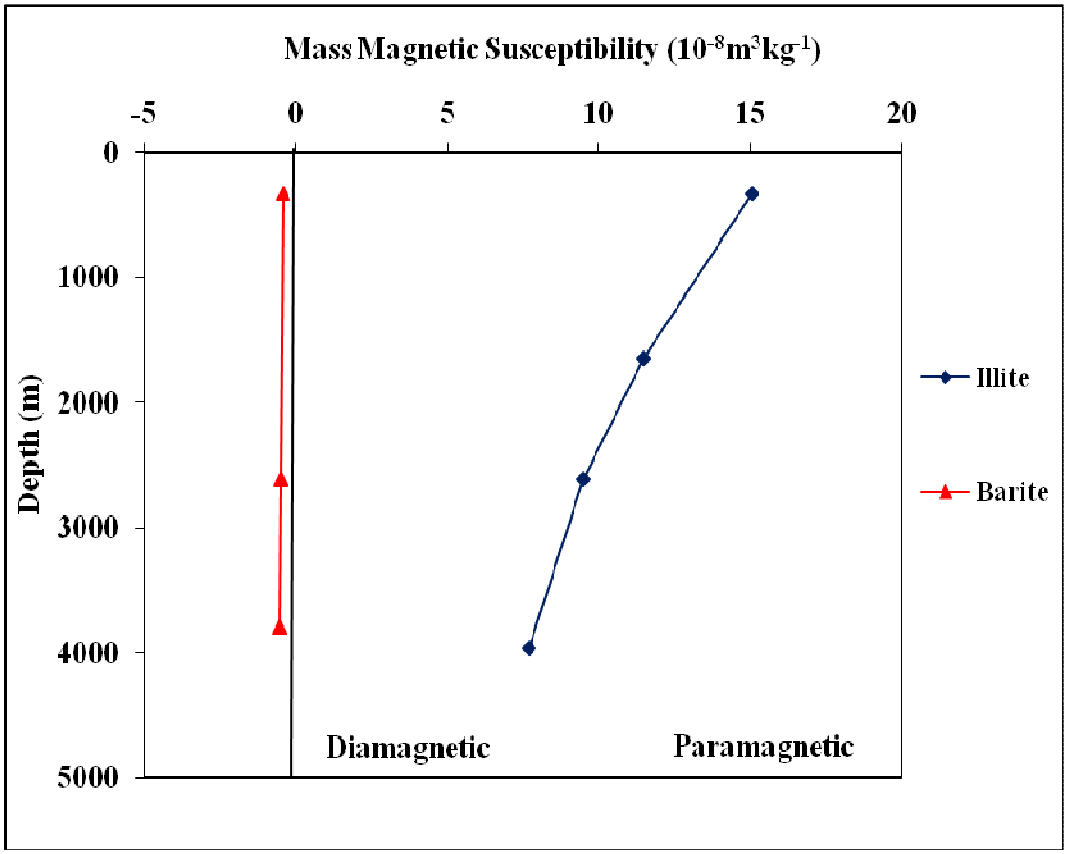

Figure 5.17: Dependence of the mass magnetic susceptibility with depth for illite and barite minerals.

5.6 Summary.

The magnetic susceptibility of paramagnetic and diamagnetic minerals is given by the high field slope on the hysteresis curve. We have shown experimentally measured magnetic hysteresis curves of pure barite, anhydrite, celestite, and gypsum (a diamagnetic mineral) and some percentage % of paramagnetic minerals (siderite and illite) and ferrimagnetic minerals (magnetite and hematite) (by weight) in a barite matrix. The presence of paramagnetic minerals would shift the high field slope of the hysteresis curve upwards. The higher the concentration of paramagnetic minerals present in a barite matrix, the higher would be the positive slope. We have drawn theoretical model templates of magnetic hysteresis curves for various concentrations of

gypsum mineral in anhydrite matrix and also various concentrations siderite and illite minerals in a barite matrix. One can see how sensitive these magnetic hysteresis measurements are for identifying and quantifying small changes in concentration which would change the high field slope of the hysteresis curve. Therefore, by experimentally measuring the magnetic hysteresis curve of a scale sample and plotting it on the model template of the corresponding mineral (known by X-ray or similar techniques), one can accurately quantify the minerals present in the sample.

CHAPTER 6: CONCLUSIONS AND RECOMMENDATIONS

6.1 Application of magnetic susceptibility to oilfield fluids analysis

Measurements of mass and volume magnetic susceptibility of reservoir fluids (brines, crude oils and scale inhibitors) have been made. There were distinct differences between the mass magnetic susceptibilities of brines and crude oils. All the samples studied are diamagnetic, but the values for the crude oils were more negative.

The values of mass magnetic susceptibility for the brines are related to their solute composition, so that an increase in ionic strength causes an increase in mass magnetic susceptibility (less negative) for most of the measured brine samples.

The values of mass magnetic susceptibility for the crude oils are also related to their physical and chemical properties, namely residue content (and group hydrocarbon content), stock tank oil gravity, and viscosity. The results suggest that the magnetic measurements could potentially be used to rapidly characterise the physical differences between various petroleum reservoir fluids.

Scale inhibitor samples which are prepared by adding (10, 100, 1000, 5000, 10000, and 20000 ppm) PPCA in sea water show that an increase in the density (or in other words increase in concentration of the scale inhibitor solutions) results in an increase in their mass magnetic susceptibility (becoming less diamagnetic).

From the values of mass magnetic susceptibility of brine solute ($CaCl_2$, $BaCl_2$, $NaSO_4$, NaCl and $MgCl_2$) with different compositions, it is clear that the increase of every

solute composition would results in a decrease of mass magnetic susceptibility (become more negative).

The values of mass magnetic susceptibility and barium concentration over a period of time for two brines, one with high scaling tendency and the other with low scaling tendency have been recorded. The interesting result is that as the barium concentration decreases with time due to scale precipitation, the mass magnetic susceptibility increases (becomes less negative). So this magnetic technique has a great potential to be used for measuring the barium concentration in fluid samples where there is a possibility of scale precipitation.

6.2 Injection water breakthrough

The mass magnetic susceptibility measurement of produced brine samples was used to identify seawater breakthrough in production lines. This is a key point of Chapter 4. The majority of reservoir fluids are diamagnetic i.e. they show negative magnetic susceptibility values. These negative susceptibilities appear due to the nature of compounds present in these fluids.

A change in the ionic compositions and densities would result in a change in the magnetic susceptibilities of brines. This also means that the mass magnetic susceptibility signal can be used to distinguish between brines of different compositions to identify the breakthrough in production wells of injection water (typically seawater), since the formation brines and sea water generally have different chemical compositions.

The results of the mass magnetic susceptibilities of 100% formation brine and 100% seawater and the mass magnetic susceptibility results for mixing different fractions of formation brine and seawater lies approximately in a straight line. An upward trend in

the magnetic susceptibility data is evident with an increase in the seawater concentration.

Therefore by taking the fluid samples from the production stream, and by measuring their mass magnetic susceptibilities, it would be possible to identify seawater breakthrough at the production wells and subsequently the seawater fraction present in the samples. Since seawater breakthrough, and consequently the onset of scale damage, can sometimes lead to loss of production within a few days, this magnetic technique may be used to alert operators of a risk of scale damage much earlier than is currently possible using conventional techniques. Also, the fact that the magnetic measurements are very rapid and are performed onsite, means that the early warning of seawater breakthrough would enable operators to take important scale prevention measures much quicker than is currently possible, and this may ultimately result in significant financial savings for the companies.

6.3 Identification and quantification of minerals in reservoir scale samples using magnetic hysteresis measurements

The magnetic hysteresis measurements can be used to rapidly and non-destructively characterise reservoir minerals. Plots of magnetisation versus applied field can be used as a universal template for identifying multiple mineral components in any reservoir mineral sample. Changes in the slope (the magnetic susceptibility) of the hysteresis curves reflect different mineral components. Straight lines with negative slope are due to diamagnetic compounds (such as the barite and calcite scale minerals, as well as reservoir fluids which are more diamagnetic than the reservoir scale minerals samples), whilst straight lines with positive slope are due to paramagnetic components (such as siderite and illite). Such straight line sections are generally apparent at high applied fields, where there is no influence from ferromagnetic components. The relative amounts of two diamagnetic minerals (e.g. barite and gypsum) or diamagnetic and paramagnetic minerals (e.g. barite and siderite) in a sample containing a mixture of the two can potentially be quantified by the slope of the straight line at high fields. At low

fields characteristic "kinks" or hysteresis loops indicate the presence of ferromagnetic minerals. The combination of high field and low field measurements provides a very powerful tool for identifying and distinguishing the different mineral components. The hysteresis plots therefore provide more information than conventional single reading low-field (initial) magnetic susceptibility measurements, which represent the sum of all the components in the sample.

The hysteresis plots can easily identify subtle increases in the amount of paramagnetic clay (which can significantly affect fluid permeability), by exhibiting more positive straight line slopes at high fields. The effects of, for instance, different mixtures of diamagnetic and paramagnetic minerals on the hysteresis curves can be theoretically modelled. This will allow a series of theoretical mineral responses to be plotted on the magnetisation versus applied field template, which can then be compared with experimental results on reservoir rocks to rapidly give one an idea of the mineral components. This could complement more conventional techniques such as X-ray diffraction.

An idea of the predominant domain state, single-domain (SD) or multi-domain (MD), of the ferromagnetic minerals (e.g. Hematite) in the samples can be obtained by plotting relevant hysteresis parameters (Hcr/Hc versus Mrs/Ms) on a Day plot.

Experimental modelling revealed changes in low-field (L_{fld}) and high-field (H_{fld}) magnetic susceptibility with temperature. Pure diamagnetic minerals (e.g. Barite) should exhibit a magnetic susceptibility that is independent of temperature. The fact that experimentally some predominantly diamagnetic reservoir samples showed slight decreases of high-field susceptibility with increasing temperature suggested that there were small amounts of paramagnetic minerals in the samples, The increasing temperature possibly caused the magnetic order of the paramagnetic material to become

more disordered, leading to slight decreases in susceptibility (more diamagnetic susceptibility) due to the paramagnetic susceptibility being reduced to some extent.

While mineral samples whose magnetic susceptibility was dominated by paramagnetic and ferromagnetic components also showed decreases in the L_{fld} and H_{fld} susceptibility with increasing temperature (e.g. illite).

6.4 RECOMMENDATIONS FOR FUTURE WORK

The following represent a (non-exhaustive) list of recommendations for further work:

- Measurements of more different types of brines, especially brines with the same density but different composition.
- Study crude oils and their physical and chemical properties.
- Study more scale inhibitor types (e.g. phosphonate).
- Model the magnetic susceptibility to monitor scaling brines tendencies over time results.
- Magnetic susceptibility to monitor other types of scale (e.g. $CaCO_3$) over time.
- Development of passive sensors for continuous monitoring of magnetic susceptibility of fluids downhole and in the laboratory. They might also be used to monitor the build-up of mineral scale and its type.

- 'Live fluids' i.e. real produced water samples with/without oil contamination. The samples could also be cleaned up using various techniques to determine whether or not the technique is viable.

- Apply the detection of injection water breakthrough technique in the field.

- Undertaking hysteresis measurements of mineral scales, particularly for identifying different components in multi-component scale.

- Construct a comprehensive series of theoretical curves for different mineral types and combinations of typical reservoir minerals on the magnetisation versus applied field cross-plot (hysteresis plot). These would become type curves for rapidly identifying and quantifying multiple mineralogies in real reservoir samples from their hysteresis characteristics.

REFERENCES

Aldana, M., Costanzo-Alvarez, V., Vitiello, D., Diaz, M., Silva, P., 1996. Casual relationship between biodegradation of hydrocarbons and magnetic susceptibility in samples from La Victoria oil field (Venezuela). AGU Fall Meeting, San Francisco. Supplement Vol., 77 (46), F163.

Allen, R. F., Walters, M., 1999. Erskine Field: Early Operating Experience. SPE Publication 56899.

Argyle, K. S., Dunlop, D. J., 1984. Theoretical domain structure in multidomain magnetite particles. Geophysical Research Letters, 11, 185-188.

Argyle, K. S., Dunlop, D. J., 1990. Low-temperature and high-temperature hysteresis of small multidomain magnetites (215–540 nm), J. Geophys. Res., 95(B5), 7069–7082.

Bagin, V. I., Ismail-zade, T. A., Malumyan, L. M., Pecherskiy, D. M., 1973. Magnetic studies of the sedimentary rocks of the productive formation in Azerbaijan. [Russian] [Magnitnye issledovaniya osadochnykh porod produktivnoy tolshchi Azerbaijana]. Proceedings of the IX conference: Problems of permanent geomagnetic field, magnetism of rocks and paleomagnetism. Part 2. Baku.

Bagin, V. I., Malumyan, L. M., 1976. Iron-containing minerals in oil-impregnated sedimentary rocks from a producing rock formation of Azerbaijan. [Russian] [Zhelezo-soderzhashchie mineraly v propitannykh neft'yu osadochnykh porodakh produktivnoy tolshchi Azerbaijana]. Proceedings of Academy of Sciences of the USSR. Physics of the Earth [Izvestiya Akademii Nauk SSSR. Fizika Zemli], 4, 73-79. English print. Bagin, V. I., Malumyan, L. M., 1976. Iron-containing minerals in oil-impregnated sedimentary rocks from a producing rock mass of Azerbaidzhan. Translated from Russian by Georgia Moritz. Izvestiya Akademii Nauk SSSR. Fizika Zemli, 4, 273-277.

Bando, Y., Kiyama, M., Yamamoto, N., Takada, T., Shinjo, T., Takaki, H., 1965. Magnetic properties of Fe_2O_3 fine particles. Journal of the Physical Society of Japan, 20, 2086.

Banerjee, S. K., 1971. New grain size limits for paleomagnetic stability in hematite. Nature, 232, 15-16.

Becker, J. R., 1988. Corrosion and scale handbook. Penn Well Publishing Company. 329 pp.

Benthien, R. H., Elmore, R. D., 1987. Origin of magnetization in the Phosphoria formation at Sheep Mountain, Wyoming – A possible relationship with hydrocarbons. Geophysical Research Letters, 14 (4), 323-326.

Bezmer, C., Bauer, K. A., 1969. Prevention of carbonate scale deposition – a well packing technique with controlled solubility phosphates. Journal of Petroleum Technology, 246, 505-514.

Beget, J. E., Stone, D. B., Hawkins, D. B., 1990. Paleoclimatic forcing of magnetic susceptibility variations in Alaskan loess during the late Quaternary. Geology 18, 40–43.

Blackett, P. M. S., 1952. Phil. Trans. Roy. Soc. London, ser. A, vol. 245, p. 303-370.

Bleil, U., Petersen, N., 1982. Magnetic properties of rocks, in Landolt-Boernstein Numerical Data and Functional Relationships in Science and Technology (K.-H. Hellwege, eds.); New Series; Group V: Geophysical and Space Research, Vol. 1B, Physical Properties of Rocks, edited by G. Angenheister, Springer-Verlag Berlin, Heidelberg, New York, 308-432.

Bruckshaw, J. McG., Robertson, E.I., 1948. Journal Scientific Instruments. vol. 25, p.444-446.

Borradaile, G.J., 1987. Anisotropy of magnetic susceptibility: rock composition versus strain. Tectonophysics 138, pp. 327-329.

Borradaile, G.J., 1988. Magnetic susceptibility, petrofabrics and strain. Tectonophysics 156, pp. 1–20

Borradaile, G. J., MacKenzie, A., Jensen E., 1990. Silicate versus trace mineral susceptibility in metamorphic rocks. Journal of Geophysical Research, Solid Earth, 95, 8447-8451.

Brace, W. F., 1965. Some new measurements of linear compressibility of rocks, J. Geophysics Res., 70, 391-398.

Butler, R. F., Banerjee, S. K., 1975. Theoretical single-domain grain size range in magnetite and titanomagnetite. Journal of Geophysical Research, 80 (29). 4049-4058.

Butler, R. F., 1992. Paleomagnetism: Magnetic domains to geologic terranes. Originally published by Blackwell Scientific Publications, 234 pp.

Carmichael, R. S., 1982. Practical Handbook of Physical Properties of Rocks, vol. II, CRC Press, Boca Raton, Fla.

Carmichael, R. S., eds., 1989. Practical handbook of physical properties of rocks and minerals. CRC Press, Boca Raton, 741 pp.

Cavanough, G. L., Holtham, P. N., 2001. Online measurement of magnetic susceptibility in titanium minerals processing. The AusIMM Proceedings 306 (2), 1–6.

Cavanough, G. L., Holtham, P. N., 2004. Rapid characterisation of magnetic separator feed stocks in titanium minerals processing, Physical Separation in Science and Engineering 13(3–4), Taylor & Francis, 141–152.

Chevallier, R., 1925. Ann. Phys., vol. 4, p. 5.

Cioppa, M. T., Al-Aasm, I. S., Symons, D. T. A., 2001. Paleomagnetic dating of diagenetic events in Paleozoic carbonate reservoirs of the Western Canada Sedimentary Basin. Conference of Rock the Foundation Convention, 18-22.

Civan, F., 2000. Reservoir formation damage: fundamentals, modeling, assessment, and mitigation. Gulf Publishing Company, 741 pp.

Cockram, D., Shields, R. and Mackay, E. J., Scale Control Using Magnets – What is the Evidence Behind the Claims?, Flow Assurance & Scale Team 2004-2007 Joint Industry Project Progress Report 3 Section 11, Heriot-Watt University (November 2005).

Cogoini, M., 1998. Determining the origin of soil magnetic susceptibility anomalies in hydrocarbon environments. AAPG Bulletin 11, 2160-2161.

Cogoini, M., 2001. Investigation the role of microbial versus chemical processes in magnetic mineral formation of soils. The IRM Quarterly, 11 (1, 2), 6-7.

Collins, I. R., Jordan, M. M., 2001. Occurrence, prediction and prevention of zinc sulfide scale within Gulf coast and North Sea high temperature/high salinity production wells. SPE paper 68317.

Collinson, D. W., 1983. Methods in rock magnetism and paleomagnetism: Techniques and Instrumentation. Chapman and Hall, London, 503 pp.

Costanzo-Alvarez, V., Aldana, M., Aristeguieta, O., Marcano, M. C., Aconcha, E., 2000. Study of magnetic contrasts in the Guafita oil field (South-Western Venezuela). Physics and Chemistry of the Earth, Part A-Solid Earth and Geodesy, 25 (5), 437-445.

Cowan, J. C., Weintritt, D. J., 1976. Water-formed scale deposits. Gulf Publishing Company, Houston, 741 pp.

Crowe, C. W., 1985. Evaluation of agents for preventing precipitation of ferric hydroxide from spent treating acid. Journal of Petroleum Technology, 691-695.

Cui, Y., Verosub, K. L., Roberts, A. P., 1994. The effect of low-temperature oxidation on large multi-domain magnetite, Geophys. Res. Lett., 21:757.

Curie, P., Chenevesu, C., 1903. Journ. Phys. Radium, No. 4, p. 769.

Day, R., Fuller, M., Schmidt, V. A., 1977. Hysteresis properties of titanomagnetites: Grain-size and compositional dependence. Physics of the Earth and Planetary Interiors, 13, 260-267.

Dearing, J. A., 1999. Environmental magnetic susceptibility using the Bartington MS2 system.

Deer, W.A., Howie, R.A., Zussman, J., 1992. An introduction to the rock forming minerals, 2nd Ed. Longman Group UK Limited.

Donovan, T. J., Forgey, R. L., Roberts, A. A., 1979. Aeromagnetic detection of diagenetic magnetite over oil fields. AAPG Bulletin, 63, 245-248.

Dorfman, Ya. G., 1961. Diamagnetism and the chemical bond. Fizmat, Moscow, 232 pp.

Drago, R. S., 1992. Physical methods for chemists. Saunders College Publishing. Second edition, 750 pp.

Dunlop, D. J., 1973a. Superparamagnetic and single-domain threshold sizes in magnetite. Journal of Geophysical Research, 78, 1780-1793.

Dunlop, D. J., 1973b. Thermoremanent magnetization in submicroscopic magnetite. Journal of Geophysical Research, 78, 7602-7613.

Dunlop, D. J., 1981. The rock-magnetism of fine particles. Phys. Earth Planet. Inter. 26, 1–26.

Dunlop, D. J., 2002. Theory and application of the Day plot (Mrs/Ms versus Hcr/Hc). Application to data for rocks, sediments, and soils. Journal of Geophysical Research, 107 (B3) doi:10.1029/2001JB000486.

Dunlop, D. J., 2002a. Theory and application of the Day plot (Mrs/Ms versus Hcr/Hc). 1. Theoretical curves and tests using titanomagnetite data. Journal of Geophysical Research, 107 (B3), 4-1 – 4-22.

Dunlop, D. J., 2002b. Theory and application of the Day plot (Mrs/Ms versus Hcr/Hc). 2. Application to data for rocks, sediments, and soils. Journal of Geophysical Research, 107 (B3), 5-1 – 5-15.

Dunlop, D. J., Bina, M. M., 1977. The coercive force spectrum of magnetite at high temperatures: Evidence for thermal activation below the blocking temperature. Geophysical Journal of the Royal Astronomical Society, 51, 121-147.

Dunlop, D. J., Ozdemir, O., 1997. Rock magnetism: Fundamentals and frontiers. Cambridge University Press, Cambridge, 573 pp.

Earnshaw, A., 1968. Introduction to magnetochemistry. Academic Pres, London, 115 pp.

Elmore, R. D., Engel, M. H., Crawford, L., Nick, K., Imbus, S., Sofer, Z., 1987. Evidence a relationship between hydrocarbons and authigenic magnetite. Nature, 325, 428-430.

Elmore, R. D., Scott, W. I., Engel, M. H., Fruit, D., 1993. Hydrocarbon and magnetization in magnetite. SEMP Special Publication 49, 181-191.

Emmons, D. H., Graham, G. C., Holt, S. P., Jordan, M. M., Lorcardel, B., 1999. On-site, near-real-time monitoring of scale deposition. SPE Publication 56776.

Enkin, R. J., Williams, W., 1994. Three-dimensional micromagnetic analysis of stability in fine magnetic grains. Journal of Geophysical Research, 99, 611-618.

Ergin, Y. V., 1983. Magnetic properties and structure of electrolyte solutions. [Russian], Nauka, Moscow, 183 pp.

Ergin, Y. V., Kostrova L. I., Subaev I. Kh., and Yarulin K. S., 1975. Magnetic properties of oils. [Russian]. Depositor of VINITI, N3265-75.

Ergin, Y. V., Yarulin, K. S., 1979. Magnetic properties of oils. [Russian], Nauka, Moscow, 200 pp.

Eventov, L., 1997. Application of magnetic methods in oil and gas exploration. The Leading Edge, 16 (5), 489-492.

Eventov, L., 2000. The nature and interpretation of geophysical and geochemical anomalies over oil and gas fields. The Leading Edge, 19 (5), 488-490.

Farshad, F.F. and Vargas, S.M. (2002). Scale prevention, a magnetic treatment approach. SPE 77850.

Farshad, F.F., Linsley, J., Kuznetsov, O. And Vargas, S. (2002). The effect of magnetic treatment on calcium sulphate scale formation. SPE 76767.

Filippycheva, L. G., Burakov, A. I., Bogdanovich, A. I., Belyaev, I. P., Gutner, A. B., 2001. Downhole magnetic stratigraphy in solving problems of correlation of heterofacial strata, sequence-stratigraphy for oil fields modelling, technology of operations, instrumentation [CD Rom]. EAGE 63th Conference and Technical Exhibition, Amsterdam, 11-15 June, 643 pp.

Foner, S., 1991. Review of magnetometry, IEEE Trans. Magn. 17 (6) 3358–3363.

Foner, S., McNiff E. J. Jr., 1968. Very low frequency integrating vibrating sample magnetometer (VLFVSM) with high differential sensitivity in high dc fields, Rev. Sci. Instrum. 39 171–179.

Fraser, D.C., 1973, Magnetite ore tonnage estimates from an aerial electromagnetic survey: Geoexploration, 11, 97-105.

Gaffney, S. H., Jackson, G. E., Lyons, A. J. S., 1988. The effect of iron (II) on the barium scale inhibition of diethylene-triamine pentamethylene phosphoric acid. In: P. H. Ogden, eds. Chemicals in the oil industry. Royal Society of Chemistry Special Publication, 67, 135-139.

Geiss, C. E., 1999. The development of rock magnetic proxies for paleoclimate reconstruction. Thesis, University of Minnesota, 254 pp.

Geiss, C. E., Heider, F., Soffel, H. C, 1996. Magnetic domain observations on magnetite and titanomaghemite grains (0.5 - 10 μm). Geophysical Journal International, 124, 75 – 88.

Gillen, K. P., Van der Voo, R., Thiessen, J. H., 1999. Late Cretaceous-early Tertiary remagnetization of the devonian Swan Hills Formation recorded in carbonate cores from the Caroline gas field, Alberta, Canada. AAPG Bulletin, 83 (8), 1223-1235.

Graham, J. W., 1964. Preliminary account of a refined technique for magnetic susceptibility anisotropy measurements of rocks, South West Center for Advanced Study Report, Dallas.

Graham G. M., Boak, L. S., Sorbie, K. S., 1997. The influence of formation calcium on the effectiveness of generally different barium sulphate oilfield scale inhibitors. Presented at the SPE International Symposium on Oilfield Chemistry, Houston, USA, 18-21 February 1997. SPE Publication 37273.

Graham G. M., Sorbie, K. S., Boak, L. S., Taylor, K. and Blilie, L.A. 1994. Development and Application of Accurate Detection and Assay Techniques for Oilfield Scale Inhibitors in Produced Water Samples, SPE No. 28997, presented at the SPE International Symposium on Oilfield Chemistry, San Antonio, Texas. 14-17 February.

Grenet, G., 1930. Ann. de Phys. Ser. 10., vol. 13, p. 309.

Gunarathne, G. P. P., and Keatch, R. W., 1995. Novel techniques for monitoring and enhancing dissolution of mineral deposits in petroleum pipelines. Presented at the Offshore Europe Conference, Aberdeen, 5-8 September. SPE Oublication 30418507-522.

Guoy, L. G., 1889. C.R Acad. Sci., Paris, 109, 935.

Hailwood, E. A., Bowen, D., Corbett, P. W. M., Ding, F., Whattler, P., 1996. Magpore-a new technique for characterizing reservoir pore fabrics, by magnetic anisotropy analysis. EAGE 58th Conference and Technical Exhibition, Petroleum Division, Amsterdam, The Netherlands, 3-7 June, P553.

Hailwood, E. A., Bowen, D., Ding, F., Corbett, P. W. M., Whattler, P., 1999. Characterizing pore fabrics in sediments by anisotropy of magnetic susceptibility

analyses. In: D. H. Tarling and P.Tuner, eds., Paleomagnetism and diagenesis in Sediments. Geological Society, London, Special Publication 151, 125-126.

Hailwood, E. A., Ding, F., 1995. Paleomagnetic reorientation of cores and the magnetic fabric of hydrocarbon reservoir sands. In: P. Turner and A. Turner, eds., Paleomagnetic application in hydrocarbon exploration and production. Geological Society Special Publication 98, 245-258.

Hall, S. A., Evans, I., 1995. Paleomagnetic and magnetic properties of hydrocarbon reservoir from the Permian basin, southeastern New Mexico, USA. In: P. Turner and A. Turner, eds. Paleomagnetic application in hydrocarbon exploration and production. Geological Society Special Publication 98, London, 79-95.

Hanson, L. S., Sauchuk, S. A., 1991, Field guide to the geology and geomorphology of the Carrabassett Formation and economic deposits in central Maine, in Fieldtrip Guide for the Summer Meeting of the Geological Society of Maine, 42 p.

Hauger, E., Lovlie, R., 1992. Paleomagnetci characteristics of drill cores from Middle Jurassic delta plain sediments, The Brent Group, North Sea. Physics of the Earth and Planetary Interiors. 71, 74-84.

Hazarika, F., Rahman, A., 2000. Temperature variation of magnetic susceptibility of samples of Lakhmoni oil field. Indian Journal of Physics, 74A (3), 273-277.

Henry, B., Jordanova, N., Le Goff, M., 2005. Transformations of magnetic mineralogy in rocks revealed by difference of hysteresis loops measured after stepwise heating: theory and case studies: Geophysical Journal International, Vol. 162, 64-78.

Hill, R., 1963. Elastic properties of reinforced solids: Some theoretical principles, J. Mech. Physics. Solids, 11, 357-372.

Hill, R. W., 1982. Advanced student experiments in paramagnetism and antiferromagnetism, Eur. J. Phys., 3, 75-79.

Hinrichsen, C. J., Brindle, K. H., 1989. Scale and corrosion control in high temperature oil production and steamflood operation. 18th Annual Indonesia Petroleum Association Convention, Jakarta, Indonesia, 24-26 October 1989. Proceeding Vol., 2, 277-300.

Hinrichsen, C. J., Edgerton, M. C., 1998. Preventing scale deposition in oil production facilities. 4th International Conference Advances in Solving Oilfield Scaling, Abeerden, 19-34.

Hoffmann, V., 1992. Greigite (Fe_3S_4): magnetic properties and first domain observations. Physics of the Earth and Planetary Interiors, 70, 288-301.

Hounslow, M. W., Maher, B. A., Thistlewood, L., 1995. Magnetic mineralogy of sandstones from the Lunde Formation (Late Triassic), northern North Sea, UK: origin of the palaeomagnetic signal. In: P. Turner and A. Turner, eds. Paleomagnetic application in hydrocarbon exploration and production. Geological Society Special Publication 98, London, 119-147.

Hrouda, F., 1973. A determination of the symmetry of the ferromagnetic mineral fabric in rocks on the basis of the magnetic susceptibility anisotropy measurements. Gerl. Beitr. Geophys., 82, 390-396.

Hrouda, F., 1994. A technique for the measurement of thermal changes of magnetic susceptibility of weakly magnetic rocks by the CS-2 apparatus and KLY-2 Kappabridge. Geophys. J. Int., 118, 604-612.

Hrouda, F., 2002. Low-field variation of magnetic susceptibility and its effect on the anisotropy of magnetic susceptibility of rocks. Geophys. J. Int., 150, 1-9.

Hrouda, F., 2003. Indices for numerical characterization of the alteration processes of magnetic minerals taking place during investigation of temperature variation of magnetic susceptibility. Stud. Geophys. Geod., 47, 847-861.

Hunt, C. P., Moskowitz, B. M., Banerjee, S. K, 1995. Rock physics and phase relations: a handbook of physical constants. AGU Reference Shelf 3. Magnetic Properties of Rocks and Minerals, 189-203.

Ivakhnenko, O.P., 2006. Magnetic analysis of petroleum reservoir fluids, matrix mineral assemblages and fluid-rock interaction. PhD thesis, Heriot-Watt University, Institute of Petroleum Engineering, Edinburgh, UK.

Ivakhnenko, O.P., Potter, D.K., 2004, Magnetic Susceptibility of Petroleum Reservoir Fluids. Physics and Chemistry of the Earth 29 (2004), pp. 899-907.

Ivakhnenko, O.P., Potter, D.K., 2006. The use of magnetic hysteresis and remanence measurements in rapidly and nondestructively characterising reservoir rocks and fluids. Society of Core Analysts held in Trondheim, Norway 12-16.

Ivakhnenko, O.P., Potter, D.K., 2008. The use of magnetic hysteresis and remanence measurements for rapidly and non-destructively characterizing reservoir rocks and fluids. Journal of Petrophysics, 49 (1), 47-56.

Jackson, M., Worm, H. U., Banerjee, S. K., 1990. Fourier analysis of digital hysteresis data: Rock magnetic applications, Phys. Earth Planet. Int., 65-78.

Jeffrey, E. L., William, H. L., Karl, J. E., 2007. An Introduction to Using Surface Geophysics to Characterize Sand and Gravel Deposits. U.S. Geological Survey, Reston, Virginia.

Jordan, M., Sjuraether, K., Collins, I., Feasey, N., Emmons, D., 2001. Life cycle management of scale control within subsea fields and its impact on flow assurance, Gulf of Mexico and the North Sea basin. SPE Publication 71557, 16pp.

Jordan, M. M., Sorbie, K. S., Jiang, P., Yuan, M., Todd, A. C., Taylor, K., Hourston, K. E., Ramstad, K., 1994. Mineralogical controls on inhibitor adsorption/desorption in Brent group sandstone and their importance in predicting and extending filed squeeze lifetime. Presented at the European Production Operations Conference and Exhibition, Aberdeen, UK, 15-17 March. SPE Publication 27607, 141-153.

Kapička, A., Hoffmann, V., Petrovsky, E., 2003. Pressure instability of magnetic susceptibility of pyrrhotite bearing rocks from the KTB borehole. Studia Geophysica et Geodaetica, 47 (2), 381-391.

Kelso, P., Tikoff, B., Jackson, M., Sun, W., 2002. A new method for the separation of paramagnetic and ferromagnetic susceptibility anisotropy using low-field and high-field methods, Geophysical Journal International 151, 345–359.

Kennedy, T., 1985. Long range order in the anisotropic quantum ferromagnetic Heisenberg model, Commun. Math. Phys. (100) pp 447.

Kittel, C., 1949. Physical theory of ferromagnetic domains. Reviews of Modern Physics, 21 (4), 541–583.

Kittel, C., 1996. Introduction to solid state physics, 7th edition, John Wiley.

Langevin, P., 1905. La physique des electrons. Revue générale des sciences pures et appliqués. [French], 16, 257–276.

Lasetr, R. M., Grander, T. R., Glasscock, F. M., 1968. Scale deposits are controlled now with liquid inhibitors. Oil and Gas Journal, January 15, 63-88.

Liu, Q. S., Liu, S. G., 1999. Magnetic and mineralogical characteristics of reservoir rocks in the Yakela oil field, northern Tarim Basin and their implications for magnetic detection of oil and gas accumulations. Chinese Science Bulletin, 44 (2), 174-177.

Liu, Q. S., Xu, W. K., Deing, S. F., Wang, X. F., 1996. A study for relationship between hydrocarbon migration and soil magnetism above oil and gas fields in China. Acta Geophysica Sinica, 39 (6), 804-812.

Liu, Q., Banerjee, S. K., Jackson, M. J., Zhu, R., Pan, Y., 2002. Effects of low-temperature oxidation on natural remanent magnetization of Chinese loess. Chinese science bulletin, 47 (24), 2100-2105.

Mackay, E. J., 2003. Modeling in-situ scale deposition: the impact of reservoir and well geometries and kinetic reaction rates. SPE Production and Facilities, February, 45-56.

Mackay, E. J., Jordan, M. M., 2003. SQUEEZE modelling: treatment design and case histories. SPE Publication 82227, 12pp.

Mackay, E. J., Jordan, M. M., Torabi, F., 2002. Predicting Brine Mixing Deep Within the Reservoir, and the Impact on Scale Control in Marginal and Deepwater Developments. Presented at the SPE International Symposium and Exhibition on Formation Damage Control, Lafayette, USA, 20-21 February 2002. SPE publication 73779, 17 pp.

Matteson, A., Tomanic, J. P., Herron, M. M., Allen, D. F., Kenyon, W. E., 2000. NMR relaxation of clay/brine mixtures. SPE Reservoir Evaluation and Engineering, 3 (5), 408-413.

Mayer-Gurr A., 1976. Petroleum Engineering. Geology of Petroleum. Vol. 3, Pitman Publishing, 208 pp.

McAndrew, J., 1957. Calibration of a Frantz isodynamic separator and its application to mineral separation, Proc. Aus. IMM 181 59–73.

McNab, T. K., Fox, R. A., Boyle, A. J. F, 1968. Some magnetic properties of magnetite (Fe3O4) crystals. Journal of Applied Physics, 39, 5703-5711.

Mee, C., Daniel, E., 1988. Magnetic recording, Vol - III, McGraw Hill.

Melnikov, N. W., Rshewski, W. W., Prodotjakonov, M. M, 1975. Handbook of physical properties of rocks. Nedra, Moscow.

Merrill, R. T., McElhinny, M., McFadden, P., 1996. The magnetic field of the Earth: Paleomagnetism, the Core and the Deep Mantle. Academic Press.

Moghadasi, J., Jamialahmadi, M., Muller-Steinhagen, H., Sharif, A., Izadpanah, M. R., 2002. Formation damage in Iranian oilfields. Presented at the SPE International Symposium and Exhibition on Formation Damage Control, Lafayette, USA, 20-21 February 2002. SPE publication 73781, 9 pp.

Moghadasi, J., Jamialahmadi, M., Muller-Steinhagen, H., Sharif, A., Ghalambor, A., Izadpanah, M. R., Motaie, E., 2003a. Scale formation in Iranian oil reservoir and production equipment during water injection. Presented at the 5th International Oilfield

Symposium and Exhibition, Aberdeen, UK, 29-30 January 2003. SPE Publication 80406, 14 pp.

Moghadasi, J., Jamialahmadi, M., Muller-Steinhagen, H., Sharif, A., 2003b. Scale formation in oil reservoir and production equipment during water injection (Kinetic of $CaSO_4$, and $CaCO_3$ crystal growth and effect on formation damage). Presented at the SPE European Formation damage Conference, The Hague, Netherlands, 13-14 May. SPE Publication 82233, 12 pp.

Mooney, H. M., 1952. Gph. vol. 27, p. 531-543, No. 3.

Moritz, A. P., and Neville, A., 2000. A novel approach for monitoring of $CaCO_3$ and $BaSO_4$ scale formation. SPE Publication 60189.

Moskowitz, B. M., 1991. Hitchhiker's guide to magnetism. Institute of Rock Magnetism, Environmental Magnetism Workshop, 48 pp.

Moskowitz, B. M., Frankel, R. B., Walton, S. A., Dickson, D. P. E., Wong, K. K. W., Douglas, T., Mann, S., 1997. Determination of the preexponential frequency factor for superparamagnetic maghemite particles in magnetoferritin. Journal of Geophysical Research, 102, 22671-22680.

Mullins, C. E., 1977. Magnetic susceptibility of the soil and its significance to soil science: a review. Journal Soil Science, 28, 233-246.

Nasr-El-Din, H. A., Al-Humaidan, A, Y., 2001. Iron sulfide scale: formation, removal and prevention. SPE Publication 68315, 13 pp.

Nagata, T., 1940. Bull. Earthquake Res. Inst., vol. 18, p. l02.

Nesset, E., Finch, J. E., 1980. Determination of magnetic parameters for field-dependent susceptibility minerals by Frantz isodynamic magnetic separator, Trans. IMM Sect. C 89 161–166.

O'Reilly, W., 1984. Rock and mineral magnetism. Blackie, Glasgow, 220 pp.

Parasnis, D. S., 1979. Principles of Applied Geophysics. 3rd eds., Chapman and Hall, London, 275 pp.

Petersen, E. U., Friesen, R. G. 1982. Metamorphism of the Geco massive sulphide deposit, Manitouwadge, Ontario. Geol. Assoc. Can./Mnieral. Assoc. Can. Program Abstr. 7, 73.

Petersen, N., 1985. Gesteinsmagnetismus. In: F. Bender, eds., Angewandte Geowissenschaften. [German], Vol. 2, Ferd. Enke Verlag, Stuttgart.

Petty, M.C., 2007. Molecular electronics: From principles to practice (Wiley series in materials for electronic and optoelectronic applications). WileyBlackwell, 208 pp.

Potter, D. K., 2004a. Magnetic susceptibility as a rapid petrophysical tool for a permeability prediction. EAGE 66th Conference and Technical Exhibition, Paris, 7-10 June 2004. Extended Abstracts, Vol. 1, Paper D018.

Potter, D. K., 2004b. Downhole magnetic susceptibility: potential applications of an environmentally friendly technique. European Geosciences Union, 1st General Assembly, Nice, France, 25-30 April. Geophysical Research Abstracts, 6, 04935.

Potter, D. K., 2005. Magnetic susceptibility as a rapid non-destructive technique for improved RCAL and SCAL parameter prediction. 2005 International Symposium of the Society of Core Analysts, Toronto, Canada. Paper SCA2005-02, 13 pp.

Potter, D. K., Corbett, P. W. M., Barclay, S. A., Haszeldine, R. S, 2004. Quantification of illite content in sedimentary rocks using magnetic susceptibility - A rapid complement or alternative to X-ray diffraction. Journal of Sedimentary Research, 74 (5), 730-735.

Potter, D. K., 2007. Magnetic susceptibility as a rapid, non-destructive technique for improved petrophysical parameter prediction. Journal of Petrophysics, 48 (3), 191-201.

Potter, D.K., Ivakhnenko, O.P., 2008. Clay typing - Sensitive quantification and anisotropy in synthetic and natural reservoir samples using low- and high-field magnetic susceptibility for improved petrophysical appraisals. Journal of Petrophysics, 49 (1), 57-66.

Poyet, J. P., Segeral, G., Toskey, E., 2002. Real-time method for the detection and characterization of scale. SPE Publication 74659, 11 pp.

Przybylinski, J. L., 2001. Iron sulfide scale deposit formation and prevention under anaerobic conditions typically found in the oil field. Presented at the SPE International Symposium on Oil Chemistry, Houston, USA, 13-16 February 2001. SPE Publication 65030, 8 pp.

Przybylinski, J. L., 2003. Ferrous sulfide solid formation and inhibition at oxidation-reduction potentials and scaling indices like those that occur in the oil field. Presented at the SPE International Symposium on Oil Chemistry, Houston, USA, 5-7 February 2003. SPE Publication 80260, 9 pp.

Richter, C., van der Pluijm, B.A., 1994. Separation of paramagnetic and ferromagnetic susceptibilities using low temperature magnetic susceptibilities and comparison with high field methods, Physics of the Earth and Planetary Interiors, 82, 113-123.

Robin, P., Bordas le Floch, N., Roure, F., Frizon, de Lamotte, D., 2000. Magnetic fabric analysis and deformation in sandstone reservoir. Geophysical Research Abstracts, Vol. 2.

Rosenblum, S., Brownfield, K., 1999. Magnetic susceptibility of minerals. USGS open-file report 99-529. [On-line] http://pubs.usgs.gov.

Selwood, P. W., 1956. Magnetochemistry. 2nd edition. Interscience publishers, New York, 435 pp.

Sepulveda, N., Thomas, I., Wikswo, J., 1994. Magnetic susceptibility tomography for a three dimensional imaging of diamagnetic and paramagnetic objects, IEEE Trans. Magn. 30 5062–5069.

Sharma, P. V., 1986. Geophysical Methods in Geology. 2nd edition, Elsevier, New York, 442 pp.

Soffel, H. C., 1971. The singledomain-multidomain transition in natural intermediate titanomagnetites. Zeitschrift fuer Geophysik, 37, 451-470.

Soffel, H. C., 1977. Pseudo-single-domain effects and single-domain - multidomain transition in natural pyrrhotite deduced from domain structure observations. Journal of Geophysics, 42, 351-359.

Soffel, H. C., 1991. Paläomagnetismus und archäomagnetismus. [German], Springer, Berlin, Heidelberg, 276 pp.

Stacey, F. D., 1960. J. Geophys. Res. vol. 65, No. 8, p. 2429-2442.

Stephenson, A., De Sa, A., 1970. A simple method for the measurement of the temperature variation of initial magnetic susceptibility between 77 and 1000 K, J. Phys. E 3 59–61.

Stone, D. B., 1962. Geophys. Jour. Roy. Astron. Soc., 7, p. 375-390.

Strangway, D. W., 1967, Magnetic characteristics of rocks: in Mining Geophysics, 2, Society of Exploration Geophysicists, p. 454-473.

Symons, D. T. A., Enkin, R. J., Cioppa, M. T., 1999. Paleomagnetism in the Western Canada Sedimentary Basin: Dating fluid flow and deformation events. Bulletin of Canadian Petroleum Geology, 47 (4), 534-547.

Tarling, D. H., 1983. Palaeomagnetism: principles and applications in geology, geophysics and archaeology. Chapman and Hall Ltd., London, 379 pp.

Tarling, D. H., Hrouda, F., 1993. The magnetic anisotropy of rocks. Chapman and Hall, London, 217 pp.

Tauxe, L., 1993. Sedimentary records of relative palaeointensity of the Geomagnetic field: Theory and Practice. Reviews of Geophysics, 31 (3), 319-354.

Telford, W. M., Geldart, L. P., Sheriff, R. E., 1990. Applied Geophysics. 2nd eds., Cambridge University Press, New York, 770 pp.

Thompson, R., Oldfield, F., 1986. Environment magnetism. Allen and Unwin, 227 pp.

Todd, A. C., Yuan, M. D., 1991. Prediction of sulphate scaling tendency in oilfield operation. SPE production Engineering Journal, February, 63-72.

Torquato, S., 1991. Random heterogeneous media: Microstructure and improved ounds on effective properties, Applied Mech. Rev., 44, 37-76.

Vasudeva, D. N., 1966. Fundamentals of Magnetism and Electricity, 7th edition, S.Chand and Co., 443-448.

Vetter, O. J., Farone, W. A., 1987. Calcium carbonate scale in oilfield operations. Presented at the 62nd Annual Technical Conference and Exhibition, Dallas, 27-30 September 1987. SPE Publication 16908.

Vetter, O. J., Farone, W. A., Veith, E., Lankford, S., 1987. Calcium carbonate scale considerations: a practical approach. Presented in the International Symposium of Production Technology, Lubbock, 16-17 November 1987. SPE Publication 17009.

Vetter, O. J., Kandarpa, V., Harvaka, A., 1982. Prediction of scale problems due to injection of incompatible waters. Journal of Petroleum Technology, February, 273-284.

Vulfson, S. G., 1998. Molecular magnetochemistry. Overseas Publishers Association, Amsterdam. Originally published in Russian in 1991. Nauka Publisher. Moscow. 474 pp.

Watt, J. P., 1988. Elastic properties of polycrystalline minerals: Comparison of theory and experiment, Phys. Chem. Minerals, 15, 579-587.

Wilson, H., Brooks, A. G., 2001. Wellbore position errors caused by drilling fluid contamination. SPE Publication 71400, 8 pp.

Wyllie, M. R. J., Gregory, A. R., Gardner, G. H. F., 1958. An experimental investigation of factors affecting elastic wave velocities in porous media, Geophysics, 23, 459-493.

Yeremin, V. N., Molostovskiy, E. A., Pervushova, Ye, V., Chernyaeva, A. F., 1986. Magnetic zonation of sedimentary rocks and the spatial distribution of authigenic iron minerals in hydrocarbon halos. [Russian] [Magnitnaya zonal'nost' osadochnykh porod i prostranstvennoye raspredeleniye autigennykh mineralov zheleza v zonakh vliyaniya UV]. Geology of oil and gas [Geologiya Nefti i Gaza], 4, 38-44. English print. Yeremin, V. N., Molostovskiy, E. A., Pervushova, Ye, V., Chernyaeva, A. F., 1986. Magnetic zonation of sedimentary rocks and the spatial distribution of authigenic iron minerals in hydrocarbon halos. International Geology Review, 28, 734-739.